Distribution Agreement

In presenting this thesis or dissertation as a partial fulfillment of the requirements for an advanced degree from Emory University, I hereby grant to Emory University and its agents the non-exclusive license to archive, make accessible, and display my thesis or dissertation in whole or in part in all forms of media, now or hereafter known, including display on the world wide web. I understand that I may select some access restrictions as part of the online submission of this thesis or dissertation. I retain all ownership rights to the copyright of the thesis or dissertation. I also retain the right to use in future works (such as articles or books) all or part of this thesis or dissertation.

Signature:

_____ _____

Gina Alesi Date

Characterization of Protein Kinase Signaling in Cancer Metastasis and Cancer Drug Resistance

By

Gina Alesi
Doctor of Philosophy

Graduate Division of Biological and Biomedical Sciences
Cancer Biology

_____
Sumin Kang, Ph.D.
Advisor

_____
Jing Chen, Ph.D.
Committee Member

_____
Haian Fu, Ph.D.
Committee Member

_____
Shi-Yong Sun, Ph.D.
Committee Member

_____
Rita Nahta, Ph.D.
Committee Member

Accepted:

_____
Lisa A. Tedesco, Ph.D.
Dean of the James T. Laney School of Graduate Studies

_____
Date

Characterization of Protein Kinase Signaling in Cancer Metastasis and Cancer Drug Resistance

By

Gina Alesi

B.S., Biomedical Engineering, University of Michigan, 2010

M.S., Biomedical Engineering, University of Michigan, 2011

Advisor: Sumin Kang, Ph.D.

An abstract of
A dissertation submitted to the Faculty of the
James T. Laney School of Graduate Studies of Emory University
in partial fulfillment of the requirements for the degree of
Doctor of Philosophy
in Graduate Division of Biological and Biomedical Sciences
Cancer Biology
2016

Abstract

Characterization of Protein Kinase Signaling in Cancer Metastasis
and Cancer Drug Resistance
By Gina Alesi

Despite improvements in cancer therapy and patient survival, there were approximately 589,000 human cancer deaths in 2015. Cancer metastases that are resistant to current therapeutic strategies are responsible for over 90% of these deaths. Over the past 20 years, the paradigm of cancer treatment has shifted toward targeted therapies, which act on cancer-specific molecular targets, such as kinases, to inhibit cancer cell survival and growth.

We recently exploited two key strategies for determining novel protein kinase targets in cancer therapy. The first strategy relies on identifying signaling effectors downstream of oncogenic kinases. Following previous research demonstrating that ribosomal S6 kinase 2 (RSK2) promotes head and neck cancer cell invasion and tumor metastasis, we performed phospho-proteomics studies to identify RSK2 signaling effectors in metastasis. Among top candidates were several potential targets involved in cell migration and cytoskeletal regulation. We validate and characterize stathmin, a novel RSK2 substrate and cytoskeletal regulatory protein that promotes microtubule destabilization. We demonstrate that RSK2 regulates microtubule stability to provide a morphological advantage for promoting cancer cell invasion and tumor metastasis, which is partly mediated through the phosphorylation and inhibition of stathmin.

The second strategy relies on the principle of synthetic lethality in cancer therapy, in which targeting a synthetic lethal gene to a chemotherapy drug could potentially increase therapeutic efficacy and decrease off-target side effects. We performed a screen for kinases that promote chemosensitization when targeted in combination with cisplatin. Genetic depletion of the top screening candidate, microtubule associated serine/threonine kinase 1 (MAST1), sensitizes various cancer cells to sub-lethal doses of cisplatin. Additional phospho-antibody array and mass spectrometry studies reveal that MAST1 signals through several protein effectors, including MEK1 and PLK1, to promote cell survival and proliferation during cisplatin treatment. Collectively, these studies expand our understanding of protein kinase signaling mechanisms underlying cancer cell metastasis and drug resistance.

Characterization of Protein Kinase Signaling in Cancer Metastasis and Cancer Drug Resistance

By

Gina Alesi

B.S., Biomedical Engineering, University of Michigan, 2010

M.S., Biomedical Engineering, University of Michigan, 2011

Advisor: Sumin Kang, Ph.D.

A dissertation submitted to the Faculty of the
James T. Laney School of Graduate Studies of Emory University
in partial fulfillment of the requirements for the degree of
Doctor of Philosophy
in Graduate Division of Biological and Biomedical Sciences
Cancer Biology
2016

Table of Contents

List of Figures

List of Abbreviations

In order of appearance:

ATP: adenosine triphosphate

ePK: eukaryotic protein kinase

RSV: Rous sarcoma virus

CNA: copy number alterations

MAPK: mitogen-activated protein kinase

DNA: deoxyribonucleic acid

GBM: glioblastoma multiforme

RTK: receptor tyrosine kinases

EGFR: epidermal growth factor receptor

PDGFRA: platelet-derived growth factor receptor α

MET: hepatocyte growth factor receptor

BCR: breakpoint cluster region

CML: chronic myeloid leukemia

PPI: protein-protein interactions

KSR: kinase suppressor of Ras

FDA: U.S. Food and Drug Administration

PI3K: phosphoinositide-3 kinase

TPMT: thiopurine methyltransferase

ABC: ATP-binding cassette

CT: computed tomography

PET: positron emission tomography

MRI: magnetic resonance imaging

RANK-L: nuclear factor kappa-B ligand

FGFR3: fibroblast growth factor receptor 3

RSK2: ribosomal S6 kinase 2

PTK6: protein tyrosine kinase 6

ING3: inhibitor of growth family member 3

MRP2: multidrug resistance-associated protein 2

ATP7A: ATPase copper transporting alpha

ATP7B: ATPase copper transporting beta

ATP11: ATP synthase mitochondrial F1 complex assembly factor 1

ERCC1: excision repair cross-complementation group 1

Bcl-2: B-cell CLL/lymphoma 2

MAST1: microtubule associated serine/threonine kinase 1

AKT: protein kinase B

ILK1: integrin-linked kinase 1

ERK: extracellular signal-regulated kinases

cAMP: cyclic adenosine monophosphate

CREB: cAMP response element-binding protein

MYT1: myelin transcription factor 1

BAD: Bcl-2 associated agonist of cell death

BIM: Bcl-2-like protein 11

FOXM1: forkhead box protein M1

CAMK: Ca^{2+}/calmodulin-dependent protein kinase

PAK1: p21 protein (Cdc42/Rac)-activated kinase 1

shRNA: short hairpin ribonucleic acid

KD: kinase dead

PCR: polymerase chain reaction

FITC: fluorescein isothiocyanate

FBS: fetal bovine serum

DMEM: Dulbecco Modified Eagle Medium

SDS-PAGE: sodium dodecyl sulfate polyacrylamide gel electrophoresis

FACS: fluorescence-activated cell sorting

PBS: phosphate-buffered saline

MOPS: 3-(N-morpholino)propanesulfonic acid

DTT: dithiothreitol

EGTA: ethylene glycol tetraacetic acid

PIPES: piperazine-N,N′-bis(2-ethanesulfonic acid)

HEPES: 4-(2-hydroxyethyl)-1-piperazineethanesulfonic acid

GFP: green fluorescent protein

BLI: bioluminescence imaging

HIPPA: Health Insurance Portability and Accountability Act

IHC: immunohistochemistry

SEM: standard error of the mean

SD: standard deviation

RNAi: RNA interference

HNSCC: head and neck squamous cell carcinoma

CA: constitutively active

WT: wild-type

rSTMN: recombinant stathmin

GST: glutathione S-transferase

PARP: poly [ADP-ribose] polymerase

PP: protein phosphatases

STAT: signal transducer activator of transcription

CDK: cyclin-dependent kinase

ASK1: apoptosis-signaling-regulating kinase 1

MEK1: mitogen-activated protein kinase kinase 1

PLK1: protein-polo-like kinase 1

ROS: reactive oxygen species

mRNA: messenger RNA

RPMI: Roswell Park Memorial Institute medium

NED: no evidence of disease

IPTG: isopropyl- β -D-1-thiogalactopyranoside

DDR: DNA damage response

H2AX: H2A histone family member X

TP53BP1: tumor protein p53 binding protein 1

Hsp27: heat shock protein 27

MT: microtubule

PKA-C: cAMP-dependent protein kinase

HGF: hepatocyte growth factor

$p27^{kip1}$: cyclin-dependent kinase inhibitor 1B

JNK: mitogen-activated protein kinase 8

HER: erb-b2 receptor tyrosine kinase

PTEN: phosphatase and tensin homolog

RAD51: RAD51 recombinase

Wee1: WEE1 G2 checkpoint kinase

CHK2: checkpoint kinase 2

Chapter 1: Introduction

1.1 Kinases

Kinases are critical for maintaining cellular homeostasis. Complex intracellular and extracellular signals are integrated through kinase signaling to coordinate important regulatory processes. Kinases are highly regulated enzymes that function in two key ways to relay these complex signals[1]. The first and most recognized role of kinases is to catalyze the transfer of the gamma-phosphate of ATP to a substrate, while the second role is to serve as a signaling scaffold protein or as an allosteric regulator of other kinases independent of phosphoryl transfer[2]. The reversible phosphorylation of substrates by kinases and phosphatases, which remove these phosphoryl groups, as well as any scaffolding or allosteric interactions between kinases and substrates, dictates the activity, reactivity, and subcellular localization of the associated substrates[3]. Kinases are broadly categorized by their substrate specificity: protein, lipid, and carbohydrate kinases. Other kinases can also act on small molecules such as nucleic acids and vitamins. Compared to kinases with non-protein substrate specificity, protein kinases are overrepresented as drivers of malignancy and implicated in a variety of human maladies, including immune related disorders, cardiovascular disease, diabetes, and cancer[4].

1.2 Mechanistic Basis of Protein Kinase Signaling

The human genome contains 518 protein kinases; comprising 1.7% of the human genome, this collection of protein kinases is commonly referred to as the kinome. The human kinome is categorized by sequence similarity of the catalytic domain. Of these

518 human protein kinases, 478 kinases constitute the typical superfamily and share a homologous eukaryotic protein kinase (ePK) catalytic sequence. The typical kinases are broadly divided into two categories based on substrate specificity – serine/threonine kinases (388 kinases) and tyrosine kinases (90 kinases); further clustering reveals that these kinases can be classified phylogenetically by 9 groups, 134 families, and 196 subfamilies[5, 6]. The remaining 40 kinases in the kinome are atypical kinases, which demonstrate protein kinase activity but lack homology to the ePK catalytic domain sequence. In addition, 48 pseudokinases, predicted to be catalytically inactive due to a lack of one or more of the three conserved ePK motifs, exist in both of the typical and atypical superfamilies[7].

Despite extensive differences in sequence variability and substrate specificity between protein kinases – even among members of the same subfamily – the ePK catalytic domain, which is responsible for mediating substrate phosphorylation, is highly conserved. Comprising 12 subunits, the bi-lobal ePK catalytic domain is a distinctly regulated mediator of typical kinase activity[6]. The N-lobe and C-lobe each contain alpha-helices and beta-sheets, and the interface between them creates a deep cleft in the protein kinase fold to permit binding of the adenine ring of ATP. In this orientation, the gamma-phosphate of ATP is aligned to the outside of the cleft for phosphoryl transfer to a bound substrate. Three key amino acid motifs are critical for kinase catalysis: the VAIK motif (subdomain II), in which the lysine residue interacts with the alpha and beta phosphates of ATP to position ATP in the binding cleft; the HRD motif (subdomain VIb), in which the catalytic aspartic acid residue acts as a base acceptor to permit proton

transfer; and the DFG motif (subdomain VII), in which the aspartic acid residue chelates a Mg^{2+} ion and orients the beta and gamma phosphates of ATP[3, 7].

Also common to all typical protein kinases is the presence of two hydrophobic spines that traverse the N- and C-lobes of the catalytic domain: the R-spine and the C-spine. Both spines were determined using local spatial pattern (LSP) alignment, a method that can identify spatially conserved amino acid residues[8]. The R-spine, or 'regulatory' spine, was discovered by comparing the spatial arrangement of residues between active and inactive typical kinases; only active kinases have a continuous, unbroken alignment of hydrophobic amino acids that results from phosphorylation of the activation loop. In contrast, the C-spine, or 'catalytic' spine, was found by comparing the spatial arrangement of all typical protein kinases. Completed by the binding of adenine from ATP in the catalytic cleft, contiguous alignment of the C-spine engages all necessary machinery for catalysis. The assembly of the R-spine and C-spine result in a kinase conformation that is primed for catalysis and increased interactions with other proteins[9].

1.3 Cancer and the Kinome

Cancer is a genetic disease that is sustained by adaptational changes on an intracellular level and interactions with growth factors, matrix components, and immune cells in the extracellular environment. Weinberg and Hanahan described six key hallmarks of cancer – and recently chronicled two additional emerging hallmarks and two enabling characteristics – to provide an organizing principle for the holistic understanding of the

complexities of this disease[10, 11]. Protein kinases contribute to many of these described characteristics.

In 1911, Peyton Rous determined that cell-free chicken sarcoma extracts induce tumor formation in other chickens; almost 70 years later, researchers studying the oncogenicity of the Rous sarcoma virus (RSV) established the first direct link between protein kinase signaling and cancer. RSV is made up of four genes: gag, pol, env, and src. Between 1978 and 1980, researchers discovered that src – the only non-viral gene of RSV – encodes a kinase with tyrosine phosphorylation activity. This src gene product, now known as the Src protein tyrosine kinase, was found to be responsible for the malignant transformation of cells by RSV[12-14]. Since then, the kinase domain was implicated as the most common protein domain encoded by cancer genes[15]. We now know that aberrant protein kinase signaling results in the pathogenesis and disease progression of cancer through a variety of mechanisms, including increased cell proliferation, survival, and motility.

Three genetic aberrations lead to dysregulated kinase signaling in cancer: somatic mutations, copy number alterations (CNA), and kinase gene fusions from chromosomal rearrangements[16, 17]. Somatic mutations are the most common genetic alteration affecting kinases. Over 1000 cancer-related somatic mutations have been documented in the protein kinase superfamily and many of these mutations are drivers of malignancy[18]**.** For example, B-Raf V600E, caused by the substitution of thymine for adenine at nucleotide 1799, is estimated to be mutated in 50% of malignant melanomas

and nearly all hairy cell leukemias, metanephric kidney adenomas, and papillary craniopharyngiomas[19]. This mutation encodes a constitutively active protein, which drives cell proliferation, survival, and invasion by continuously signaling downstream through the mitogen-activated protein kinase (MAPK) pathway. CNAs, in which somatic changes to chromosome structure result in the deletion or duplication of a DNA sequence, are also prevalent among kinases. The most common malignant adult brain tumor, glioblastoma multiforme (GBM), features CNA of receptor tyrosine kinases (RTKs). Focal amplification of epidermal growth factor receptor (EGFR; 46%), platelet-derived growth factor receptor α (PDGFRA; 16%), and hepatocyte growth factor receptor (MET; 2.6%) was determined in over 400 cases of GBM. In addition to extensive single-receptor focal CNA, many of these analyzed GBMs have co-amplification of two or more RTKs. Although the immediate clinical relevance of this finding is unclear, this may help explain poor clinical trial outcomes of small-molecule inhibitors targeting an individual RTK[20]. Similar to CNAs, chromosomal rearrangements also alter the native chromosome structure; however, instead of affecting gene copy number, these rearrangements often lead to the formation of overactivated chimeric kinases. The most notorious chromosomal rearrangement is the reciprocal translocation between chromosome 9 and chromosome 22, which fuses the Abelson (ABL1) tyrosine kinase to the Breakpoint Cluster Region (BCR) gene. The resulting fusion protein, Bcr-Abl, causes increased proliferative signaling that directly results in the formation of Chronic Myeloid Leukemia (CML).

A few fundamental non-genetic mechanisms also control kinase activity in cancer, including protein-protein interactions (PPIs) and feedback regulation[21, 22]. One example where these mechanisms work in tandem to regulate kinase activity is the Raf/MEK/ERK MAPK pathway. Upon mitogenic stimulation, Ras-GTP recruits and activates the three Raf paralogs (A/B/C-Raf) at the plasma membrane. B- and C-Raf subsequently form homo- and heterodimers in which one monomer, usually B-Raf, allosterically activates the other monomer. PPIs between Raf and scaffold proteins influence the extent and duration of Raf kinase activation to modulate downstream MAPK signaling. For example, Kinase Suppressor of Ras (KSR) pseudokinases dimerize with Raf to regulate Raf:Raf dimer formation and subsequent kinase activity[23]. 14-3-3 proteins also bind to Raf and act as 'molecular handcuffs' to either inhibit or promote Raf kinase activity. Raf signals through MEK1/2 to activate ERK1/2 and stimulate a variety of biological responses. At the same time, active ERK1/2 phosphorylates Raf and MEK1/2 to promote feedback inhibition of MAPK pathway activity[24].

1.4 Targeting Protein Kinases in Cancer

Traditionally, cancer treatment involves a regimen consisting of surgery, radiation, and chemotherapy; surgery removes the primary tumor while radiation and chemotherapy exploit the genetic and signaling abnormalities of cancer cells to eliminate any residual tumor cells. Although this regimen can result in durable clinical responses, systemic chemotherapy also harms rapidly proliferating normal cells. This leads to negative side-effects that can dramatically impact a patient's quality of life short-term or result in the formation of a secondary cancer long-term. Over the past 20 years, the paradigm of

cancer treatment has shifted toward targeted therapy, which is considered to be more effective and less toxic. Instead of interfering with all dividing cells, targeted therapies act on cancer-specific molecular targets, such as kinases, to inhibit cancer cell survival and growth[25].

In 2001, imatinib (Gleevec), a small-molecule drug that inhibits Bcr-Abl in CML, became the first FDA-approved targeted therapy for an oncological indication. Since then, 27 additional small-molecule kinase inhibitors have been approved by the FDA to treat a variety of cancers[26]. Clinical adoption of kinase inhibitors has revolutionized cancer treatment outcomes; for example, the five-year survival rate for patients diagnosed with CML has more than doubled between the early 1990s (31%) and mid 2000s (63%)[27].

Small-molecule kinase inhibitors are classified as either irreversible or reversible. Usually resulting from covalent binding between an inhibitor and a reactive amino acid residue next to the ATP-binding site, irreversible inhibitors permanently block ATP-binding to prevent kinase activation. There are four types of reversible inhibitors that transiently suppress kinase activity: Type 1, which bind to active kinases at the ATP-binding site in the catalytic cleft; Type 2, which bind to inactive kinases at the ATP-binding site; Type 3, which bind to a pocket adjacent to the ATP-binding site to allosterically inhibit kinase activity; and Type 4, which bind to a pocket distant of the ATP-binding site to allosterically inhibit kinase activity. Of the 28 FDA-approved kinase inhibitors, 26 kinases are reversible. Only two inhibitors are irreversible and all but one

inhibit protein kinases; the exception is idelalisib, an inhibitor of the phosphoinositide-3 kinase (PI3K) lipid kinase[26].

Antibody-based therapies also inhibit kinase activity; however, this class of drugs inhibits a distinct family of kinases – RTKs – that bridge extracellular signals and cellular responses. Activation of RTKs by extracellular growth factors results in a marked increase of intracellular protein phosphorylation due to downstream kinase cascade signaling. Biologic kinase inhibitors are monoclonal antibodies that bind extracellularly to RTKs and inhibit receptor activation and any subsequent downstream signaling.

1.5 Clinical Challenges of Cancer Therapy

Despite improvements in cancer therapy and patient survival, there are two major challenges facing cancer research and treatment: drug resistance and tumor metastasis. According to the National Cancer Institute, there were approximately 589,000 human cancer deaths in 2015. Cancer metastases that are resistant to current therapeutic approaches are responsible for over 90% of these deaths.

1.5.1 Cancer Metastasis

The dissemination of tumor cells from a primary site and subsequent recolonization of these cells at a distant site leads to the formation of cancer metastasis. Primary tumors commonly metastasize to the brain, bones, lungs, and liver[28]. In rare cases, cancer metastasis is diagnosed without prior knowledge of a primary tumor. Clinically addressing cancer metastasis has proved difficult for five main reasons:

Detection limitations of metastases: although there is no single test to check for metastasis, it is usually detected using lab tests and advanced imaging modalities. These include computed tomography (CT), positron emission tomography (PET), and magnetic resonance imaging (MRI) scans. However, these imaging modalities are only able to detect larger metastatic lesions. Therefore, many patients are not diagnosed with distant metastasis until it becomes detectable; at that time, the cancer is considered to be incurable.

Inadvertent pro-metastatic effects of primary tumor growth control: therapy aimed at reducing the primary tumor can promote cancer cell metastasis. The most striking example is the tumor bed effect, in which radiation therapy of the primary tumor site induces hypoxic signaling factors that lead to local recurrent tumors with more aggressive phenotypes and increased metastatic propensity. Moreover, current postirradiation treatments with angiogenic inhibitors may also unintentionally promote metastasis by increasing hypoxia[29].

Lack of treatment options: therapeutic treatment of metastases mirrors that of primary tumors, even though gene expression patterns and phenotypic characteristics are often quite different[30]. However, targeted molecular and biological therapies that recognize the specific biology of metastatic cells show promise of controlling metastatic burden. One example is the recent observation that metastatic cancer cells in the bone interact with osteoblasts and osteoclasts to promote metastatic growth[31]. Bisphosphonates and receptor activator of nuclear factor kappa-B ligand (RANK-L) inhibitors suppress

osteoclast formation, which provides a rationale for the use of these therapies for the control and treatment of bone metastases[32]. Despite this example, metastasis-specific treatment options are limited due to a lack of knowledge of metastatic formation and growth.

Poor biological understanding of the metastatic process: the progression from a primary to a metastatic cancer is inadequately characterized. Cancer cells must complete complex cellular signaling changes to overcome barriers that typically prevent metastasis. However, the molecular processes underlying these cellular changes are not well characterized[33]. A better understanding of the key signaling modalities underlying the steps of metastatic dissemination and organotropic colonization is necessary to develop molecular therapies to treat and prevent metastases[34].

Inefficient clinical trials process: the methods in which clinical trials are conducted preclude the collection of necessary information to determine the efficacy of potential anti-metastatic therapies. Due to the high cost associated with increasing the duration of clinical trials, the inclusion of metastasis as an end-point is rarely observed. Therefore, many clinical trials do not directly assess metastatic outcomes of a particular drug and potentially useful clinical data for the development and evaluation of future therapies is lost. To determine metastasis related effects of a drug in clinical trials, primary endpoints need to include the development of a new metastasis. Furthermore, observations made during the clinical treatment of metastatic cancers need to feed back into basic research efforts[35].

1.5.2 Drug Resistance

Clinical drug resistance is classified as either acquired or intrinsic. In conjunction with surgery and radiation, systemic chemotherapy and targeted therapies produce clinical responses in a subset of patients. Unfortunately, many of these patients that initially respond to treatment eventually experience tumor relapse, in which the recurrent tumor or metastasis is resistant to previously used therapeutic agents. This forms the basis of acquired resistance – initially sensitive tumors can develop acquired drug resistance through various adaptive responses during treatment. Another subset of patients never respond to certain therapies because they harbor tumors that are intrinsically resistant. Occurring before a patient receives therapy, intrinsic resistance is caused by preexisting resistance-mediating factors in the bulk of tumor cells that make the therapy ineffective[36]. Five broad categories serve as a framework to describe the mechanisms underlying drug resistance[37]:

Systemic resistance: differing pharmacogenomic profiles across patients influences effective drug dosing. Recent sequencing technologies allow the detection of acquired and inherited genetic variations that cause drug absorption, distribution, metabolism, and elimination differences between patients. These factors alter the effective dose of a systemically administered drug, which may help explain unexpected treatment responses or toxicities[38]. One example is the case of 6-mercaptopurine, an antimetabolite that inhibits DNA synthesis to treat leukemia and lymphoma. Therapeutic efficacy and side effects of 6-mercaptopurine treatment is dictated by the activity of thiopurine methyltransferase (TPMT), an enzyme that inactivates 6-mercaptopurine to regulate

abundance and clearance of the drug. Of the 20+ identified *TPMT* human gene variants, many of these encode TPMT protein with attenuated enzymatic activity; patients with these variants that are administered uncorrected doses experience decreased efficacy and severe toxicity due to increased 6-mercaptopurine accumulation[39]. The FDA now recommends genotyping *TPMT* before 6-mercaptopurine administration to optimize interpatient dosing.

Pre-target resistance: drugs are actively pumped out of cells or inactivated before they can reach their target. ABC transporters in the plasma membrane are involved in mediating drug efflux by promoting the elimination of various hydrophobic drug compounds, thereby limiting the amount of drug that is delivered to an intracellular target. Drug inactivation or lack of activation can also occur to limit the amount of active drug that reaches its target. For example, the therapeutic efficacy and reactivity of platinum drugs is influenced by activation-specific upstream mechanisms of resistance. Cisplatin must be activated by spontaneous aquation reactions upon entry into the cell. Subsequent cytoplasmic inactivations of cisplatin can also occur when exposed to endogenous antioxidants such as glutathione[40].

On-target resistance: mutations or gene amplification of a drug target reduces or inhibits the efficacy of the drug. Many cases of on-target resistance for targeted kinase therapy occur as a result of gatekeeper mutations. Most small-molecule kinase inhibitors exploit a conserved threonine residue within the ATP-binding site for binding specificity. Substitution of the gatekeeper threonine residue with a residue containing bulky side

chains prevents inhibitor binding in the ATP-binding site. For example, the T315I Bcr-Abl gatekeeper residue mutation results in steric hindrance that precludes imatinib binding[41]. Target gene amplification, which occurs through increased target protein expression or stability, also leads to on-target resistance; previously optimized drug doses no longer result in therapeutic responses because more drug is required to inhibit the increased amount of targets.

Post-target resistance: efficacy of drug treatment is diminished by adaptive responses downstream of the drug target. In addition to the classic examples of downstream resistance (e.g. deregulation of apoptosis), other mechanisms are drug-specific. For example, the goal of cisplatin therapy is to induce cancer cell apoptosis through extensive DNA damage. However, cisplatin-mediated DNA damage also induces cell cycle arrest and genomic instability. Cell-cycle arrest allows cancer cells to repair the DNA damage instead of undergoing apoptosis. Likewise, genomic instability leads to adaptive changes that promote cancer cell tolerance to DNA damage.

Off-target resistance: inhibition of a drug target is bypassed by the activation of alternative pathways. For instance, EGFR stimulates activation of several downstream signaling pathways that are critical for cell survival and proliferation, including the MAPK pathway. Treatment with EGFR inhibitors such as erlotinib or cetuximab blocks activation of these downstream pathways, which results in cancer cell death. In response to EGFR inhibition, cancer cells can bypass EGFR and upregulate other RTKs that can activate the downstream effectors of EGFR signaling.

One or more of these mechanisms of resistance can lead to treatment failure. Therefore, a more comprehensive understanding of the biological mechanisms that contribute to drug resistance is imperative for developing better therapies and improving clinical outcomes in cancer patients.

1.6 Identifying Novel Protein Kinase Therapeutic Targets for Cancer Therapy

There are two key strategies for determining kinase targets and rational drug administration for cancer therapy. The first is to determine druggable genetic or non-genetic aberrations in kinase signaling that are necessary for cancer cell survival and metastasis. The second strategy is to exploit potential synergies between kinase signaling and mechanisms of resistance to a current therapy to specifically induce a synthetic lethal therapeutic effect in cancer cells[42]. Both of these strategies are utilized in the Kang lab to identify novel kinase targets for cancer therapy.

In line with the first strategy, the Kang lab previously performed phospho-proteomics studies to identify downstream signaling effectors of the leukemogenic tyrosine kinase fibroblast growth factor receptor 3 (FGFR3). In that study, ribosomal S6 kinase 2 (RSK2) was identified as a critical effector of FGFR3-mediated hematopoietic transformation[43]. Subsequent research established that RSK2 is important for cancer initiation and cancer cell survival, proliferation, and metastasis, in which the role of RSK2 in these functions varies amongst tumor types[44-46]. Following previous research demonstrating that RSK2 promotes head and neck cancer cell invasion and tumor

metastasis, we performed additional phospho-proteomics studies to identify RSK2 signaling effectors in metastasis. Among top candidates were several potential targets involved in cell migration and cytoskeletal regulation. Chapter 2 presents data in which we validate and characterize the novel RSK2 substrate stathmin, a microtubule regulatory protein that promotes microtubule destabilization. We demonstrate that RSK2 regulates microtubule stability to provide a morphological advantage that promotes cancer cell invasion and tumor metastasis, which is partly mediated through phosphorylating and inhibiting stathmin.

The second strategy relies on the principle of synthetic lethality, in which the mutation or inhibition of two genes together leads to cell death, whereas modulation of one gene alone allows viability. Synthetic lethality approaches can also be applied to cancer therapy – targeting a gene that is synthetic lethal to a chemotherapy drug could potentially increase therapeutic efficacy and decrease off-target side effects. The Kang lab recently performed a screen for kinases involved in mediating cisplatin resistance; various cisplatin resistant cancer cells were treated with a sublethal dose of cisplatin in conjunction with systematic individual knockdown of all kinase-related genes. Genetic depletion of the top screening candidate, microtubule associated serine/threonine kinase 1 (MAST1), sensitized various cisplatin resistant cancer cells to sublethal doses of cisplatin. Chapter 3 presents data characterizing the role of MAST1 in cisplatin resistant cancer. We reveal MAST1 signals through several protein effectors, including MEK1 and PLK1, to promote cell survival and proliferation during cisplatin treatment.

Chapter 2: RSK2 signals through stathmin to promote microtubule dynamics and tumor metastasis

2.1 Author's Contribution and Acknowledgement of Reproduction

This chapter is reproduced with minor edits from Alesi, G.N., et al., *RSK2 signals through stathmin to promote microtubule dynamics and tumor metastasis.* Oncogene, 2016[47]. Y.K., Z.G.C., D.M.S. and F.R.K. provided critical reagents. L.J. performed IHC staining and BLI study. K.R.M. performed histopathological study. G.N.A. and D.L. performed all the other experiments. G.N.A., L.J. and S.K. designed the study and wrote the manuscript.

2.2 Abstract

Metastasis is responsible for over 90% of cancer related deaths. Complex signaling in cancer cells orchestrates the progression from a primary to a metastatic cancer. However, the mechanisms of these cellular changes remain elusive. We previously demonstrated that p90 ribosomal S6 kinase 2 (RSK2) promotes tumor metastasis. Here, we investigated the role of RSK2 in the regulation of microtubule dynamics and its potential implication in cancer cell invasion and tumor metastasis. Stable knockdown of RSK2 disrupted microtubule stability and decreased phosphorylation of stathmin, a microtubule destabilizing protein, at serine 16 in metastatic human cancer cells. We found that RSK2 directly binds and phosphorylates stathmin at the leading edge of cancer cells. Phosphorylation of stathmin by RSK2 reduced stathmin- mediated microtubule depolymerization. Moreover, overexpression of phospho-mimetic mutant stathmin S16D significantly rescued the decreased invasive and metastatic potential mediated by RSK2 knockdown *in vitro* and *in vivo*. Furthermore, stathmin phosphorylation positively correlated with RSK2 expression and metastatic cancer progression in primary patient tumor samples. Our finding demonstrates that RSK2 directly phosphorylates stathmin and regulates microtubule polymerization to provide a pro-invasive and pro-metastatic advantage to cancer cells. Therefore, the RSK2-stathmin pathway represents a promising therapeutic target and a prognostic marker for metastatic human cancers.

2.3 Introduction

Metastasis remains difficult to treat and therefore continues to be responsible for about 90% of human cancer deaths[48, 49]. Cancer cell metastasis is a multi-stage process characterized by loss of cellular adhesion, increased motility and invasiveness, entry and survival in the circulation, exit into new tissue, and eventual colonization at a distant site[28, 48, 50]. However, the molecular processes underlying these cellular changes remain elusive. Therefore, defining pro-metastatic signaling pathways is necessary to develop molecular therapies for metastasis and improve clinical outcomes.

Protein kinases are key mediators of extracellular and intracellular signaling and are often implicated in human cancer metastases. For example, AKT and ILK1 play important roles in breast cancer cell invasion and tumor metastasis[51, 52]. We previously found that p90 ribosomal S6 kinase 2 (RSK2) signaling is commonly important in providing anoikis resistance, cell invasion, and pro-metastatic signals in diverse metastatic human cancer cells, including lung, breast, and head and neck cancer[53-55]. RSK2 belongs to the RSK serine/threonine kinase family and is a downstream substrate of ERK. RSKs are involved in various cellular processes including gene expression, cell cycle, and cell survival by phosphorylating multiple signaling effectors, including cAMP response element-binding (CREB)[56], myelin transcription factor 1 (Myt1)[57], BAD, and Bim[58, 59], respectively[60-62].

Metastasis requires cell motility, which is partly driven by dynamic instability of microtubules[63, 64]. Microtubules are protein filaments comprised of heterodimeric α-

/β-tubulin subunits that dynamically switch between self-assembly and disassembly phases. This dynamic instability is largely regulated by stathmin (a.k.a. STMN, oncoprotein 18, OP18, metablastin, and p19)[64]. Stathmin binds to the end of microtubules to sequester free tubulin and promote microtubule depolymerization, resulting in increased microtubule catastrophe and dynamics in cells[65]. Studies in sarcoma, colorectal, hepatoma, nasopharyngeal, breast cancer, and gastric cancer cells report that stathmin expression positively correlates with metastatic potential[66-70]. Several transcription factors downstream of growth signaling pathways, including E2F, c-Jun, FoxM1, and CREB are reported to increase stathmin expression in cancer cells[71-74]. Conversely, studies show that stathmin protein is downregulated in metastatic breast cancer[75]. Stathmin is also regulated at the post-translational level via phosphorylation at N-terminal serines, S16, S25, S38, and S63. Phosphorylation is critical for inhibiting stathmin activity[76-79]. Increased phosphorylation of stathmin promotes dissociation from tubulin, which permits microtubule stabilization and polymerization[79]. Studies suggest a model of increasing stathmin phosphorylation by several pro-mitogenic kinases as the cell-cycle progresses to allow for proper spindle formation and mitosis[80]. Ca^{2+}/calmodulin-dependent protein kinases (CaMKs) are shown to phosphorylate stathmin at S16 in response to Ca^{2+} stimulation. In addition, activation of Rac/Cdc42 proteins induces p21-activated kinase 1 (PAK1)-dependent stathmin phosphorylation[76, 77, 80]. A clinically relevant point mutation in the N-terminal regulatory region of stathmin has been found to greatly enhance its microtubule sequestering ability, thereby causing aggressive invasion in comparison to its overexpressed wild-type counterpart[66, 81, 82].

These findings suggest that stathmin plays an important role in many types of cancers and may therefore be a promising target for cancer therapy[80]. Although stathmin activity is highly regulated via phosphorylation on N-terminal serine residues, the regulation of stathmin phosphorylation in metastatic cancers is not fully understood. Here we report that RSK2 signals through stathmin to regulate cytoskeleton stability and promotes cancer cell invasion and tumor metastasis in human cancers.

2.4 Materials and Methods

Reagents ShRNA constructs for RSK2, sense strand GCCTGAAGATACATTCTATTT for clone #1 and CGCTGAGAATGGACAGCAAAT for clone #2, were purchased from Dharmacon, GE Healthcare Life Sciences (Lafeyette, CO, USA). The RSK2 constructs, pDEST27-RSK2 and pLHCX-mycRSK2 variants, have been previously described[43, 53]. Human RSK2 constitutively active (CA) mutant Y707A or a kinase dead (KD) mutant Y707A/K100A[83], which are resistant to RSK2 shRNA by introducing silent mutations in the shRNA target sequence, were generated using QuikChange-XL site-directed mutagenesis kit (Stratagene, San Diego, CA, USA). The image clone for stathmin1 (GenBank accession number BC082228, clone ID 2822803) was purchased from GE Healthcare Life Sciences. Flag tag was added to stathmin by PCR and subcloned into the pLHCX-Gateway vector. A549 and SKBR3 cells were from American Type Culture Collection (Manassas, VA, USA). 212LN cells were obtained as described previously[54]. A549-Luc-GFP cell line was generated from A549 cells using a bioluminescent and fluorescent imaging vector[84]. Purified recombinant active and inactive RSK2 were obtained from Invitrogen. Purified bovine tubulin, rhodamine-labeled tubulin, and *in vitro* tubulin polymerization assay kit were from Cytoskeleton, Inc (Denver, CO, USA).

Antibodies Antibodies against β-actin (A1978/AC-15), flag (F7425), glutathione-S-transferase (G1160/GST-2), and α-tubulin conjugated with FITC (F2168/DM1A) were from Sigma Aldrich (St. Louis, MO, USA). Anti-phospho-S16 stathmin (3353), phospho-S38 stathmin (4191/D19H10), stathmin (3352), phospho-T286 CAMK II (3361), pan

CAMKII (4436/D11A10), phospho- PAK1/2 S199/S204 (2605) and PAK1 (2602) antibodies were purchased from Cell Signaling Technology Inc (Danvers, MA, USA). Antibodies against tubulin (sc23948/B-5-1-2), RSK2 (sc9986/E-1) and phospho-S16 stathmin (sc12948-R) were from Santa Cruz Biotechnology (Dallas, TX, USA). Anti-phospho-S16 stathmin antibody (ab47328) for immunohistochemistry and western blot, stathmin (ab52906) for immunoprecipitation and western blot, phospho-S25 stathmin (ab62336/EP2124Y), phospho- S63 stathmin (ab76583/EPR1574) antibodies were obtained from Abcam (Cambridge, MA, USA). Anti-RSK2 antibody (NB110-57472/Y82) for immunohistochemistry was from Novus Biologicals (Littleton, CO, USA).

Cell Culture A549 cells were cultured in RPMI 1640 medium with 10% fetal bovine serum (FBS). 212LN cells were cultured in Dulbecco Modified Eagle Medium (DMEM)/Ham's F-12 50/50 mix medium in the presence of 10% FBS. 293T and SKBR3 cells were cultured in DMEM with 10% FBS. Cell lines with stable RSK2 knockdown and overexpression of flag-tagged stathmin variants were obtained by lentiviral and retroviral infection as previously described[85].

Microtubule sedimentation assay The level of polymerized and depolymerized forms of tubulin in cells were measured using a modification of the procedure that was previously described[75]. In brief, equal numbers of cells with or without RSK2 knockdown were lysed in the presence of 1 mg/ml paclitaxel. The cell lysates were centrifuged at 12,000 g for 10 minutes. The tubulin contents in the pellet and supernatant were analyzed

by SDS-PAGE followed by immunoblotting with anti-tubulin antibody. The fraction of tubulin in the polymerized state was calculated by taking the ratio of tubulin in the pellet divided by the sum of the ratios of tubulin in the pellet and its corresponding supernatant.

FACS (fluorescence-activated cell sorting)-based whole cell analysis of tubulin polymerization Polymerized tubulin in cells was quantified as previously described with slight modifications[86]. Briefly, $3x10^5$ cells were fixed for 10 minutes with 1 ml of 0.5% glutaraldehyde in Microtubule Stabilizing Buffer (80 mM PIPES, 1 mM $MgCl_2$, 5 mM EDTA, and 0.5% Triton X-100, pH 6.8). 0.7 ml of 1 mg/ml $BaBH_4$ was added and cells were pelleted by centrifugation at 1000 g for 10 min. The collected cells were incubated with 50 μg/ml RNase A for 12 hours in Antibody Diluting Buffer (PBS, 0.2% Triton X-100, 2% BSA and 0.1% NaN_3) followed by staining with anti-α-tubulin-FITC antibody (1:250) for 3 hours. The samples were diluted in 0.5 ml of PBS containing 50 μg/ml propidium iodide and analyzed by flow cytometry.

In vitro **microtubule polymerization assay** Recombinant stathmin (6.4 μg) and/or RSK2 (1μg) were mixed into 100 μl of tubulin polymerization buffer (80 mM PIPES, 0.5 mM EGTA, 2 mM $MgCl_2$, 1 mM GTP, 3.75% glycerol, pH 6.9) after *in vitro* RSK2 kinase assay with purified tubulin (0.5 mg/ml), and incubated for 1 hour at 37°C. Samples were centrifuged for 20 minutes at 40,000 rpm, 37°C. The amount of microtubules in the pellet and supernatant were analyzed by SDS-PAGE and Coomassie blue staining. Fluorescence studies were performed as previously described[87]. In brief,

2 mg/ml tubulin was polymerized with rhodamine-labeled tubulin in a 4:1 ratio at 37 °C for 60 minutes. Microtubules were spotted on a glass slide with mounting solution. Images were collected on Leica SP8 confocal microscope (Leica Microsystems GmbH, Wetzlar, Germany). For the fluorimetry-based tubulin-polymerization assay, microtubule assembly was measured using a Tubulin Polymerization Assay Kit (Cytoskeleton, Inc.) according to the manufacturer's instructions.

In vitro **RSK2 kinase assay** Protein purification and proteolytic digestion were performed as previously described[43]. Purified recombinant flag-tagged stathmin wild-type, S16A, and S31A were incubated with recombinant active RSK2 in 20 mM MOPS, 1 mM DTT, 5 mM EGTA, 1 mM Na_3VO_4, 25 mM β-glycerol phosphate, 15 mM $MgCl_2$ along with 10 mM MgAc and 0.1 mM ATP for 30 minutes at 30°C. Phosphorylation of stathmin at serine 16 was detected by phospho-Ser16 stathmin specific antibody.

Immunofluorescence staining A549 cells were seeded on coverslips and fixed in PHEMO buffer (68 mM PIPES, 25 mM HEPES, 15 mM EGTA, and 3 mM $MgCl_2$, 3.7% formaldehyde, 0.05% glutaraldehyde, 0.5% Triton X-100). Cells were blocked in 10% goat serum and then stained with anti-tubulin antibody and anti-phospho S16 stathmin antibody followed by Alexa Fluor 633-conjugated anti-mouse IgG antibody and Alexa 488-conjugated anti-rabbit IgG antibody, respectively. The coverslips were washed, mounted, and imaged on a Zeiss LSM 510 META confocal microscope (Carl Zeiss, Oberkochen, Germany).

***In vitro* cell invasion assay** Transwell inserts with 8 μm pores (BD Biosciences) were coated with Matrigel (BD Biosciences, San Jose, CA, USA). Approximately, 4 x 10^4 cells were seeded on Matrigel coated upper chambers with 0.3 ml serum free media and 0.5 ml of medium with 10% FBS was placed in the lower wells. The invaded cells were fixed and stained in 25% methanol and 0.5% crystal violet after 48 hour incubation. Proliferation was determined by using the Celltiter96AQ$_{ueous}$ One solution proliferation kit (Promega, Madison, WI, USA). Invasion was assessed as the number of cells that had invaded through the membrane normalized by the proliferation.

***In vivo* xenograft assay and bioluminescence imaging** Animal experiments were performed according to protocols approved by the Institutional Animal Care and Use Committee of Emory University. Nude mice (athymic nu/nu, female, 4-6 weeks old, Harlan, Indianapolis, IN, USA) were intravenously injected with 2.5 x 10^6 of A549-luc-GFP cells with RSK2 knockdown and expression of stathmin mutants. Metastasis was monitored by BLI analysis as described[84]. In brief, xenograft mice were administered 75 mg/kg of D-luciferin intraperitoneally three minutes before the BLI imaging (Perkin Elmer, 15 mg/mL solution in sterile phosphate-buffered saline). BLI images were acquired by using Xenogen IVIS system coupled to Living Image acquisition and analysis software (Perkin Elmer, Waltham, MA, USA).

Tissue microarray analysis Approval of use of human specimens was given by the Emory University Institutional Review Board. All of the clinical samples were collected with informed consent under Health Insurance Portability and Accountability Act

(HIPAA) approved protocols. Paraffin embedded lung cancer with matched lymph node metastasis tissue array (LC814) was obtained from US Biomax, Inc (Rockville, MD, USA). Immunohistochemistry (IHC) analysis of RSK2 expression and stathmin phosphorylation was performed using tissue array samples as previously described[88]. In brief, human tissue sections were incubated in 3% hydrogen peroxide after deparaffinization and rehydration. Antigen retrieval was achieved by microwaving the sections in 100 mM Tris (pH 10.0) and 10 mM sodium citrate (pH 6.0) for RSK2 and phospho-stathmin S16 staining, respectively. The slides were subsequently blocked with 2.5% horse serum and avidin–biotin complex system (Vector Laboratories, Burlingame, CA). The primary antibodies, anti-RSK2 antibody and anti-phospho-stathmin S16 antibody were applied at a dilution of 1:100. Detection was achieved with 3,3'-diaminobenzidine and counterstained with hematoxylin. IHC staining results were scored as 0 for no staining, 1+ for weak staining, 2+ for moderate staining, and 3+ for strong staining.

Statistics Statistical analysis was performed using GraphPad Prism 6.0. Data shown as images are from one representative experiment of multiple experiments. Data with error bars represent mean ± SEM for Figure 2.7 and mean ± SD for all the other figures. Statistical analysis of significance was based on chi-square test for Figure 2.8D and Student's *t*-test for all the other figures.

Reproducibility of experiments The results of one representative experiment from at least two independent experiments are shown except data shown in Figs 2.7 and 2.8.

Precise numbers of independent repeats are stated in each figure legend. There is no estimate of variation in each group of data and the variance is similar between the groups. No statistical method was used to predetermine sample size. The experiments were not randomized. The investigators were not blinded to allocation during experiments and outcome assessment. All data are expected to have normal distribution.

2.5 Results

RNAi-mediated RSK2 knockdown attenuates microtubule polymerization in metastatic cancer cells. To better understand the role of RSK2 in pro-metastatic signaling, we tested the effect of blocking RSK2 on microtubule dynamics. Targeted downregulation of RSK2 using two different shRNA clones resulted in significant reduction of microtubule polymerization in metastatic lung cancer A549 and head and neck squamous cell carcinoma (HNSCC) 212LN cell lines as measured by microtubule sedimentation assay (Figure 2.1A), immunofluorescence staining (Figure 2.1B), and fluorescence-based quantitative whole cell microtubule analysis (Figure 2.1C). Immunofluorescence imaging revealed that tubulin was evenly distributed as bundles in control A549 cells transduced with an empty vector, whereas it was predominantly depolymerized in cells with stable RSK2 knockdown (Figure 2.1B). Moreover, overexpression of shRNA-resistant human constitutively active (CA; Y707A) RSK2, but not kinase dead (KD; Y707A/K100A) RSK2, rescued the tubulin depolymerization induced by RSK2 knockdown (Figure 2.1D). These data suggest that RSK2 promotes microtubule polymerization in metastatic cancer cells in a kinase-dependent manner.

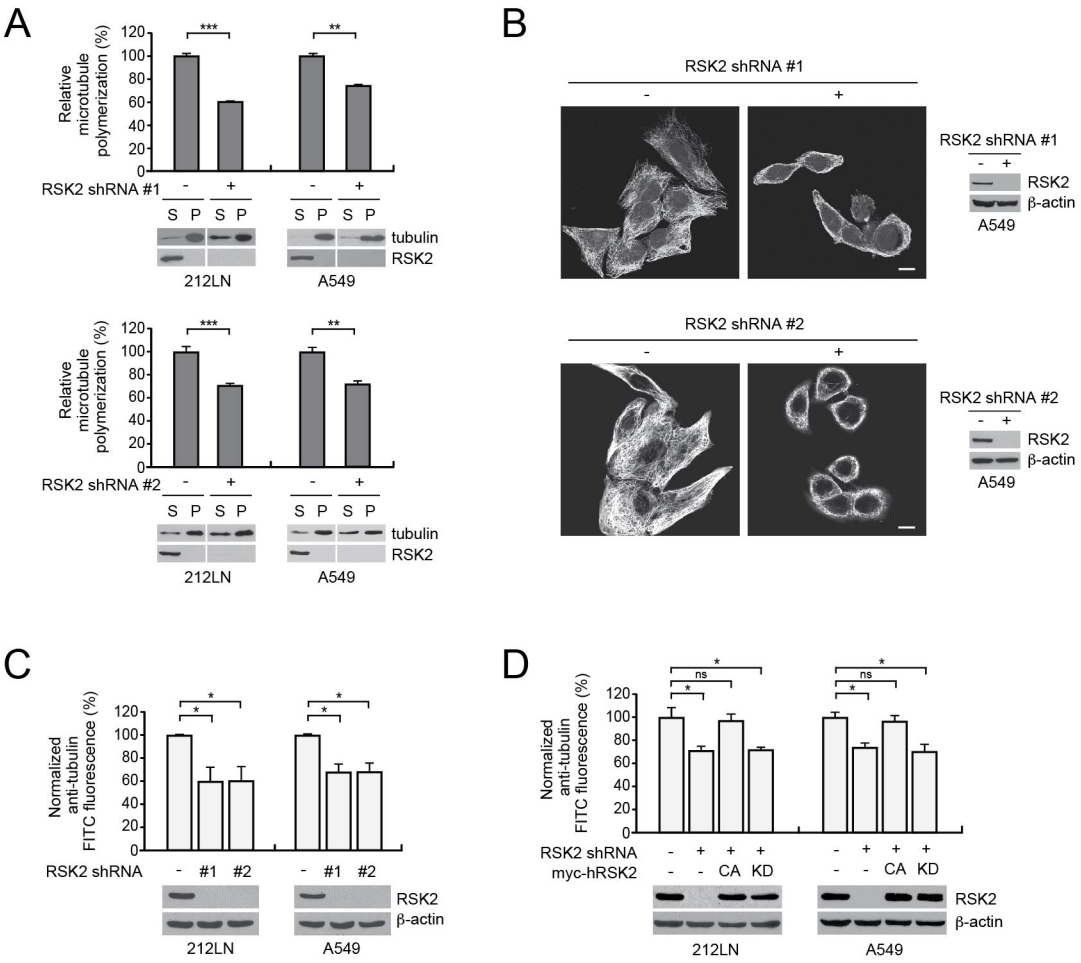

Figure 2.1. Targeted downregulation of RSK2 attenuates microtubule polymerization in metastatic human cancer cells. (A) Microtubule polymerization in 212LN cells (*left*) and A549 cells (*right)*. *Lower:* Tubulin immunoblots show soluble and polymerized tubulin in the supernatant (S) and pellet (P), respectively. *Upper:* Relative tubulin polymerization was determined by density analysis. The amount of polymerized tubulin in cells with RSK2 knockdown was normalized to the tubulin polymerization of control cells. **(B)** Immunofluorescence staining of tubulin in A549 cells with RSK2 knockdown. Scale bar represents 10 μm. Western blot shows RSK2 knockdown. **(C)** FACS-based whole cell analysis of polymerized microtubules in RSK2 knockdown cells. FITC fluorescence intensity was normalized to control cells. **(D)** FACS-based whole cell microtubule analysis using RSK2 knockdown cells with overexpression of shRNA- resistant CA or KD human RSK2. Stable RSK2 knockdown cells were transiently transfected with CA or KD RSK2 cDNA prior to microtubule analysis. Statistical significance was determined using two-tailed Student's *t* test (ns: not significant; *: $0.01<p<0.05$; **: $0.001<p<0.01$; ***: $p<0.001$).

Targeted downregulation of RSK2 attenuates stathmin phosphorylation at serine 16. Dysregulation of microtubule formation and stability in cancer can lead to increased cell motility and metastasis. Microtubule dynamics are mainly modulated by stathmin. Stathmin binds tubulin heterodimers and destabilizes microtubules. Phosphorylation of stathmin at N- terminal serines inhibits stathmin activity and is crucial for promoting microtubule stability. To demonstrate whether RSK2 phosphorylates stathmin to promote microtubule polymerization, we determined the phosphorylation of stathmin at S16, S25, S38, and S63 in diverse metastatic cancer cell lines with RSK2 knockdown. We found that stable knockdown of RSK2 using two different shRNA clones decreased stathmin phosphorylation at S16 in A549, 212LN, and breast cancer SKBR3 cell lines (Figure 2.2A). Conversely, RSK2 knockdown did not alter stathmin phosphorylation at other N-terminal serines: S25, S38, and S63 (Figure 2.2B). Moreover, RSK2 knockdown did not affect the activity of CaMKII and PAK1, known stathmin kinases, in all tested cell lines (Figure 2.2C). CaMKII and PAK1 activity was assessed by auto-phosphorylation at T286 and S199/S204, respectively. In addition, we performed immunofluorescent staining to determine the effect of RSK2 knockdown on stathmin S16 phosphorylation in A549 cells (Figure 2.2D). A significant portion of phosphorylated stathmin localized to the leading edge of control cells as indicated by arrows. RSK2 knockdown ablated the phosphorylation and localization of stathmin at the leading edge. These data suggest that RSK2 contributes to stathmin phosphorylation at S16 at the leading edge of cancer cells independent of CaMKII or PAK1 kinase activity.

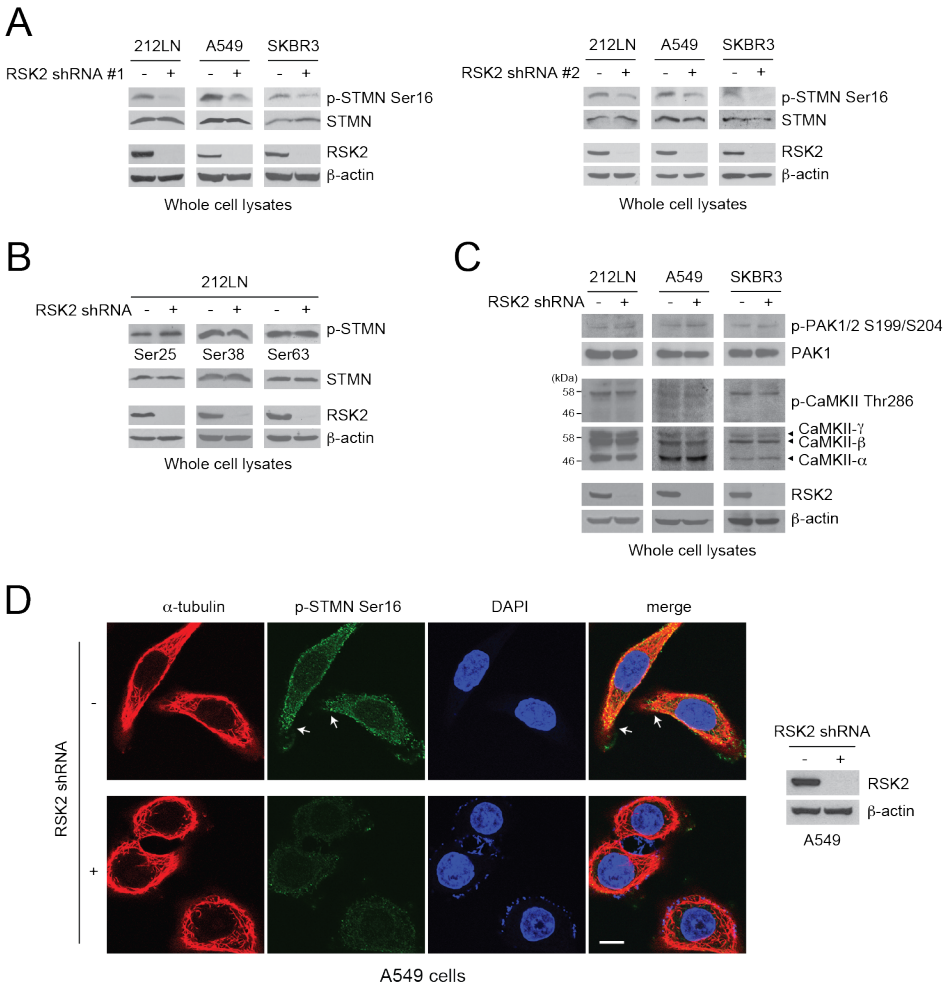

Figure 2.2. RSK2 promotes stathmin phosphorylation in diverse metastatic cancer cells. (A-B) Effect of RSK2 stable knockdown on stathmin (STMN) phosphorylation at N-terminal serine residues, S16 (A), S25, S38, and S68 (B) in metastatic human cancer cells, 212LN, A549, and SKBR3. **(C)** RSK2 knockdown effect on the activity of CaMKII and PAK1, known upstream kinases of stathmin**.** PAK1 and CAMKII activity was assessed by autophosphorylation at S199/S204 and T286, respectively. SKBR3 cells were stimulated with 0.5 M sorbitol for phospho-PAK1 detection. **(D)** Immunofluorescence assay shows the localization of phosphorylated stathmin and tubulin in A549 cells with or without RSK2 knockdown. Scale bar represents 10 μm.

RSK2 phosphorylates stathmin at serine 16. Next, we tested whether RSK2 directly phosphorylates stathmin at S16. Purified recombinant stathmin variants, wild- type (WT) and phospho-deficient mutants S16A and S31A, were incubated with recombinant active RSK2 in an *in vitro* kinase assay. As shown in Figure 2.3A, both WT and S31A stathmin were phosphorylated at S16 by RSK2, whereas S16 phosphorylation was not observed for the stathmin S16A mutant. The structural properties of the recombinant stathmin variants were evaluated by proteolytic digestion (Figure 2.3B). Purified recombinant flag-tagged stathmin WT, S16A, and S31A were incubated with chymotrypsin. The digestion patterns of the mutant proteins and WT were similar, suggesting that the global structure of mutant proteins was not altered and the observed phosphorylation patterns were not caused by a structural change.

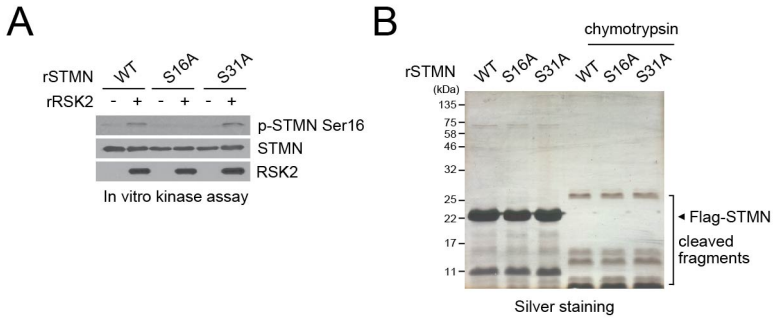

Figure 2.3. RSK2 directly phosphorylates stathmin. (A) RSK2 directly phosphorylates stathmin (STMN) at S16. Purified recombinant stathmin (rSTMN) variants, wild type, S16A, and S31A, were incubated with recombinant active RSK2. Phosphorylation at serine 16 of stathmin was detected by Western blot using specific antibody against phospho-stathmin at S16. **(B)** Partial protease digestion demonstrates that the global structure of stathmin is not changed by point mutations. 0.5 units of chymotrypsin were incubated with recombinant stathmin variants at 30°C for 30 minutes and the digestion patterns were compared.

RSK2 interacts with stathmin. To further investigate the RSK2-dependent phosphorylation of stathmin in cells, we tested whether RSK2 interacts with stathmin. First, we found that stathmin predominantly colocalizes with RSK2 in the cytosol (Figures 2.4A and 2.4B). Binding was confirmed by co- immunoprecipitation using 293T cell lysates expressing flag-tagged stathmin and GST-fused RSK2. Flag-stathmin was detected in the bead-bound GST-RSK2 sample, but not the GST control sample, suggesting that RSK2 interacts with stathmin in cells (Figure 2.4C). Moreover, endogenous RSK2 and stathmin interact in A549 and 212LN cancer cells (Figure 2.4D). These data together suggest that RSK2 binds to stathmin.

Although RSK2 and stathmin colocalize and bind in cancer cells, their interaction is relatively weak. We tested the interaction between endogenous stathmin and RSK2 after modulating the phosphorylation of stathmin with nocodazole[75]. As shown in Figure 2.4E, nocodazole treatment induces the phosphorylation of stathmin and increases binding between phosphorylated stathmin and RSK2. In addition, RSK2 CA binds with higher affinity to GST-stathmin-WT compared to GST-stathmin-S16A (Figure 2.4F). These data suggest that the interaction between RSK2 and stathmin may transiently occur while RSK2 phosphorylates stathmin in cancer cells.

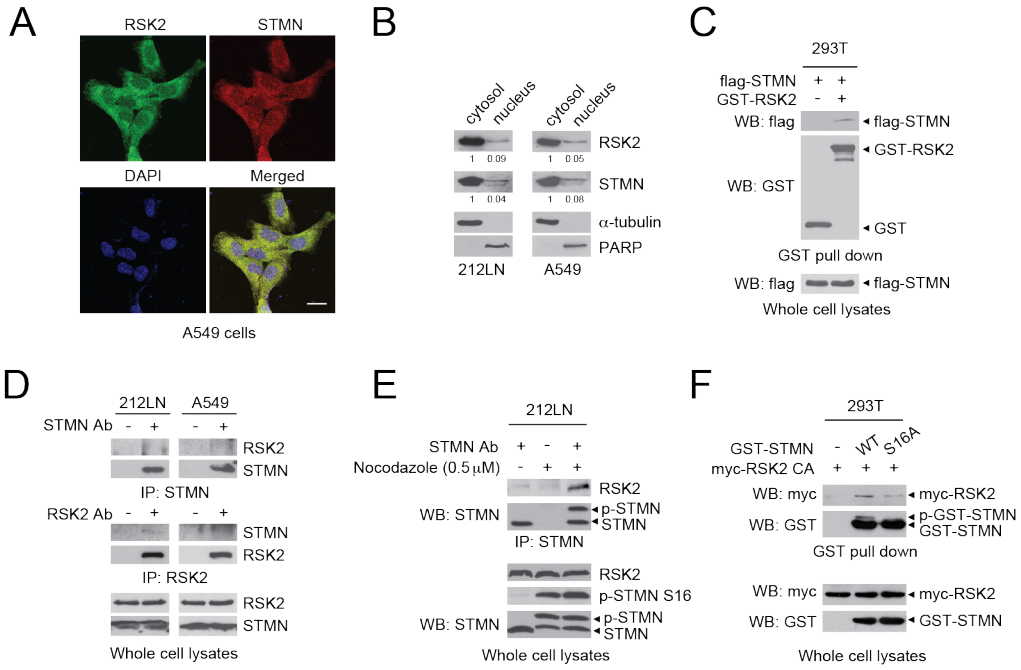

Figure 2.4. RSK2 interacts with stathmin in cells. (A) Immunofluorescence assay of RSK2 and stathmin in A549 cells. Scale bar represents 20 μm. **(B)** Western blots of the cytosolic/nuclear localization of RSK2 and stathmin. α-tubulin and PARP were used as control markers for cytosol and nucleus, respectively. **(C)** GST or GST-fused RSK2 was pulled down from 293T cells transfected with flag-tagged stathmin. Binding between stathmin and bead-bound GST-RSK2 was detected by Western blot. **(D)** Co-immunoprecipitation of endogenous RSK2 and stathmin in 212LN and A549 cells. (E) Immunoprecipitation of stathmin in 212LN cells treated with nocodazole. Binding between stathmin and RSK2 was detected by Western blot. **(F)** myc-RSK2 CA and GST-fused stathmin WT or S16A were co-transfected into 293T cells. GST-stathmin was pulled down from the cell lysates and binding between RSK2 and stathmin was detected by Western blot.

RSK2-dependent phosphorylation of stathmin attenuates microtubule-destabilizing activity of stathmin. To further investigate the role of RSK2-dependent phosphorylation in stathmin activation, we performed a series of coupled *in vitro* kinase assays and microtubule polymerization assays (Figures 2.5A-2.5E). Stathmin was phosphorylated via an *in vitro* RSK2 kinase assay and was subsequently incubated with purified bovine tubulin for polymerization. Polymerized tubulin was assessed using three different assays: microtubule sedimentation (Figures 2.5A-2.5C), immunofluorescence staining (Figure 2.5D), and fluorimetry-based tubulin polymerization (Figure 2.5E). RSK2 alone did not affect tubulin polymerization (Figures 2.5B-2.5E, left samples). Incubation with stathmin markedly reduced tubulin polymer formation, whereas phosphorylation of stathmin by RSK2 significantly attenuated stathmin activity and partially restored tubulin polymerization *in vitro* (Figures 2.5B-2.5E, right samples). Moreover, incubation of stathmin with recombinant inactive RSK2 (KD) *in vitro* (Figure 2.5E) or overexpression of kinase dead RSK2 (KD) in RSK2 knockdown cells (Figure 2.5F) did not alter the tubulin depolymerizing activity of stathmin, suggesting that RSK2-mediated regulation of stathmin is phosphorylation dependent. Furthermore, co-overexpression of CA RSK2 and WT stathmin, but not S16A stathmin, restored the decreased tubulin polymerization in cells with RSK2 knockdown (Figure 2.5F). These data suggest that RSK2 promotes tubulin polymerization by phosphorylating stathmin at serine16 and consequently inhibiting stathmin activity.

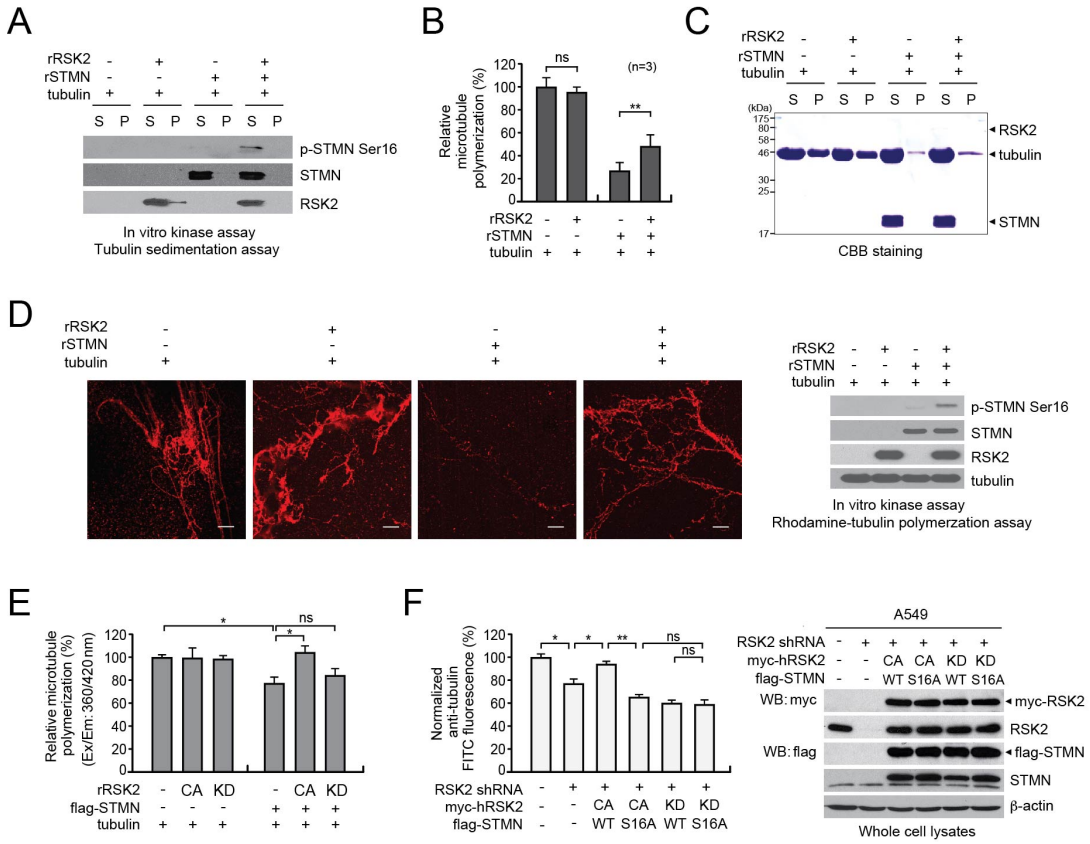

Figure 2.5. RSK2-dependent phosphorylation of stathmin promotes microtubule polymerization. Purified stathmin (STMN) was phosphorylated via an *in vitro* RSK2 kinase assay and incubated with tubulin. **(A)** Stathmin phosphorylation in supernatant and pellet fractions is shown by Western blot analysis. **(B-C)** Polymerized tubulin was analyzed by Coomassie blue staining. S: supernatant, P: pellet. Relative tubulin polymerization in the absence or presence of RSK2 and/or stathmin was quantified by analyzing three independent repeats of microtubule polymerization assays (B). Representative image is shown (C). **(D)** Rhodamine- labeled tubulin was polymerized with stathmin alone or with stathmin pre-incubated with RSK2 and analyzed by fluorescence microscopy. Scale bars represent 30 µm. **(E)** Tubulin polymerization in the presence of recombinant stathmin, active RSK2 (CA), or inactive RSK2 (KD) as indicated. Polymerized tubulin was quantified using fluorimetry-based tubulin polymerization assay kit. **(F)** FACS-based whole cell microtubule analysis of RSK2 knockdown cells overexpressing shRNA-resistant CA or KD RSK2 along with wild-type (WT) or S16A stathmin. Stable RSK2 knockdown cells were transiently transfected with distinct RSK2 and stathmin variants prior to whole cell microtubule analysis. Data represent mean ± SD. Statistical significance was determined using two-tailed Student's *t*-test (ns: not significant; *:0.01<p<0.05; **:0.001<p<0.01).

RSK2 phosphorylates stathmin to promote cancer cell invasion. To demonstrate whether stathmin, as a downstream phosphorylation target of RSK2, contributes to RSK2-dependent pro-invasive and pro-metastatic signals in cancer cells, metastatic cancer cell lines with stable knockdown of RSK2 and forced expression of phospho-mimetic or -deficient mutants of stathmin were generated and examined for invasive and metastatic potential *in vitro* and *in vivo* (Figure 2.6). Silencing RSK2 using two different shRNA clones significantly attenuated the invasive capacity of metastatic A549 and 212LN cells, whereas expression of stathmin phospho-mimetic mutant S16D, but not the phospho-deficient mutant S16A, significantly rescued the decrease in cell invasion due to RSK2 knockdown (Figure 2.6A-2.6B).

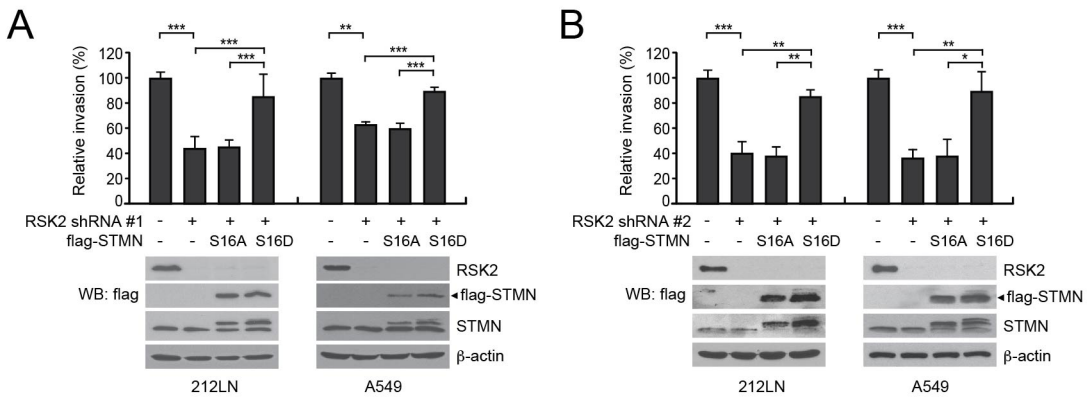

Figure 2.6. RSK2 promotes cancer cell invasion partly through phosphorylation of stathmin. (A-B) Matrigel invasion assay using RSK2 knockdown cells with stathmin (STMN) variants. Stable expression of phospho-mimetic mutant S16D stathmin but not phospho-deficient mutant S16A stathmin restored the cancer cell invasion attenuated by RSK2 knockdown in 212LN and A549 cells. Statistical significance was determined using two-tailed Student's *t*-test (*: $0.01<p<0.05$; **: $0.001<p<0.01$; ***: $p<0.001$).

Phosphorylation of stathmin by RSK2 is required for RSK2-driven tumor metastasis. Next we tested whether phosphorylation of stathmin by RSK2 is required to promote tumor metastasis *in vivo* using a xenograft mouse model. Luciferase-labeled A549 cells with stable RSK2 knockdown and S16A or S16D stathmin overexpression (Figure 2.7A and 2.7D) were injected intravenously into nude mice and subjected to bioluminescent imaging (BLI). The group injected with RSK2 knockdown cells showed significantly attenuated lung metastasis compared to the control group (Figure 2.7B and 2.7E). Overexpression of the stathmin phospho-mimetic mutant S16D, but not the phospho-deficient mutant S16A, significantly rescued the decrease in metastatic potential caused by RSK2 knockdown *in vivo* (Figure 2.7C and 2.7F). Taken together, these analyses show that RSK2 signals through stathmin by phosphorylation at serine 16 to promote tumor metastasis.

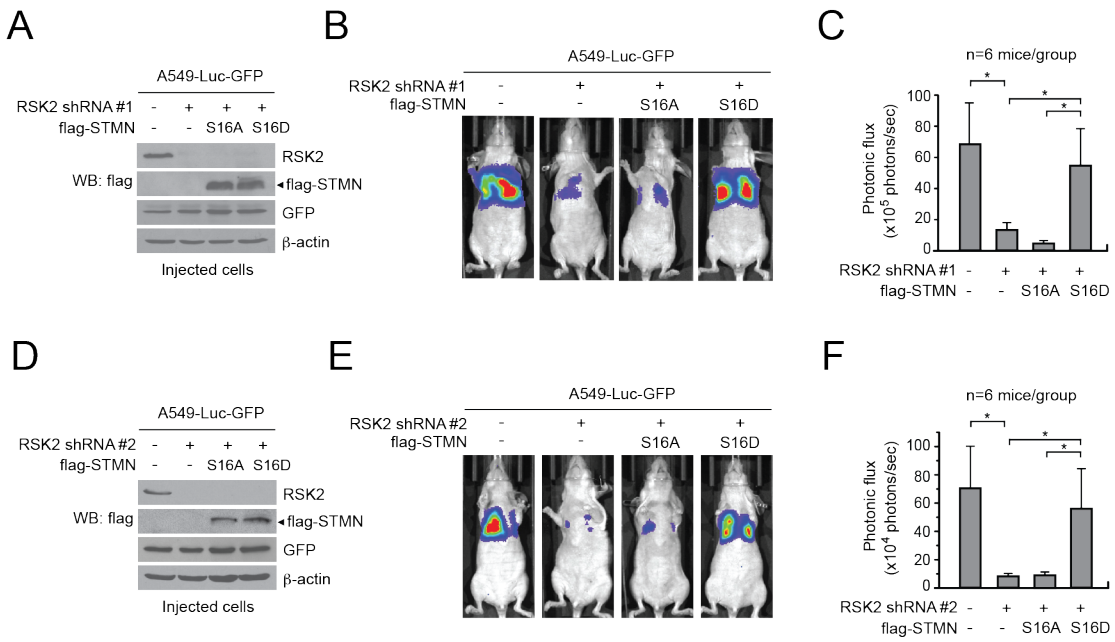

Figure 2.7. RSK2 promotes tumor metastasis, in part, through phosphorylation of stathmin. (A) RSK2, flag-tagged stathmin S16A and S16D expression was detected by immunoblotting in A549-luc-GFP cells (RSK2 shRNA #1) used for tail-vein injection. **(B)** BLI imaging of representative mice injected with A549-luc-GFP cells with RSK2 shRNA #1 knockdown and S16A or S16D stathmin expression at day 52 post injection. **(C)** Average photonic flux of each group at week 6-8 is shown. **(D)** RSK2, flag-tagged stathmin S16A and S16D expression was detected by immunoblotting in A549-luc-GFP cells (RSK2 shRNA #2) used for tail-vein injection. **(E)** BLI imaging of representative mice injected with A549-luc-GFP cells with RSK2 shRNA #2 knockdown and S16A or S16D stathmin expression at day 42 post injection. **(F)** Average photonic flux of each group at week 4-6 is shown. (C, E) Data represent mean ± SEM from six mice for each group. Statistical significance was determined using one- tailed Student's *t* test (*: $0.01<p<0.05$; **: $0.001<p<0.01$; ***: $p<0.001$).

Stathmin phosphorylation and RSK2 expression patterns correlate in primary human tumor tissue samples from lung cancer patients. To further explore the clinical importance of the RSK2-stathmin signaling axis in tumor metastasis, we examined whether stathmin phosphorylation positively correlates with metastatic cancer progression and with RSK2 expression in primary human lung cancer tissue samples. Tissue microarray containing 40 cases of primary lung cancer with matched lymph node metastasis was used for immunohistochemistry (IHC) to detect phospho-S16 stathmin and RSK2 expression (Figure 2.8). As shown in Figure 6A, RSK2 and phospho-stathmin S16 staining intensity in the tumor cells was scored on a scale of 0-3+ (Figure 2.8A). The IHC studies demonstrate that the levels of RSK2 expression and stathmin phosphorylation positively correlate with metastatic progression. Both RSK2 and phospho-stathmin staining levels were significantly higher in tumor tissue samples from metastatic lymph nodes compared to the paired primary tumor specimens (Figure 2.8B). Furthermore, we found a positive correlation between staining scores of RSK2 and phospho-S16 stathmin (Figure 2.8C). These data together support a functional cooperation between RSK2 and stathmin in tumor metastasis of human lung cancer.

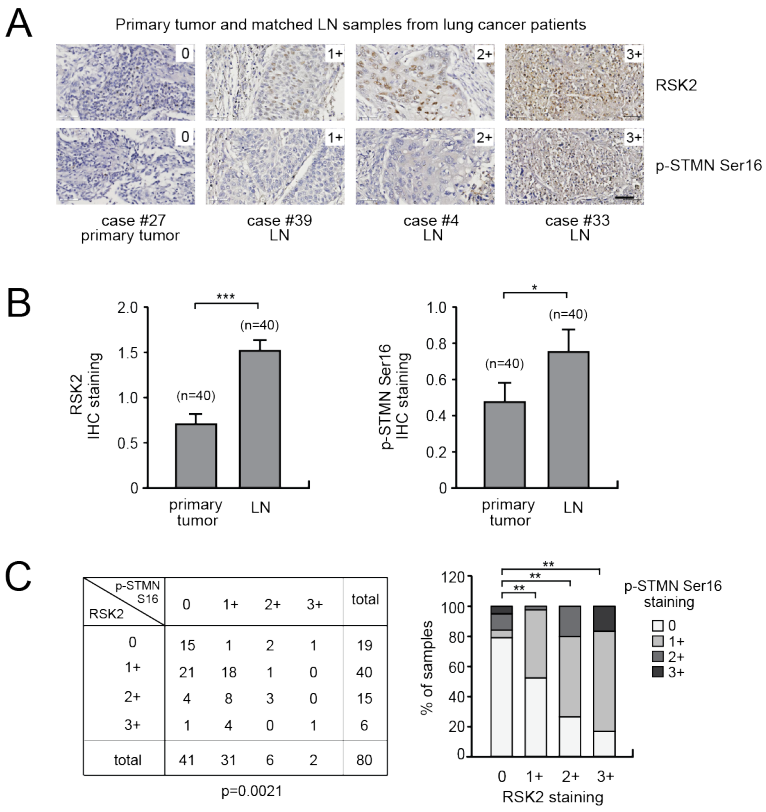

RSK2 \ p-STMN S16	0	1+	2+	3+	total
0	15	1	2	1	19
1+	21	18	1	0	40
2+	4	8	3	0	15
3+	1	4	0	1	6
total	41	31	6	2	80

Figure 2.8. RSK2 and phospho-S16 stathmin correlate with metastatic cancer progression in primary human tumor tissue samples from lung cancer patients. The levels of RSK2 and STMN phosphorylation in 40 cases of human lung cancer with matched lymph node (LN) metastasis were determined by IHC staining using lung cancer tissue microarray. **(A)** Representative tumor specimens with staining intensity of 0 (negative), 1+ (weak), 2+ (moderate), and 3+ (strong) of RSK2 and phospho-stathmin S16 are shown. Scale bar represents 50 μm. **(B)** Levels of RSK2 expression (*left*) and stathmin phosphorylation (*right*) in primary tumors and matched tumors from lymph nodes. The staining intensity was scored as 0-3+. Data represent mean ± SEM from n=40/group. **(C)** The correlation between RSK2 and phospho-stathmin S16 was determined. Bar graph representation is shown on the right. P values were determined by two-tailed paired Student's *t*-test for (B) and chi-square test for (C) (*:0.01<p<0.05; **: 0.001<p<0.01; ***: p<0.001).

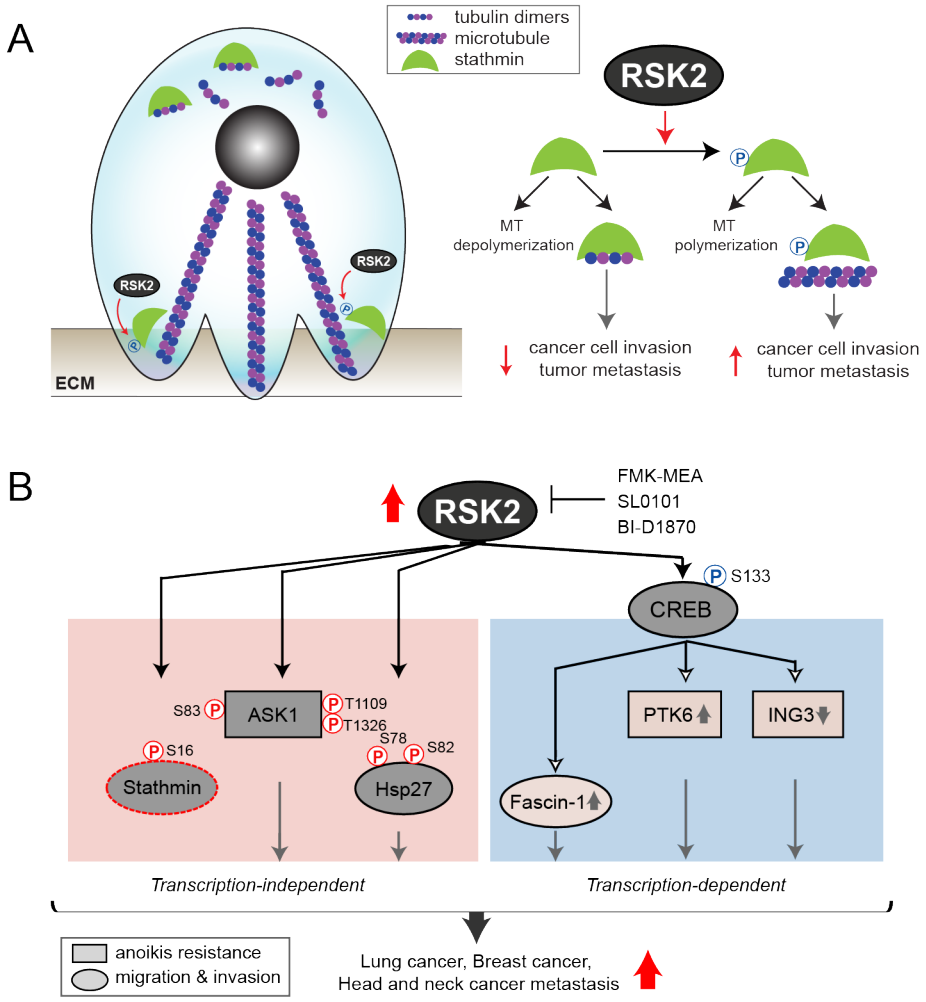

Figure 2.9. Proposed model of RSK2 signaling in cancer metastasis. (A) RSK2 regulates microtubule polymerization to induce morphological changes that promote cancer cell invasion and tumor metastasis, which is mediated in part through phosphorylating stathmin at the leading edge of the cell. **(B)** RSK2 mediates anoikis resistance, cell invasion, and tumor metastasis by phosphorylating a spectrum of downstream factors in cancer cells. Together, these factors form a network to promote RSK2 transcription-dependent (Fascin-1, PTK6, ING3) and –independent (STMN, ASK1, Hsp27) metastatic signaling in human cancers.

2.6 Discussion

Our data support that RSK2 signals through stathmin and inhibits its microtubule-destabilizing activity. We provide evidence that targeting RSK2 reduces the invasive and metastatic potential of cancer cells, while overexpression of the phospho-mimetic mutant S16D but not the phospho-deficient mutant S16A form of stathmin can partially rescue the reduced cancer cell invasion and tumor metastasis due to the attenuation of RSK2 *in vitro* and *in vivo*. Clinically, we observed that the phosphorylation level of stathmin at S16 positively correlates with RSK2 expression and metastatic tumor progression in patient tumor tissues. These findings link RSK2 signaling to microtubule dynamics through stathmin providing a pro-invasive and pro-metastatic advantage to human cancers. Therefore, the RSK2-stathmin pathway may represent a promising prognostic marker and a therapeutic target for the treatment of metastatic human cancers.

Stathmin is a promising anti-cancer target due to its critical role in microtubule dynamics and cell migration. Our study supports that stathmin serves as a signaling effector of RSK2 and contributes to RSK2-mediated microtubule polymerization. We previously reported Hsp27 as an alternative RSK2 phosphorylation target. RSK2 phosphorylates Hsp27 at S78 and S82 to promote actin filament formation and cell invasion[54]. In addition, we reported that the RSK2-CREB pathway promotes filopodia formation by upregulating Fascin-1, a major bundling protein in filopodia[55]. Together, our studies suggest that RSK2 functions as a signal integrator to modulate dynamics of the cytoskeleton including microtubules, microfilaments, and filopodia via a network of phosphorylation targets and transcription targets of RSK2 in both transcription-

independent and -dependent manners. Further research is warranted to explore the coordinated potential between different RSK2 targets, which may ultimately provide RSK2-dependent anti-anoikis, pro-migratory, pro-invasive, and pro-metastatic signaling in human cancers.

RNAi-mediated downregulation of RSK2 partially decreased the polymerized tubulin biomass in cells. Although RSK2 significantly affected cellular tubulin polymerization, RSK2 likely acts in tandem with other critical signaling factors that mediate microtubule dynamics in cancer cells. It is worth considering that the phosphorylation of stathmin by RSK2 partially rescued the microtubule depolymerizing activity of stathmin *in vitro*. This indicates that the phosphorylation of stathmin at S16 could be modulated through not only RSK2 but also other protein kinases including PKA, CaMKII, PAK1, and Aurora[80]. In addition, phosphatases such as PP1, PP2A, or PP2B could be involved in the dephosphorylation of stathmin[89, 90]. Nevertheless, phosphorylation of stathmin at S16 was significantly diminished upon RSK2 knockdown in cancer cells, indicating that RSK2 is the predominant upstream stathmin kinase in the cancer cells we tested. Further comprehensive comparison using additional cell lines and cancer types would be required to determine the contribution of kinases and phosphatases to stathmin activation in distinct cancer cells.

Although serine phosphorylation at the N-terminal residues is the most commonly known mechanism of stathmin modulation, the activity of stathmin is also controlled by protein sequestration. Signal transducer and activator of transcription 3 (STAT3) and the cyclin-

dependent kinase (CDK) inhibitor $p27^{Kip1}$ bind to stathmin and block its ability to sequester free α-/β-tubulin dimers from microtubules. We demonstrated that RSK2 not only phosphorylates stathmin, but also associates with stathmin in cells. In addition, we found that inactive RSK2 does not alter tubulin polymerization and stathmin activity *in vitro* and *in vivo*. Therefore, RSK2 likely interacts with stathmin to modulate cell motility in a phosphorylation-dependent manner.

Lastly, stathmin contributes to several biological processes including control of cell cycle progression, apoptosis, and cell migration. Stathmin is a target of apoptosis-signaling-regulating kinase 1 (ASK1)-p38[91]. We recently reported that RSK2 signals through ASK1 to mediate resistance to anoikis, an apoptotic process induced by loss of cell adhesion[53]. Therefore, stathmin may not only contribute to RSK2-dependent pro-migratory potential but also to anoikis resistance through ASK1 in cancer cells. The comprehensive characterization of RSK2 and its essential downstream signaling effectors will provide critical information to advance our understanding of the signaling mechanisms underlying metastatic progression.

2.7 Acknowledgements

We acknowledge Dr. Anthea Hammond for editorial assistance. We thank the shared resources facilities of the Winship Cancer Institute and the Integrated Cellular Imaging Core of Emory University. We also acknowledge and thank Dr. Shi-Yong Sun for his insightful scientific input in the development of this work. This work was supported in part by NIH grants R01 CA175316 (S.K.), F31 CA183365 (G.N.A), and ACS grant RSG-11-081-01 (S.K.). G.N.A. is an NIH pre-doctoral fellow. F.R.K. and S.K. are Georgia Cancer Coalition Scholars. S. K is a Robbins Scholar and an American Cancer Society Basic Research Scholar.

Chapter 3: Microtubule-associated serine/threonine kinase 1 (MAST1) kinase activity is important for cisplatin resistance in human cancers

3.1 Abstract

Cisplatin is a cornerstone of cancer chemotherapy. However, the efficacy of cisplatin therapy is limited by the pervasiveness of intrinsic and acquired drug resistance. Cisplatin chemoresistance occurs through complex signaling mechanisms that are poorly understood. To identify novel kinases involved in mediating resistance to cisplatin, we utilized RNAi targeting 781 kinase and kinase-related genes and performed a viability-based screen. We identified microtubule-associated serine/threonine kinase 1 (MAST1) is important for cell viability and cell cycle progression in cisplatin resistant cancer cells during cisplatin treatment. We performed phospho-proteomics studies to identify potential downstream signaling effectors of MAST1 signaling in cancer cells and found MAST1 directly phosphorylates mitogen-activated protein kinase kinase 1 (MEK1) at S221, which consequently activates MEK1 to promote cell survival during cisplatin treatment. Furthermore, we show that MAST1 interacts with and phosphorylates polo-like kinase-1 (PLK1), an essential kinase in cell cycle regulation. We show MAST1 knockdown cells experience G2/M cell cycle arrest when treated with a sublethal dose of cisplatin. Importantly, expression of phospho-mimetic mutant PLK1-T210D but not phosphor-deficient mutant PLK1 T210A partially overcomes the requirement for MAST1 in mitotic progression after cisplatin treatment. These data suggest MAST1 confers cisplatin resistance in cancer cells through MEK1 and PLK1. Investigation of the clinical significance of MAST1 in head and neck cancer patient tumors shows MAST1

expression negatively correlates with clinical response to cisplatin treatment in head and neck cancer patients. Taken together, our mechanistic studies support that MAST1 is a novel kinase that mediates cisplatin resistance in part through activation of several downstream substrates including MEK1 and PLK1. Clinically, MAST1 represents a novel therapeutic target for cisplatin chemosensitization, as well as a promising prognostic marker for predicting tumor responsiveness to cisplatin therapy.

3.2 Introduction

Cisplatin is a platinum-based compound that is highly effective for treating solid tumors, including lung, ovarian, head and neck, and testicular cancers [92-94]. Cisplatin binds to purine DNA bases, forms inter- and intra-strand crosslinks, and induces extensive DNA damage that promotes apoptosis [40, 95]. In addition, cisplatin simultaneously tips the cellular redox balance toward a more oxidative environment by binding to reductive scavenger proteins, resulting in reactive oxygen species (ROS) formation that further exacerbates cisplatin-induced DNA damage and/or stimulates apoptosis. Because cisplatin enters cells non-selectively, systemic cisplatin therapy also harms rapidly proliferating normal cells and causes nephrotoxicity, neurotoxicity, and ototoxicity [96]. Nonetheless, cisplatin-based therapy is still widely used in spite of these contraindications, particularly in head and neck cancer, in which 80-90% of patients experience significant initial therapeutic responses [97]. In metastatic testicular cancer, the advent of cisplatin-based therapy increased the cure rate twelve-fold (5% to 60%) [98].

Although some tumors are initially sensitive to cisplatin-based therapy, many patients unfortunately experience tumor relapse and develop chemoresistance [97, 99]. For example, although 70% of ovarian cancer patients initially respond to cisplatin-based therapy, tumor relapse after primary treatment results in a five-year survival rate between 15% and 20% [40]. Many studies have shown that cisplatin-DNA adducts induce DNA distortions that are recognized by several DNA repair pathway proteins. When the extent of DNA damage is beyond repair, as is the case for cisplatin-sensitive tumors at clinically relevant concentrations, these repair proteins signal to promote apoptotic cell death and tumor regression. Conversely, cisplatin-resistant tumors at these same clinical concentrations activate the DNA damage response to promote cell cycle arrest, particularly at the G2/M checkpoint. This allows resistant tumor cells time to partially restore DNA fidelity, prevent abortive mitosis, and consequently sustain proliferation. Despite this knowledge, there are still extensive gaps in the understanding of cisplatin activity, cisplatin-mediated cellular effects, and cisplatin chemoresistance.

Cisplatin resistance is underscored by a complex combination of pre-target, on-target, post-target, and off-target resistance mechanisms (where DNA is the primary target) that encourages cancer cell survival [96]. Over the past few decades, many proteins have been implicated in cisplatin resistance, including ATP7A/7B/11B [100-102], MRP2 [103, 104], ERCC1 [105-107], Bcl-2 family proteins [108, 109], and survivin [110]. Many of these proteins have well established roles in pre-target (ATP7A/7B/11B, MRP2), on-target (ERCC1), and post-target (Bcl-2 proteins, survivin) resistance. However, the contribution of off-target proteins, typically kinases, to cisplatin resistance is not well

known. Since cisplatin resistance is multifactorial (i.e. many molecular mechanisms simultaneously promote a resistant phenotype), a holistic understanding of the molecular mechanisms of cisplatin chemoresistance will be critical for developing novel ways to improve therapeutic outcomes [111, 112].

One proposed strategy to circumvent clinical platinum resistance is combining cisplatin treatment with novel molecular targeted therapies [113], which archetypally inhibit kinases. To better understand the contribution of kinases to off-target cisplatin-resistance and potentially identify a novel cisplatin-sensitizing drug target or predictive biomarker, we performed two consecutive shRNA-based viability screening assays with or without sublethal cisplatin exposure. Microtubule-associated serine/threonine-protein kinase 1 (MAST1, SAST170) emerged as the top screening candidate that is critical for cell viability specifically during cisplatin treatment. MAST1 functions as a scaffold protein to link the dystrophin/utrophin network with microfilaments *via* Syntrophin [114-117]. In addition, recurrent gene rearrangement of MAST1 has been observed in breast cancer cell lines and tissues [118]. However, MAST1 is poorly studied in general, and any major role for MAST1 in cancer chemoresistance has not been reported. Here, we investigate the contribution of MAST1 signaling in response to cisplatin in cancer cells.

3.3 Materials and Methods

Reagents. MAST1 shRNA constructs (sense strand: 5'-CCACTTCCTCTCCAAACACTT-3' for clone #1; 5'-CCACGGTCTACTTCTATGAAT-3' for clone #2; 5'- CGTGATGATGAATCACGTCTA-3' for clone #3) were purchased from Open Biosystems. The MAST1 gene was amplified using mRNA of the KB-3-1 human cancer cell line. The MAST1 construct was myc tagged by PCR and subcloned into pDEST27 and a pLHCX-derived Gateway destination vector as described previously [85]. The PLK1 and MEK1 constructs (graciously provided by Jing Chen) were Flag tagged by PCR and subcloned into pDEST27 and pLHCX (human cell line expression) and pET53 (bacterial recombinant protein purification). PLK1, MEK1 and MAST1 mutant constructs were generated using QuikChange-XL Site-directed Mutagenesis Kit (Stratagene). 15A HNSCC cells were obtained as previously described [54, 119, 120]. KB-3-1 cells were obtained as previously described [121, 122]. A549 lung cancer cells were obtained from American Type Culture Collection. A2780 ovarian cancer cells were obtained from Sigma Aldrich. Cisplatin resistant strains (cisR) of KB-3-1, 15A, A549, and A2780 were generated by serial passage in the presence of increasing cisplatin concentrations (cisR cells courtesy of Dan Li).

Antibodies. MAST1 antibodies for IHC (NBP1-81453) and Western blot (NBP2-17228) were obtained from Novus Biologicals. Antibodies against myc, MEK1 **(**2352/61B12**)**, phospho-MEK1 (S217/S221) (9154/41G9), PLK1 (4513/208G4), and phospho-PLK1 (Thr210) (5472) were obtained from Cell Signaling Technology, Inc. Antibodies against Flag (F7425), glutathione S-transferase (G1160/GST-2), and β-actin (A1978/AC-15)

were obtained from Sigma Aldrich. Anti-pan phospho-serine/threonine antibody is from Abcam.

Cell Culture. A549 and A2780 cells were cultured in RPMI 1640 medium with 10% FBS. $A549^{cisR}$ and $A2780^{cisR}$ cells were cultured in RPMI supplemented with 10% FBS and 0.5μg/mL cisplatin. 15A cells were cultured in Dulbecco Modified Eagle Medium (DMEM)/Ham's F-12 50/50 mix medium with 10% FBS. $15A^{cisR}$ cells were cultured with DMEM/F-12 50/50 with 10% FBS and 0.5μg/mL cisplatin. KB-3-1 and 293T cells were cultured in DMEM with 10% FBS. KB-3-1^{cisR} cells were cultured in DMEM with 10% FBS and 0.5μg/mL cisplatin. Cell lines with stable MAST1 knockdown and overexpression of flag-tagged PLK1 or flag-tagged MEK1 variants were obtained by lentiviral and retroviral infection as previously described [83].

RNAi Screening. To identify protein kinase genes required for cisplatin resistance, we performed two screening assays using the human kinome shRNA library (OpenBiosystems), which contains 4,518 short hairpin RNA constructs and targets 781 human kinases and kinase-related genes. Each gene was individually targeted by approximately five different shRNA constructs. The primary screen was performed by transducing KB-3-1 cisplatin resistant human carcinoma cells (KB-3-1^{cisR}) with lentivirus pools targeting each gene individually. After infection, cells were divided into replica plates; half were treated with a sub-lethal dose of cisplatin and the other half were treated with PBS. Gene candidates that induced cell death (shRNA alone <85% cell viability) and/or had poor shRNA transduction (<25% as assessed by puromycin selection) were

excluded. The secondary screen assayed the 50 top ranking candidate genes from the primary screen in four cancer cell lines (PCI-15A^{cisR}, A549^{cisR}, A2780^{cisR}, KB-3-1^{cisR}). Cell viability was determined using CellTiter-Glo Luminescent Viability Assay (Promega).

Cell Proliferation and Viability Assays. 1x10^5 cells were seeded in a six-well plate. At the indicated time points, the cells were collected and counted using a hemocytometer with trypan blue exclusion. For experiments involving cisplatin treatment, cells were treated with cisplatin and counted as previously mentioned. To determine IC50 values, 5000 cells were seeded in triplicate in a 96 well plate and treated with indicated cisplatin concentrations for 48 hours. Viability was measured using CellTiter-Glo (Promega). IC50 values were calculated using GraphPad Prism.

Colony Formation Assays. KB-3-1cisR (500 cells), A549cisR (200 cells), and A2780cisR (300 cells) cells stably infected with pLKO.1 or MAST1 shRNA were seeded in 35-mm dishes and treated with PBS or cisplatin until the experimental endpoint two weeks later. Colonies were fixed, stained with 0.5% crystal violet, and counted using ImageJ. Relative colony numbers were determined by normalizing the data to the pLKO.1 and PBS condition.

Xenograft Studies. Animal experiments were performed according to protocols approved by the Institutional Animal Care and Use Committee of Emory University. Nude mice (athymic nu/nu, female, 4–6 weeks old; Harlan) were subcutaneously injected

with $5x10^5$ KB-3-1^{cisR} cells harboring MAST1 vector variants in 30% Matrigel. One week after injection, 5mg/kg cisplatin was intraperitoneally injected every 2-3 days for 20 days. Tumor growth was recorded by measurement of two perpendicular diameters of the tumors and tumor size was calculated using the formula $\frac{4\pi}{3} x \left(\frac{width}{2}\right)^2 x \left(\frac{length}{2}\right)$. The tumors were harvested and weighed at the experimental endpoint. Tumor proliferation was determined by Ki-67 IHC staining.

Immunohistochemical Staining. Archived, formalin-fixed, paraffin-embedded tumor specimens from HNSCC patients were provided in collaboration with Drs. Nabil Saba and Kelly Magliocca. Approval for use and care of these specimens was given from the Institutional Review Board of Emory University School of Medicine. Clinical information for the patients was obtained from the pathology files at Emory University Hospital under the guidelines and with approval from the Institutional Review Board of Emory University School of Medicine and according to the Health Insurance Portability and Accountability Act. Two groups of patient tumor samples were used: patients with no evidence of disease (NED) over two years after cisplatin therapy, and patients with tumor recurrence within two years of cisplatin therapy. After deparaffinization and rehydration, human tissue sections were incubated in 3% hydrogen peroxide to suppress endogenous peroxidase activity. Antigen retrieval was achieved by microwaving the sections in 10mM Tris-Cl (pH 9). Sections were then blocked by incubation in 2.5% horse serum. The rabbit anti-MAST1 antibody was applied to the slides at a dilution of 1:50 and incubated at 4°C overnight. Detection was achieved with the Avidin-Biotin Complex System (Vector Laboratories). Slides were stained with 3,3′-diaminobenzidine, washed,

counterstained with hematoxylin, dehydrated, treated with xylene, and mounted. Immunohistochemical staining results were reviewed and scored as follows: 0, no staining and no background; 1+, weak staining; 2+, moderate staining; and 3+, strong staining [54].

Cell Cycle Analysis. Cells were harvested and fixed in ice-cold 70% ethanol overnight. Cells were washed with PBS and subsequently stained with propidium iodide. Cell cycle distribution was analyzed using flow cytometry as previously described [123].

Phospho-protein Profiling by Phospho-antibody Array. The experiment was performed by Full Moon BioSystems Inc as previously described with modifications [54]. Lysates obtained from KB-3-1^{cisR}-pLKO.1 and KB-3-1^{cisR}-pLKO.1-MAST1 shRNA cells treated with PBS or cisplatin were applied to the Phospho Explorer Antibody Array (Full Moon Biosystems Inc). The array contains 1318 antibodies from over 30 signaling pathways, each of which has two replicates that are printed on standard-size coated glass microscope slides. In brief, cell lysates were labeled with biotin in 10 μg/μL N,N-dimethyformamide; at the same time, the array slides were blocked with Blocking Solution and washed extensively with Milli-Q grade water. The biotin-labeled proteins were diluted in Coupling Solution and applied to the array for conjugation. After 1-2 hours incubation, the array slides were washed extensively with 1X Wash Solution and Milli-Q grade water. The array slides were then incubated with Cy3-conjugated streptavidin diluted in Detection Buffer for 20 minutes, washed extensively with 1X Wash Solution and Milli-Q grade water, and dried with compressed nitrogen. The

conjugated labeled proteins were detected using the Full Moon Biosystems Antibody Array Scanning Service. To identify leading candidates, we computed the following phosphorylation ratio for each antibody:

$$\frac{KB-3-1^{cisR}-MAST1\ shRNA\ (+cisplatin)}{KB-3-1^{cisR}-pLKO.1\ (-cisplatin)}$$

Purification of Recombinant PLK1 Proteins. Flag-PLK1 WT and K82M proteins were purified by sonication of Escherichia coli BL21(DE3)/pLysS cells (Invitrogen) obtained from 250 ml of culture with 0.5 mM isopropyl-β-D-1-thiogalactopyranoside (IPTG) induction at 25°C. Cell lysates were loaded onto a Ni-NTA column (Qiagen) in equilibration buffer (20 mM imidazole, 20 mM Tris (pH7.5), 150 mM NaCl) and eluted with elution buffer (250 mM imidazole, 20 mM Tris (pH7.5), 150 mM NaCl). Proteins were desalted on a PD-10 column (GE Healthcare Life Sciences). Purification efficiency was examined by Coomassie Brilliant Blue staining and immunoblotting.

In vitro **Kinase Assays.** 293T cells were transfected with GST-MAST1 WT or KD for 24 hours. GST-MAST1 variants were precipitated from cell lysates with a glutathione-Sepharose 4B column. Purified recombinant flag-tagged PLK1 WT and K82M or MEK1 K79A were incubated with bead-bound GST-MAST1 in kinase assay buffer (25mM Tris-HCl (pH 7.5), 10 mM $MgCl_2$, 0.5 mM Na_3VO_4, 1mM DTT, 0.01% Triton X-100) for 30 min at 30 °C. Phosphorylation of PLK1 at Thr210 was detected by phospho-Thr210 PLK1-specific antibody. Phosphorylation of MEK1 at Ser221 was detected by phospho-Ser221 MEK1 specific antibody.

Statistics Statistical analysis was performed using GraphPad Prism 6.0. Data shown as images are from one representative experiment of multiple experiments. Data with error bars represent mean ± SEM for Figure 3.6A and 3.6B and mean ± SD for all the other figures. Statistical analysis of significance was based on chi-square test for Figure 3.6B and Student's *t*-test for all the other figures.

3.4 Results

Cisplatin resistant generated cells are over seven-fold more resistant than corresponding parental cells. We generated four cisplatin resistant (cisR) cancer cell lines to use as a screening platform by culturing parental cell lines (KB-3-1 squamous cell carcinoma cells, A549 lung cancer cells, A2780 ovarian cancer cells, PCI-15A head and neck cancer (HNSCC) cells) with sub-lethal concentrations of cisplatin. We assayed cisplatin IC50 and found that cisR cells are over seven times more resistant to cisplatin than the paired parental cell lines (Figure 3.1A-3.1D). These cisR cells likely rely on critical intracellular signaling mechanisms to promote cell survival and proliferation during cisplatin treatment and thus provide a platform for interrogating important mediators of cisplatin resistance.

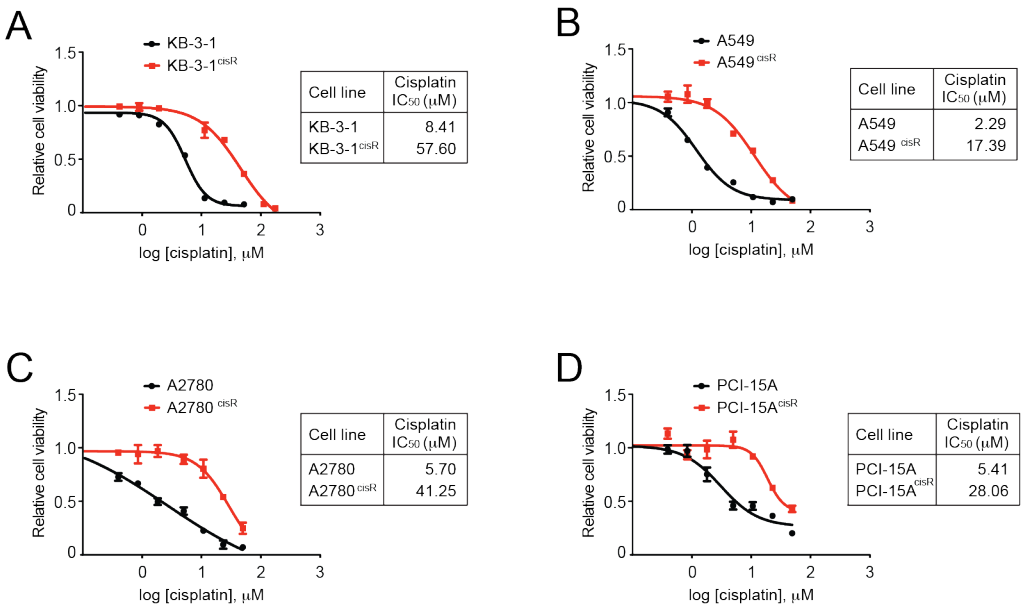

Figure 3.1. Generated cisR cells are over seven-fold more cisplatin resistant than corresponding parental cell lines. (A-D) Parental KB-3-1 and cisplatin resistant KB-3-1^{cisR}(A), parental A549 and cisplatin resistant A549^{cisR}(B), parental A2780 and cisplatin resistant A2780^{cisR}(C), and parental PCI-15A and cisplatin resistant PCI-15A^{cisR}(D) cells were treated with the indicated cisplatin concentrations for 48 hours and assayed for relative cell viability using the CellTiter-Glo assay. IC50 values of all cell lines were calculated using GraphPad Prism.

Two RNAi screening assays identified MAST1 as a novel synthetic lethal kinase in cisplatin resistance. To identify novel kinases that contribute to cisplatin resistance, we performed two sequential cell viability-based screening assays. In the first screening assay, we transduced KB-3-1^{cisR} cells with shRNA individually targeting 781 kinase and kinase-like genes and treated replica plates with or without sub-lethal doses of cisplatin. We identified 50 top candidates that induce cancer cell death in combination with cisplatin treatment (Figure 3.2A *(left)*; data courtesy of Lingtao Jin). Many leading candidates are reported to function in cell proliferation and survival (e.g. MEK2, MEK5, SPHK1) and cell cycle progression (e.g. CDK7, CDC7). Interestingly, little is known about the function of other leading candidates (e.g. MAST1, VCPIP1) (Figure 3.2A *(right)*; data courtesy of Lingtao Jin). We subsequently screened the top 50 candidates from the primary screen in four different cisR cell lines (KB-3-1^{cisR}, PCI-15A^{cisR}, A2780^{cisR}, A549^{cisR}) to determine kinase genes that are fundamental mediators of cisplatin resistance across different cancer types (Figure 3.2B *(left)*; data courtesy of Dan Li). Based on our results, we identified microtubule-associated serine/threonine kinase 1 (MAST1) as the top candidate from the secondary screen and subsequently focused on elucidating its role in cisplatin resistance (Figure 3.2B *(right)*; data courtesy of Dan Li).

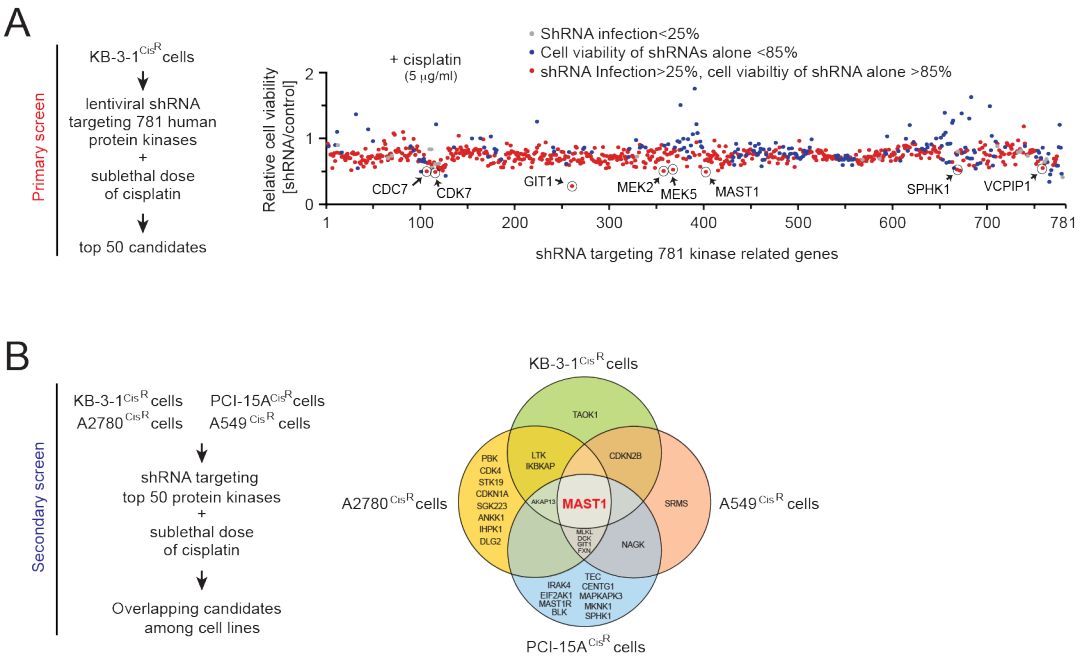

Figure 3.2. Two RNAi screening assays identified MAST1 as a novel synthetic lethal kinase in cisplatin resistance. (A) Primary screen. KB-3-1^{cisR} cells were transduced with shRNA lentivirus targeting 781 individual kinase and kinase-related genes and subsequently treated with a sub-lethal dose (5 μg/ml) of cisplatin. Cell viability was determined after 48 hours using the CellTiter-Glo assay. Gene candidates with low infection efficiency (<25%; grey) and shRNA-induced cell death (>15%; blue) were excluded. **(B)** Secondary screen. The top 50 candidates from the primary screen were assayed in four cisplatin resistant cancer cell lines. 30 leads showing more than 10% cell death upon shRNA and cisplatin treatment are shown.

MAST1 family kinases share significant sequence homology. As shown in Figure 3.3, MAST1 belongs to the MAST protein kinase family (MAST1-4). MAST family proteins are characterized by four domains: 1) domain of unknown function 1908 (DUF1908), which has no characterized function; 2) serine/threonine kinase domain (S_TKc), which mediates kinase catalytic activity; 3) AGC-kinase C-terminal domain (STKX), which distinguishes AGC kinases from other ePKs [124]; and 4) PDZ, which mediates PPIs as a specialized scaffolding domain. The active site of all four isoforms is represented as a red diamond and corresponds to the aspartate of the HRD motif, which acts as a base to deprotonate the substrate serine/threonine side chain [125, 126], at MAST1 residue 497 (Figure 3.3). Beyond these shared domains, the MAST family also shares >60% sequence homology N-terminal of the S_TKc domain and <40% sequence homology C-terminal of the PDZ domain[114]. MAST1 kinase activity and substrate specificity is likely to be regulated differentially by the four distinct MAST1 domains (Figure 3.3).

Although MAST1 is the leading candidate from our screening assays (Figure 3.1; data courtesy of Dan Li), MAST2 (rank: 169/781) and MAST 4 (rank: 332/781) are among the top ~20% and ~40% of candidates from the primary screen, respectively (data not shown). MAST3 was not included in the primary screen. Therefore, MAST family kinases may share enough sequence homology to commonly promote cisplatin resistance; however, divergent sequences between MAST family members likely support a specialized role for MAST1 in cisplatin resistance.

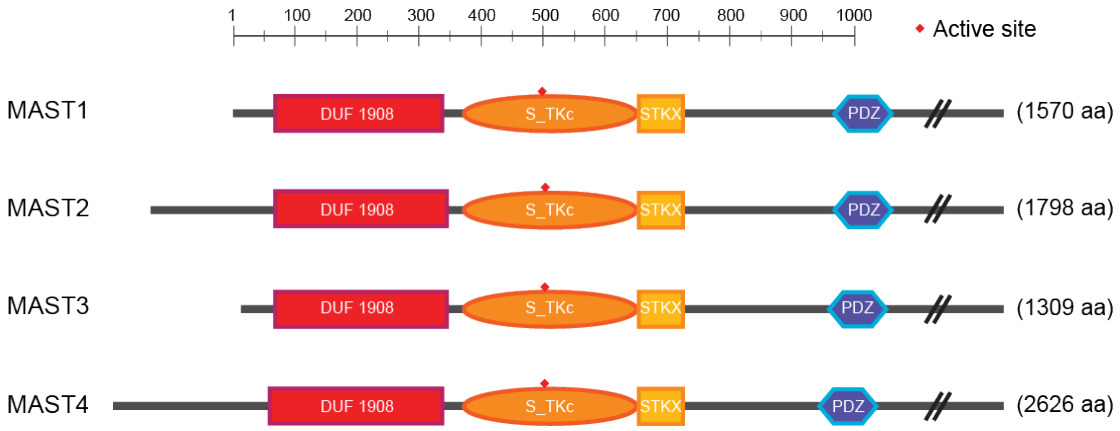

Figure 3.3. MAST1 family kinases share significant sequence homology. Schematic diagram of MAST1-4 isoforms domain schematic. The MAST1 kinase active site (proton acceptor) is the aspartate 497 residue.

MAST1 promotes cell proliferation in diverse cisplatin resistant cancer cells during cisplatin treatment. Most patients' tumors initially respond to cisplatin therapy; however, through selective pressure that favors the survival of intrinsically resistant cells or mutations that promote acquired resistance, residual tumor cells induce tumor formation and disease relapse despite ongoing cisplatin therapy. To validate the role of MAST1 in cisplatin resistance, we tested the effect of targeting MAST1 in combination with cisplatin on *in vitro* cancer cell proliferation and *in vivo* tumor growth. To confirm our screening result, we utilized three different shRNA clones to deplete MAST1 expression in cisR cells and checked cell proliferation with or without cisplatin treatment (Figure 3.4A; data courtesy of Dan Li). As we observed in the primary and secondary screens, concurrent MAST1 knockdown and cisplatin treatment dramatically reduces cell proliferation. Furthermore, MAST1 knockdown without cisplatin treatment does not affect cell proliferation. We also checked whether MAST1 sustains cell proliferation in $A549^{cisR}$ and $A2780^{cisR}$ cells under cisplatin treatment (Figure 3.4B; data courtesy of Dan Li). Indeed, stable knockdown of MAST1 does not impact cell proliferation in KB-3-1^{cisR} cells; however, MAST1 knockdown cells treated with cisplatin proliferate significantly slower than control cells with empty vector. This suggests MAST1 is important for cisplatin resistant cancer cell proliferation during cisplatin treatment.

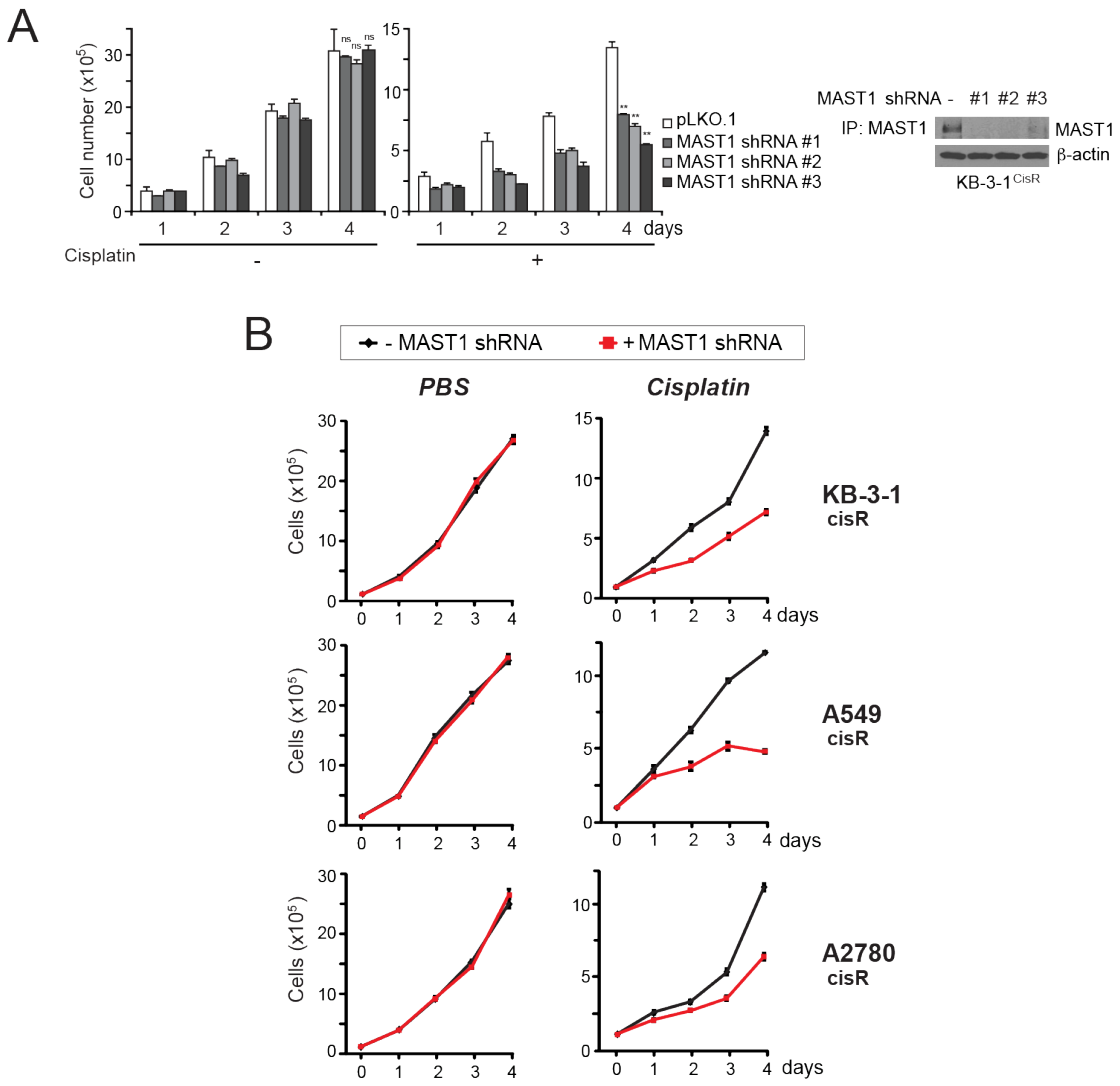

Figure 3.4. MAST1 promotes cell proliferation in diverse cisplatin resistant cancer cells during cisplatin treatment. (A) KB-3-1^{cisR} cells were infected with three different MAST1 shRNA clones followed by 5 μg/ml cisplatin or vehicle treatment. Proliferation was measured by trypan blue exclusion cell counting. **(B)** KB-3-1^{cisR} *(top)*, A549^{cisR} *(middle)*, and A2780^{cisR} *(bottom)* cells were infected with MAST1 shRNA. KB-3-1^{cisR} and A2780^{cisR} were treated with PBS or 2 μg/mL cisplatin. A549^{cisR} cells were treated with PBS or 0.75 μg/mL cisplatin. At the indicated time points, cells were collected and counted by trypan blue exclusion.

Targeting MAST1 attenuates *in vitro* colony formation during cisplatin treatment. We next tested whether MAST1 is important for mediating tumor formation *in vitro* using a colony formation assay. KB-3-1^{cisR}, A549^{cisR}, and A2780^{cisR} cells with or without stable MAST1 knockdown were treated with PBS or cisplatin for two weeks. As shown in Figure 3.5A-3.5B (data courtesy of Dan Li), cisR cells with concurrent MAST1 knockdown and cisplatin treatment (sample 4) form ~70% (KB-3-1^{cisR}), ~30% (A549^{cisR}), or ~50% (A2780^{cisR}) fewer colonies compared to cisplatin treated cells expressing MAST1 (sample 3). In addition, MAST1 knockdown does not impact colony formation without cisplatin treatment (sample 2). Thus, this suggests MAST1 is dispensible for cancer cell colony formation in the absence of cisplatin; however, MAST1 expression in cancer cells is critical for *in vitro* colony formation during cisplatin treatment.

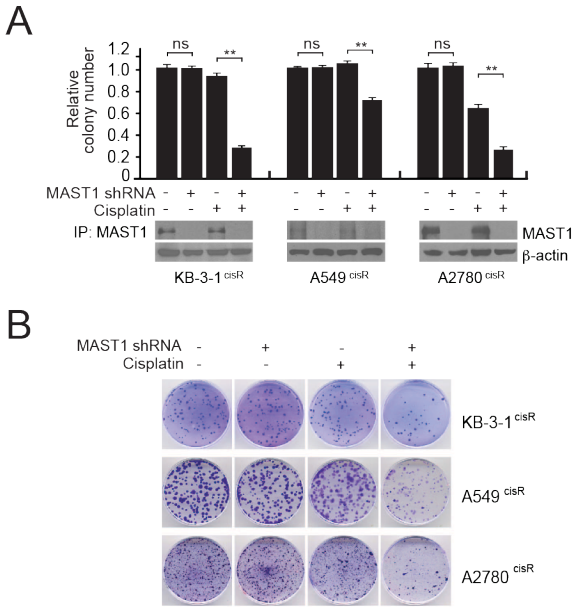

Figure 3.5. Targeting MAST1 attenuates *in vitro* colony formation during cisplatin treatment. (A) KB-3-1cisR (500 cells/dish), A549cisR (200 cells/dish), and A2780cisR (300 cells/dish) cells were seeded in 35-mm dishes. KB-3-1^{cisR} and A2780^{cisR} were treated with PBS or 2 μg/mL cisplatin. A549^{cisR} cells were treated with PBS or 0.75 μg/mL cisplatin. Colonies were fixed and stained with crystal violet. Relative colony numbers were determined using ImageJ. **(B)** Representative images of colony formation assay results are shown.

MAST1 promotes *in vivo* tumor growth during cisplatin treatment. We performed a xenograft experiment to interrogate whether MAST1 influences *in vivo* tumor formation and growth of cisplatin resistant cancer cells. KB-3-1^{cisR} cells with or without stable MAST1 knockdown were injected subcutaneously into nude mice. As shown in Figure 3.6A (data courtesy of Dan Li), mice injected with MAST1 knockdown cells and treated with cisplatin have a significantly slower tumor growth rate compared with MAST1 expressing cells treated with cisplatin. Moreover, harvested tumors from mice injected with MAST1 knockdown cells and treated with cisplatin are significantly smaller than tumors harvested from mice treated with cisplatin alone (Figure 3.6B and 3.6C *(bottom)*; data courtesy of Dan Li). To measure *in vivo* cell proliferation of the different tumors, we performed IHC and stained harvested tumors for Ki-67, a marker of cell proliferation. In agreement with our previous observations, harvested tumors comprised of cisplatin-treated MAST1 knockdown cells have the lowest cell proliferation as indicated by the absence of Ki-67 staining (Figure 3.6C *(top)*; data courtesy of Dan Li). Finally, stable MAST1 knockdown was observed in the corresponding harvested tumor samples (Figure 3.6C *(middle)*; data courtesy of Dan Li), which confirms expected MAST1 protein expression in each tumor group. Taken together, this data suggests that MAST1 is important for *in vivo* cisplatin resistant tumor formation and proliferation specifically during cisplatin treatment.

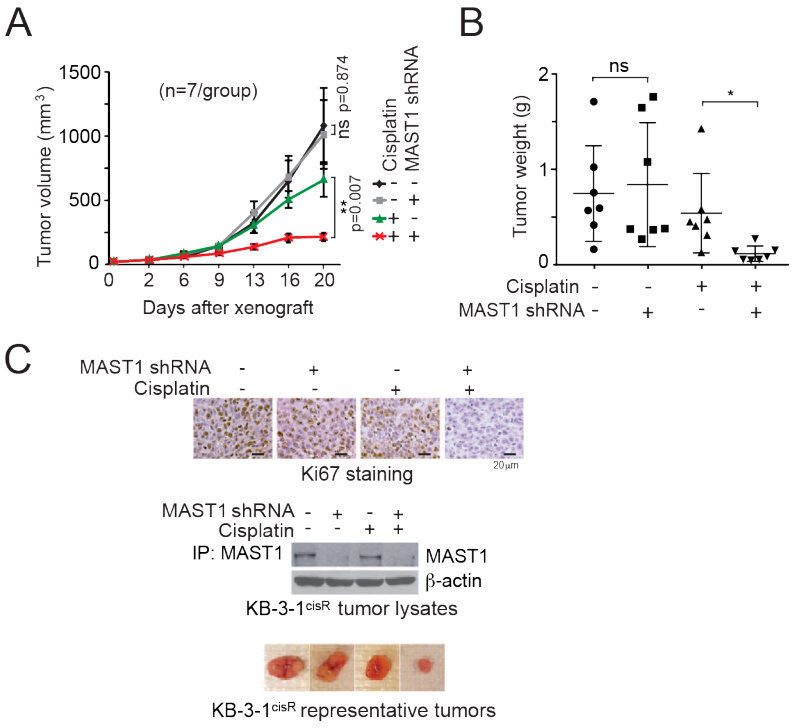

Figure 3.6. MAST1 promotes *in vivo* tumor growth during cisplatin treatment. Xenograft mice experiment using KB-3-1^{cisR} cells. **(A)** Tumor volume was measured and cisplatin treated mice were injected with 5mg/kg cisplatin every 2-3 days until the experimental endpoint. **(B)** Tumor weight of the harvested tumors. **(C)** Ki-67 IHC staining *(top)*, MAST1 expression immunoblot *(middle)*, and representative images *(bottom)* of the harvested tumors from each group are shown.

MAST1 functions independent of the DNA damage response to promote cisplatin resistant cancer cell cycle progression and survival during cisplatin treatment. Cisplatin induces G2/M cell cycle arrest, which allows cells to repair DNA damage before cell division. Cancer cells must strike a fine balance between repairing enough DNA damage to prevent cell death and progressing through cell cycle checkpoints in order to proliferate. Therefore, we performed DNA damage, cell cycle, and apoptosis assays to understand how MAST1 promotes cancer cell proliferation during cisplatin treatment.

First, we determined whether MAST1 influences cisplatin-mediated DNA damage or the DNA damage response (DDR) in cisplatin-resistant cancer cells with or without MAST1 knockdown during cisplatin treatment (data not shown; data courtesy of Lingtao Jin). We found MAST1 influences neither the amount of cisplatin-mediated DNA damage (assessed by relative quantification of DNA-cisplatin adducts) nor the DDR (assessed by p-H2AX and p-TP53BP1 staining). Therefore, MAST1 functions independent of cisplatin activity and cisplatin-mediated DDRs.

Second, we investigated the role of MAST1 in cisplatin-mediated G2/M cell cycle arrest using A2780^{cisR} (A), KB-3-1^{cisR} (B), and A549^{cisR} (C) cells with or without MAST1 knockdown (Figure 3.7). As expected, cisplatin treatment induced G2/M arrest as measured by propidium iodide staining (sample 3). Moreover, concurrent MAST1 knockdown and cisplatin treatment significantly increased G2/M arrest (sample 4). These data indicate that MAST1 promotes cell cycle progression

Finally, we tested whether MAST1 affects cisplatin-mediated cell survival by Annexin V staining and FACS analysis (data not shown; data courtesy of Dan Li). Upon cisplatin treatment, approximately two-fold more KB-3-1^{cisR} cells with MAST1 knockdown undergo apoptosis compared to MAST1 expressing cells.

These data suggest MAST1 promotes cancer cell proliferation by coordinating increased cell cycle progression and cell viability upon cisplatin treatment. Furthermore, MAST1 does not influence cisplatin drug activity or DNA damage responses in cancer cells.

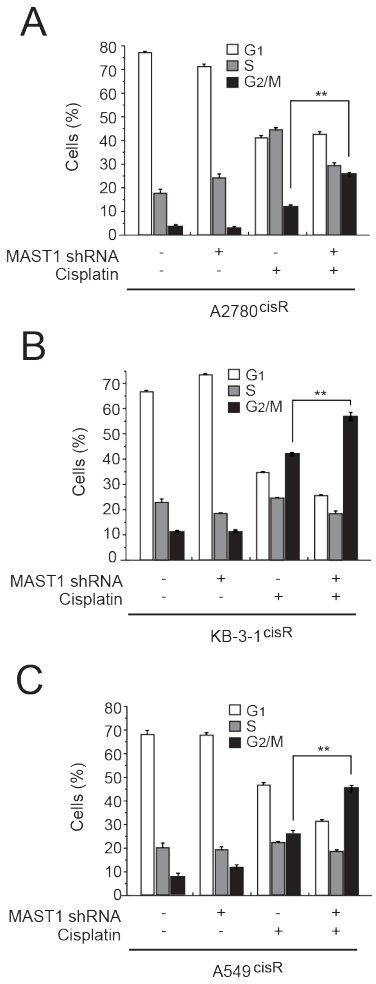

Figure 3.7. MAST1 promotes cancer cell cycle progression during cisplatin treatment. (A) A2780^{cisR}, **(B)** KB-3-1^{cisR}, and **(C)** A549^{cisR} cells with or without MAST1 knockdown were treated with PBS or 5 μg/ml of cisplatin. Cell cycle distribution was assayed 48 hours after cisplatin treatment using propidium iodide and FACS analysis.

MAST1 kinase activity mediates cisplatin resistance. We next tested whether MAST1 kinase activity is required for MAST1-mediated cisplatin resistance. To permit experimental study of MAST1 kinase function, we generated and characterized a MAST1 kinase dead (KD) mutant by introducing a point mutation at the active site depicted in Figure 3.3 and performing a MAST1 *in vitro kinase* assay. As shown in Figure 3.8A (data courtesy of Dan Li), the D497A mutation abolishes MAST1 auto-phosphorylation and kinase activity determined using myelin basic protein (MBP) as a substrate. This data validates the use of MAST1 D497A as a kinase dead mutant to investigate the contribution of MAST1 kinase activity to cisplatin resistance in cancer cells.

We overexpressed MAST1 WT or KD in parental KB-3-1 and A549 cells treated with cisplatin and checked cell viability. Expression of MAST1 WT, but not KD, significantly increases viability (Figure 3.8B; data courtesy of Dan Li). As demonstrated previously, KB-3-1^{cisR} *(left)* and A549^{cisR} *(right)* MAST1 knockdown cells treated with cisplatin have significantly less cell viability compared to MAST1 expressing cells (sample 2). Moreover, expression of shRNA-resistant MAST1 WT fully rescues cell viability (sample 3); conversely, MAST1 KD expression does not influence cell viability (sample 4). These data provide evidence that the kinase activity of MAST1 is required for cell proliferation and acquisition of cisplatin resistance during cisplatin treatment in cancer cells.

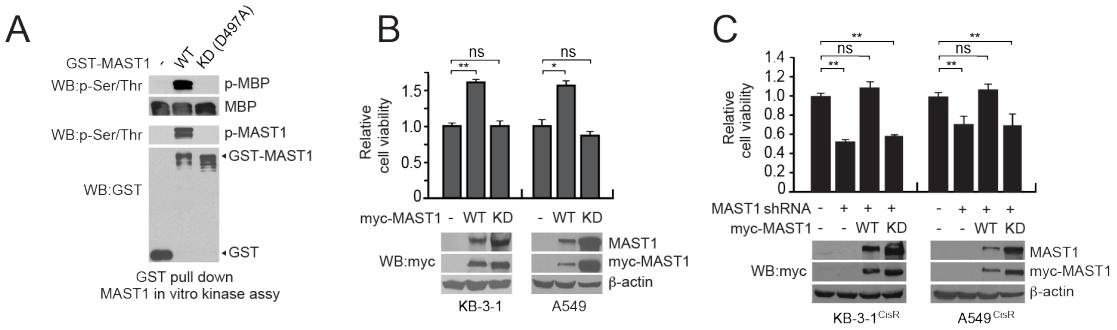

Figure 3.8. MAST1 kinase activity mediates cisplatin resistance. (A) GST-fused MAST1 constructs were transfected and pulled down from 293T cells. *In vitro* kinase assay was performed by incubating bead bound GST-MAST1 WT or KD and MBP substrate. Phosphorylation of MBP was detected by immunoblotting using anti-pan-phospho-serine/threonine antibody. **(B)** Relative cell viability was assayed by trypan blue exclusion cell counting in myc-MAST1 WT- or KD-expressing cisplatin sensitive KB-3-1 and A549 cells treated with 0.15 μg/mL and 0.25 μg/mL cisplatin, respectively. Protein expression was detected by immunoblotting. **(C)** shRNA-resistant MAST1 WT or KD was expressed in KB-3-1^{cisR} and A549^{cisR} cells with stable endogenous MAST1 knockdown. Cells were treated with 2 μg/mL (KB-3-1^{cisR}) or 0.75 μg/mL (A549^{cisR}) cisplatin and relative cell viability was assessed 48 hours post-treatment by trypan blue exclusion cell counting.

MAST1 promotes cell survival by phosphorylating MEK1 at serine 221. Our data provides evidence that MAST1 kinase activity is required for mediating cisplatin resistance. To understand MAST1 signaling in cisplatin chemoresistance, we performed a phospho-antibody array using KB-3-1^{cisR} cell lysates to determine potential substrates of MAST1 kinase activity (Figure 3.9A; data courtesy of Dan Li). Cisplatin treatment decreased phosphorylation of mitogen-activated protein kinase 1 (MEK1) at serine 221 by approximately 50% in MAST1 knockdown cells compared to MAST1 expressing cells. Thus, we investigated the functional connection between MAST1 and MEK1 using immunoblotting, *in vitro* kinase assays, and immunoprecipitation assays.

First, we tested exogenous binding between GST-fused MAST1 WT or KD mutants and endogenous MEK1 in 293T cells (Figure 3.9B; data courtesy of Dan Li). Both MAST1 proteins can bind MEK1, which suggests binding is not dependent on kinase domain activity. We also tested endogenous binding in A2780 cells and found that MAST1 and MEK1 bind endogenously (data courtesy of Lingtao Jin; data not shown). Next, we examined whether MAST1 mediates MEK1 phosphorylation in cisR cancer cells during cisplatin treatment and found that MEK1 S221 phosphorylation is significantly attenuated in cisR MAST1 knockdown cells treated with cisplatin (Figure 3.9C; data courtesy of Lingtao Jin and Dan Li). Moreover, MAST1 directly phosphorylates MEK1 at S221 *in vitro* (Figure 3.9D; data courtesy of Dan Li).

MEK1 is generally known to stimulate cell survival. To understand whether MAST1 phosphorylation of MEK1 at S221 functionally promotes cell survival during cisplatin

treatment, we expressed flag-tagged MEK1 S221A or S221D in KB-3-1 and KB-3-1^{cisR} cells with stable MAST1 knockdown. Cells were treated with or without cisplatin and apoptosis was assessed 48 hours post-treatment by Annexin V staining and FACS analysis. As previously demonstrated, approximately two-fold more MAST1 knockdown cells undergo apoptosis compared to MAST1 expressing cells upon cisplatin treatment. Furthermore, expression of phospho-mimetic MEK1 S221D, but not phospho-deficient MEK1 S221A, in MAST1 knockdown cells rescues apoptosis to the level observed in MAST1 expressing cells (data not shown; data courtesy of Lingtao Jin).

Thus, these data demonstrate that MAST1 binds and phosphorylates MEK1 to promote cell survival during cisplatin treatment in cancer cells (Figure 3.16 *(left)*).

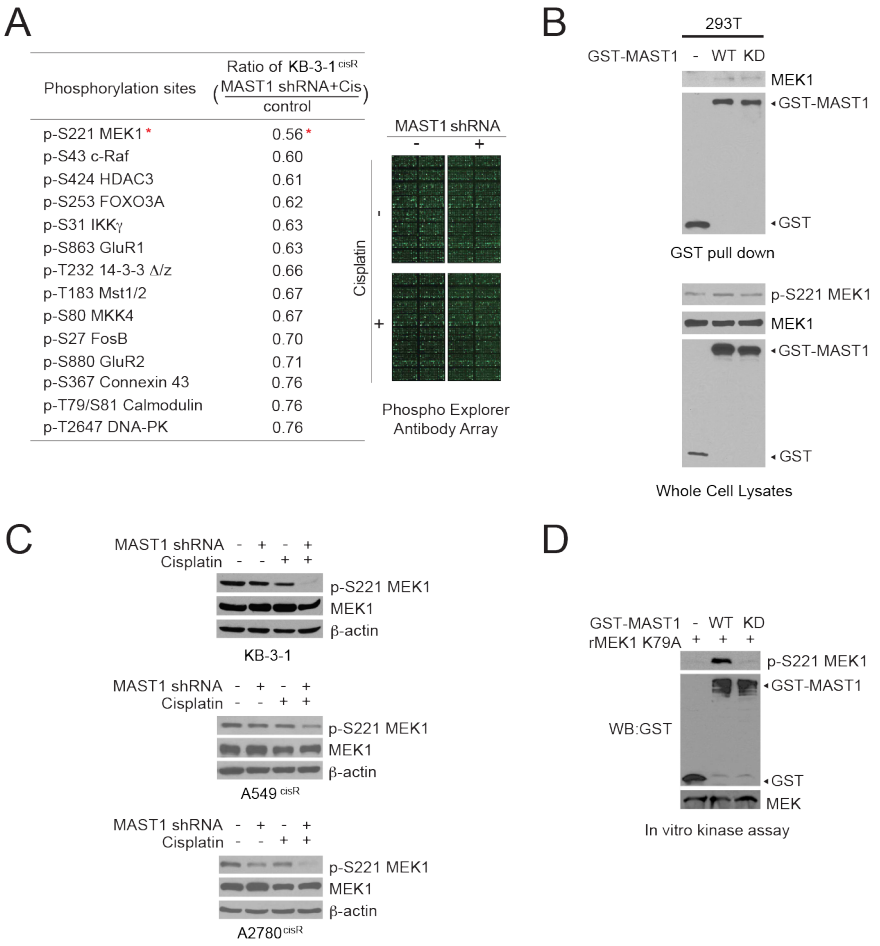

Figure 3.9. MAST1 phosphorylates MEK1 at serine 221. (A) KB-3-1^{cisR} cells with or without stable MAST1 knockdown were treated with cisplatin or PBS for 48 hours. The Phospho Explorer Antibody Array was performed with the various KB-3-1^{cisR} cell lysates to determine potential downstream MAST1 protein substrates. Potential MAST1 substrates were ranked by the phosphorylation site ratio, in which the phosphorylation amount of a specific protein in KB-3-1^{cisR}-MAST1shRNA+cisplatin was divided by the phosphorylation amount of the same protein in KB-3-1^{cisR}–pLKO.1-cisplatin (control) cells. Array images are shown on the right. **(B)** GST-MAST1 WT or KD was transfected in 293T cells. Binding between GST-MAST1 and endogenous MEK1 was assessed using a GST pull down assay from the collected 293T lysates and immunoblotting. **(C)** KB-3-1 *(top)*, A549^{cisR} (*middle)*, and A2780^{cisR} *(bottom)* cells with or without MAST1 knockdown and cisplatin treatment were assayed for p-S221 MEK1and MEK1 protein expression by immunoblotting. **(D)** GST-fused MAST1 constructs were transfected and pulled down from 293T cells. *In vitro* kinase assay was performed by incubating bead bound GST-MAST1 WT or KD with recombinant inactive MEK1 as a substrate. Phosphorylation of S221 MEK1 was detected by immunoblotting.

PLK1 is a novel MAST1 binding partner. We expressed GST-MAST1 in 293T cells and performed mass spectrometry analysis to determine binding partners that may mediate MAST1 signaling in cisplatin resistance (Figure 3.10A; data courtesy of Dan Li). Among known tubulin protein binding partners, we identified a key cell cycle regulatory protein – polo- like kinase 1 (PLK1) – as a potential binding partner.

Intracellular DNA damage activates checkpoint mechanisms to allow time for DNA repair before mitosis. Cells subsequently can mount three different responses based on the severity of DNA damage and the fidelity of DNA repair mechanisms: checkpoint recovery, checkpoint adaptation, or apoptosis. Cells with good repair fidelity and limited DNA damage undergo checkpoint recovery, in which cells successfully repair all DNA damage and re-enter the cell cycle. Cells with poor repair fidelity and low to moderate levels of damage can also re-enter the cell cycle without fully repairing DNA damage in a process called checkpoint adaptation, which promotes tumorigenesis and genomic instability. Finally, cells overwhelmed by the severity of DNA damage undergo cell death. PLK1 activity is critical for regulating all of these responses to DNA-damaging therapies [127].

As shown in Figure 3.10B, PLK1 is characterized by two functional domains: 1) a serine/threonine kinase domain (S_TKc), which mediates kinase catalytic activity; and 2) two Polo-box domains, which regulates PLK1 subcellular localization[128] and substrate binding in phosphorylation-dependent and -independent manners[129].

A

Group	Gene	Total Peptides	Description	Mass (kDa)
1.1	MAST1	81	microtubule-associated serine/threonine-protein kinase 1 [Homo sapiens]	171
7.2	HSPA9	18	stress-70 protein, mitochondrial precursor [Homo sapiens]	74
10.1	GSTM2	21	glutathione S-transferase Mu 2 isoform 1 [Homo sapiens]	26
10.2	GSTM3	20	glutathione S-transferase Mu 3 [Homo sapiens]	27
36.1	TUBA1A	15	tubulin alpha-1A chain isoform 2 [Homo sapiens]	46
37.1	TUBB	15	tubulin beta chain [Homo sapiens]	50
37.2	TUBB2A	13	tubulin beta-2A chain [Homo sapiens]	50
37.3	TUBB2B	13	tubulin beta-2B chain [Homo sapiens]	50
37.4	TUBB6	5	tubulin beta-6 chain [Homo sapiens]	50
75.1	PLK1	10	serine/threonine-protein kinase PLK1 [Homo sapiens]	68
102.1	CDC37	8	hsp90 co-chaperone Cdc37 [Homo sapiens]	44

B

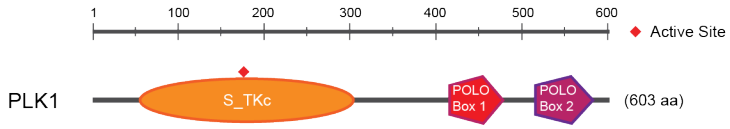

Figure 3.10. Identification of PLK1 as a novel MAST1 binding partner. (A) GST-fused MAST1 was expressed in 293T cells. Cell lysates were collected and analyzed using mass spectrometry analysis to determine novel MAST1-binding proteins. In addition to previously reported binding proteins (e.g. tubulin isoforms), polo-like kinase 1 (PLK1) was identified in the screen. **(B)** Schematic diagram of PLK1 protein domains.

MAST1 exogenously interacts with PLK1. To confirm interaction between MAST1 and PLK1, we performed a series of exogenous binding experiments in human embryonic kidney 293T cells. As shown in Figure 3.11A, Flag-tagged or GST-fused PLK1 interacts with endogenously or exogenously overexpressed MAST1 in cells. Exogenous Flag-tagged PLK1 binds to GST-fused MAST1 (Figure 3.11A) and myc-tagged MAST1 (Figure 3.11B). GST-fused PLK1 also binds to endogenous MAST1 (Figure 3.11C).

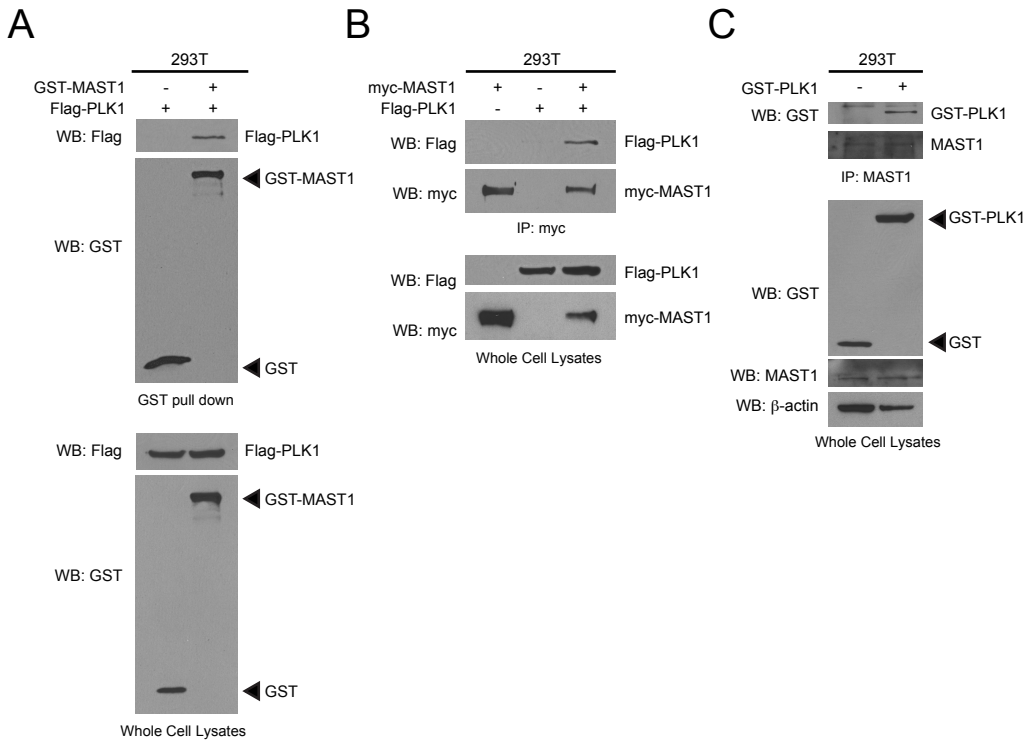

Figure 3.11. MAST1 exogenously interacts with PLK1. (A) GST-fused MAST1 and Flag-tagged PLK1 were co-transfected into 293T cells. The 239T cells were lysed and used for a GST pull down assay. Interaction between Flag-PLK1 and GST-MAST1 was detected by immunoblotting. **(B)** Myc-MAST1 and Flag-PLK1 were co-transfected in 293T cells. Myc was immunoprecipitated from the collected 293T lysates. Interaction between Flag-PLK1 and myc-MAST1 was detected by immunoblotting. **(C)** GST-PLK1 was transfected in 293T cells. Endogenous MAST1 was immunoprecipitated from the collected 293T lysates and GST-PLK1 was detected in the immunoprecipitated MAST1 sample.

MAST1 endogenously interacts with PLK1. We also performed a series of endogenous binding experiments in diverse cisplatin resistant cancer cells. As shown in Figure 3.11, endogenous MAST1 and PLK1 interact in (A) A2780^{cisR}, (B) KB-3-1^{cisR}, and (C) A549^{cisR} cells. These data together demonstrate that MAST1 physiologically binds to PLK1 in cancer cells.

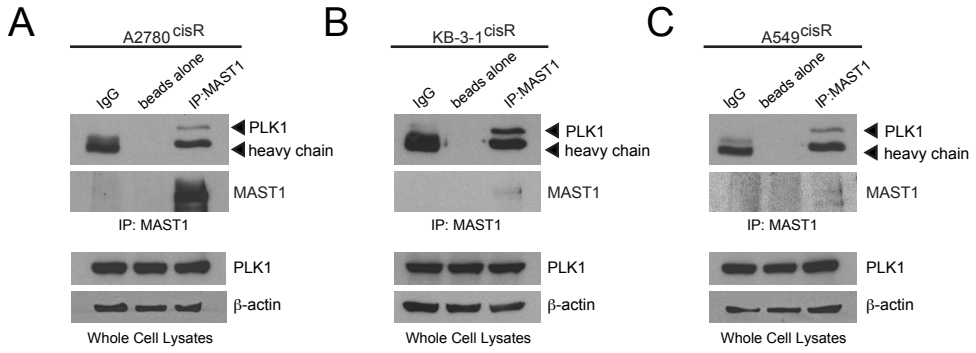

Figure 3.12. MAST1 endogenously interacts with PLK1. (A-C) Interaction between endogenous MAST1 and GST-PLK1 was detected by immunoblotting. MAST1 was immunoprecipitated from A2780^{cisR} (A), KB-3-1^{cisR} (B), and A549^{cisR} (C) cells and assayed for PLK1 binding by immunoblotting.

Targeted down-regulation of MAST1 attenuates PLK1 phosphorylation in cisplatin resistant cancer cells. We next examined whether MAST1 induces PLK1 phosphorylation and activation in (A) $A549^{cisR}$ and (B) $A2780^{cisR}$ cells with cisplatin treatment (Figure 3.13). PLK1 T210 phosphorylation is significantly attenuated in cisR MAST1 knockdown cells treated with cisplatin. Phosphorylation of PLK1 at threonine 210 is required for PLK1 activation [130]. Thus, MAST1 likely promotes PLK1 phosphorylation and activation when cancer cells are treated with cisplatin.

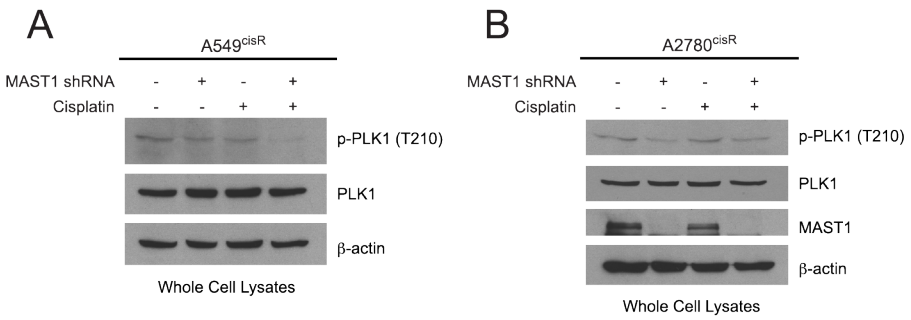

Figure 3.13. Targeted down-regulation of MAST1 attenuates PLK1 phosphorylation in cisplatin resistant cancer cells. (A) A549^{cisR} cells and **(B)** A2780^{cisR} cells with or without stable MAST1 knockdown were treated with PBS or 5 μg/ml of cisplatin for four hours. Phosphorylation of PLK1 at T210, which is required for PLK1 activity, was assayed by immunoblotting.

MAST1 phosphorylates PLK1 at threonine 210. To investigate whether MAST1 directly phosphorylates PLK1, we generated recombinant PLK1 protein and performed a MAST1 *in vitro* kinase assay (Figure 3.14). We expressed and purified PLK1 WT *(left)* and KD (K82M) *(right)* protein from *E. Coli* (Figure 3.14A). Both proteins were efficiently purified as assessed by immunoblotting *(top)* and Coomassie blue staining *(bottom)* (Figure 3.14B). Therefore, we performed a MAST1 *in vitro kinase* assay using GST-MAST1 and these purified, recombinant PLK1 proteins as substrates (Figure 3.14C). We found that GST-fused MAST1 phosphorylates WT and KD PLK1 proteins *in vitro* at threonine 210. Furthermore, PLK1 KD incubated with GST alone lacks T210 phosphorylation, which validates the PLK1 K82M mutant as a kinase dead protein void of autophosphorylation activity [131].

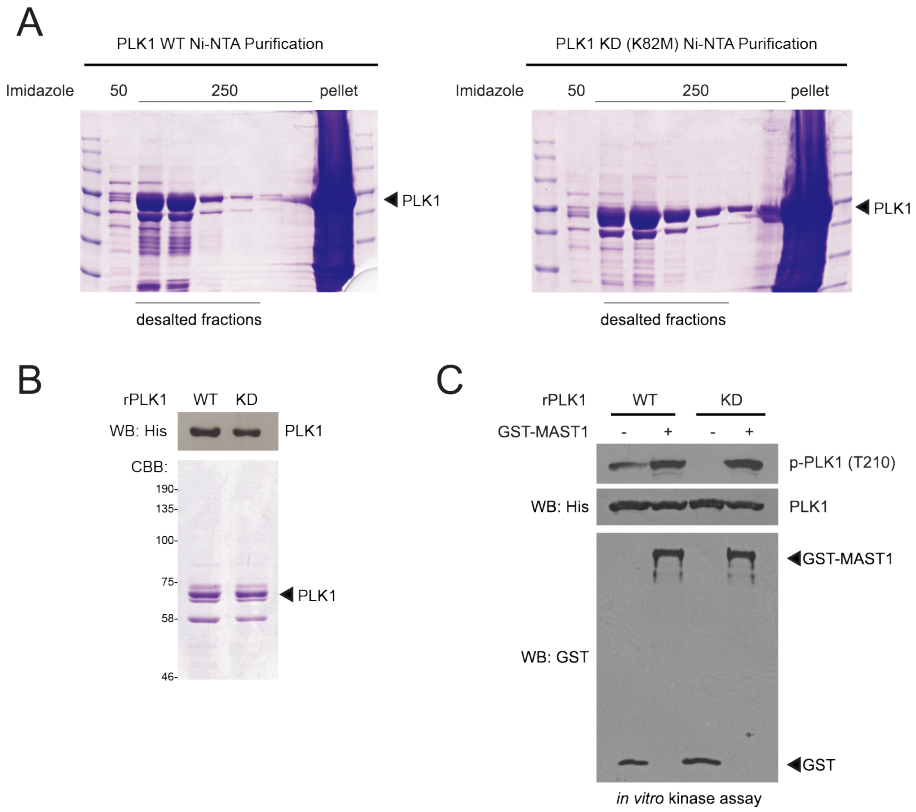

Figure 3.14. MAST1 phosphorylates PLK1 at threonine 210. (A) Histidine-tagged Flag-PLK1 WT *(left)* or Flag-PLK1 KD (K82M) *(right)* recombinant protein was purified from *E.coli* BL21(DE3)/pLysS cells using a Ni-NTA column. Indicated eluted fractions were combined and desalted using a PD-10 column. **(B)** Purification efficiency of recombinant PLK1 proteins was examined by Coomassie Brilliant Blue staining and immunoblotting. **(C)** GST-fused MAST1 was transfected and pulled down from 293T cells. *In vitro* kinase assay was performed by incubating bead bound GST-MAST1 and recombinant PLK1 WT or KD as a substrate. Phosphorylation of T210 PLK1 was detected by immunoblotting.

Constitutively active PLK1 rescues G2/M arrest of MAST1 knockdown cells during cisplatin treatment. PLK1 activity stimulates mitotic progression after DNA damage [130, 132]. To understand whether MAST1-mediated phosphorylation of PLK1 at T210 functionally promotes G2/M cell cycle progression during cisplatin treatment, we expressed flag-tagged PLK1 K82M (kinase dead; KD) or T210D (constitutively active; CA) in A2780^{cisR} cells with stable MAST1 knockdown (Figure 3.15A). Cells were treated with or without cisplatin and cell cycle distribution was assessed 48 hours post-treatment by propidium iodide staining and FACS analysis (Figure 3.15B). As previously demonstrated, G2/M cell cycle arrest is significantly higher in MAST1 knockdown cells compared to MAST1 expressing cells during cisplatin treatment. Importantly, expression of PLK1-T210D phospho-mimetic mutant partially overcomes the requirement for MAST1 in mitotic progression after cisplatin treatment. These data suggest that MAST1 may phosphorylate PLK1 to promote cancer cell cycle progression past cisplatin-induced G2/M checkpoint arrest (Figure 3.16 *(right)*).

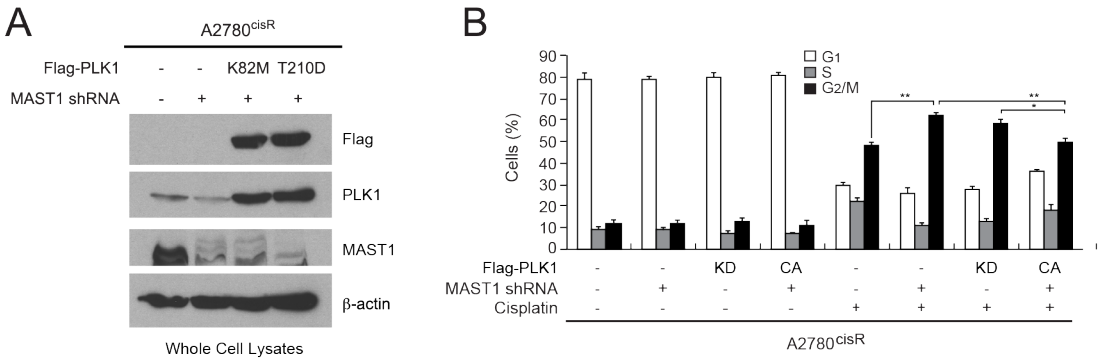

Figure 3.15. Constitutively active PLK1 rescues G2/M arrest of MAST1 knockdown cells during cisplatin treatment. (A) Flag-tagged PLK1was expressed in A2780^{cisR} cells with MAST1 knockdown. Exogenous expression of PLK1 mutants and MAST1 knockdown was confirmed by immunoblotting. **(B)** Cell cycle distribution amongst G1, S, and G2/M was quantified in variant A2780^{cisR} cells. Flag-tagged PLK1 KD or CA was expressed in A2780^{cisR} cells with stable MAST1 knockdown. Cells were treated with or without cisplatin (5 μg/ml) and cell cycle was assessed 48 hours post-treatment by propidium iodide staining and FACS analysis.

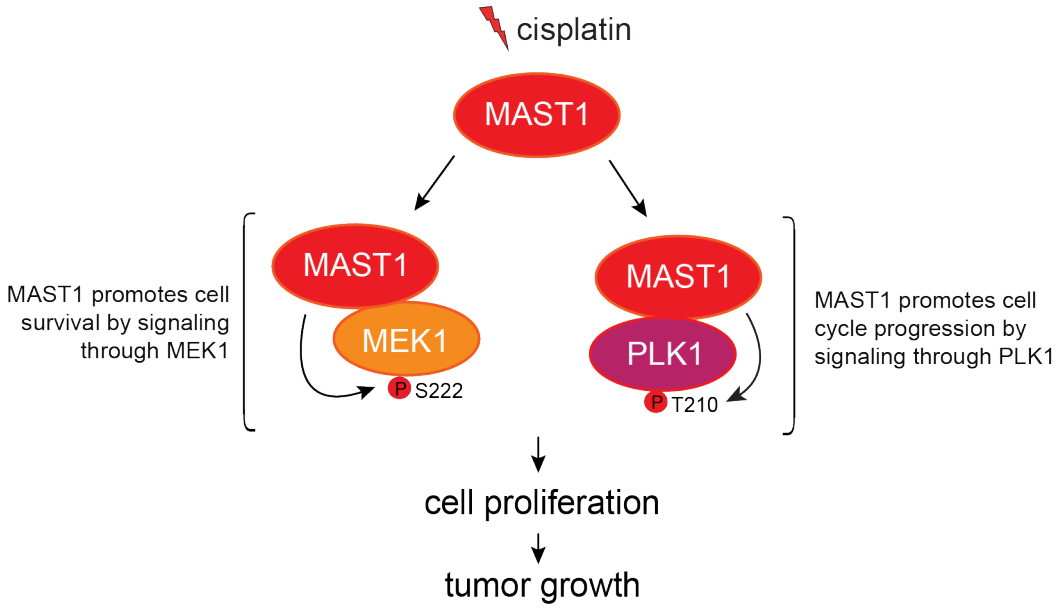

Figure 3.16. Proposed model of MAST1 function during cisplatin treatment. We show that microtubule-associated serine/threonine kinase 1 (MAST1) is important for mediating cisplatin resistant cancer cell proliferation and tumor growth in two key ways. First, MAST1 binds and phosphorylates mitogen-activated protein kinase kinase 1 (MEK1) at S221, which consequently activates MEK1 to promote cell survival during cisplatin treatment *(left)*. Second, MAST1 directly binds and phosphorylates polo-like kinase 1 (PLK1), which functions to activate PLK1 to stimulate mitotic progression during cisplatin treatment *(right)*. Taken together, these data demonstrate that MAST1 is a novel kinase that mediates *in vitro* and *in vivo* cisplatin resistance partly through activation of MEK1 and PLK1.

MAST1 expression positively correlates with disease recurrence. The primary goal of cancer therapy is permanent ablation of cancer cell survival. Unfortunately, tumor cells develop ways to evade death from chemotherapy and targeted therapies, thereby resulting in disease recurrence. In relation to our study, we performed a pilot experiment to understand whether MAST1 expression in primary head and neck squamous cell carcinoma (HNSCC) patient tumor samples correlates with HNSCC disease recurrence after cisplatin therapy (Figure 3.17; data courtesy of Dan Li).

We first developed a platform to study MAST1 expression in patient tumor samples by identifying a MAST1-specific antibody and optimizing MAST1 immunohistochemistry staining conditions in HNSCC tumor tissue (Figure 3.17A-3.17B; data courtesy of Dan Li). Using this platform, we examined MAST1 tumor expression at biopsy in two distinct HNSCC patient populations: patients with either no evidence of disease (NED) or recurrent disease two years after cisplatin chemotherapy (Figure 3.17C; data courtesy of Dan Li). We denoted patients with NED as cisplatin sensitive and patients with disease recurrence as cisplatin resistant. We found that MAST1 expression is significantly higher in primary tumor tissue collected from cisplatin resistant HNSCC patients compared to cisplatin sensitive HNSCC patients (Figure 3.17D-3.17E; data courtesy of Dan Li). This experiment suggests that MAST1 may be a potential biomarker to predict HNSCC cisplatin treatment patient responses. However, large-scale studies are needed to validate MAST1 as a prognostic indicator of cisplatin resistance in HNSCC.

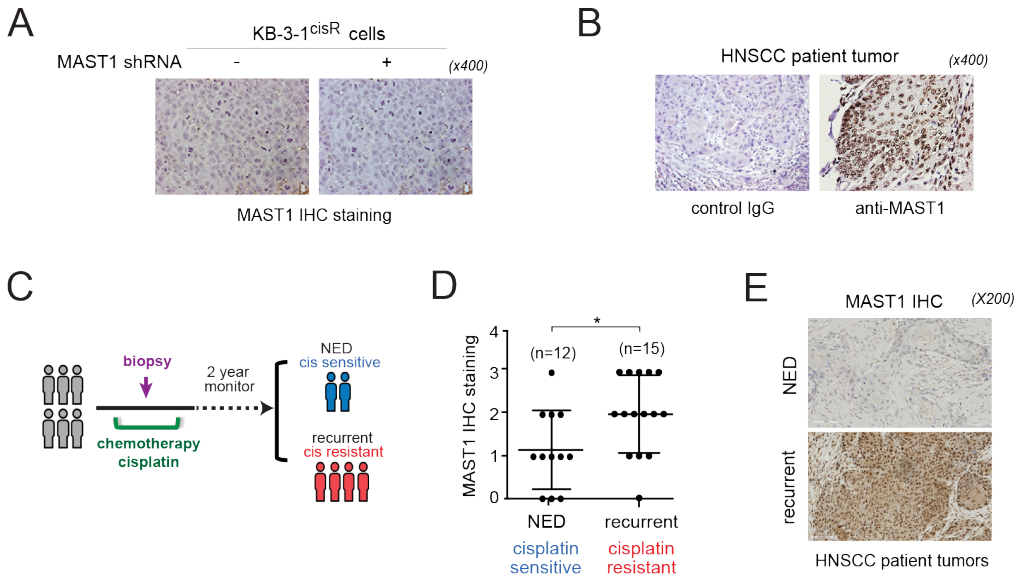

Figure 3.17. MAST1 expression positively correlates with disease recurrence. (A) KB-3-1^{cisR} cells with or without MAST1 knockdown were used for immunohistochemistry (IHC) staining to test anti-MAST1 antibody IHC specificity. **(B)** anti-MAST1 antibody was optimized for IHC in paraffin embedded formalin fixed HNSCC patient tumors. Representative images are shown. **(C)** HNSCC patient pilot experiment schematic. Two patient groups were monitored for two years after the cisplatin therapy: patients with no evidence of disease (NED) over two years after cisplatin therapy (cisplatin sensitive group) and patients with tumor recurrence within two years of cisplatin therapy (cisplatin resistant group). Tumor tissue samples were collected at biopsy. **(D)** MAST1 expression was determined in the two patient tumor tissue groups using IHC and scored based on staining intensity (0-3+). **(E)** Representative IHC images for each group are shown.

3.5 Discussion

Our data demonstrate that MAST1 kinase activity plays a multi-faceted role in cisplatin resistance. In response to cisplatin treatment, MAST1 activates two critical proteins involved in cell proliferation and tumor growth. First, we show that MAST1 directly binds, phosphorylates, and activates mitogen-activated protein kinase kinase 1 (MEK1) at S221 to promote cell survival during cisplatin treatment. Second, we demonstrate that MAST1 directly binds, phosphorylates, and activates polo-like kinase 1 (PLK1) to stimulate checkpoint progression during cisplatin treatment. Taken together, these data define a function for the MAST1 kinase in mediating cisplatin resistance partly through activation of MEK1 and PLK1.

Clinical drug resistance is classified as either acquired or intrinsic. Acquired drug resistance occurs due to drug-induced developments of mutations and other intracellular aberrations that allow tumor cells to adapt and survive. Conversely, intrinsic resistance occurs before a patient receives therapy and is caused by preexisting resistance-mediating factors in the bulk of tumor cells that make the therapy ineffective [36]. We found a positive correlation between MAST1 protein expression and response to cisplatin treatment *in vivo*, which suggests that MAST1 may mediate intrinsic cisplatin resistance. We also see a significant increase of MAST1 mRNA *in vitro* after cisplatin treatment (data not shown; data courtesy of Lingtao Jin). Therefore, MAST1 may be involved in both intrinsic and acquired cisplatin resistance. Further interrogation of key regulatory mechanisms of MAST1 protein expression and stability before, during, and after cisplatin treatment is necessary to understand the contribution of MAST1 expression to cisplatin

resistance.

Cisplatin induces G2/M cell cycle arrest as part of the DNA damage response (DDR). The DDR in cisplatin-sensitive cells, overwhelmed by the amount of DNA damage, directly signals to induce apoptosis. In contrast, the DDR in cisplatin-resistant cells induces repair mechanisms that promote cell cycle re-entry followed by successful cell division. We show that MAST1 promotes cell cycle progression and cell survival through PLK1 and MEK1 downstream signaling upon cisplatin treatment. Therefore, MAST1 likely facilitates cell cycle re-entry after checkpoint arrest to induce cell survival and proliferation in the presence of cisplatin. Importantly, this data suggests that inhibition of MAST1 activity induces a cisplatin-sensitive phenotype. Further studies are needed to validate MAST1 as a novel cisplatin-sensitizing drug target. In addition, MAST1 may phosphorylate and activate substrates other than MEK1 and PLK1 to mediate cisplatin resistance. Further characterization of MAST1 downstream effectors and signaling networks in cancer cells before, during, and after cisplatin treatment is warranted.

Excluding kinase-related domains, MAST1 has two functional domains: DUF1908 and PDZ. The DUF1908 domain has no characterized function; however, other DUF domains are shown to function under certain cellular conditions, including low nutrient conditions [133]. The PDZ domain mediates protein-protein interactions with other PDZ domain-containing proteins. For example, binding between MAST1 and PTEN, a tumor suppressor phosphatase that contains a PDZ domain, occurs at the PDZ domains. Moreover, MAST1 phosphorylation of PTEN is potentiated upon PDZ domain binding

[117]. It would be interesting to perform comprehensive studies to assess the contribution of these domains in MAST1 function during cisplatin treatment.

Tumors resistant to cisplatin are typically cross-resistant to other unrelated anticancer agents, which suggests that cisplatin likely shares mechanisms of chemoresistance with other therapies [40]. We found that MAST1 does not influence cancer cell growth and proliferation in response to taxol, a chemotherapy agent that stabilizes microtubules to induce mitotic failure and apoptosis (data not shown; data courtesy of Dan Li). However, MAST1 may play a common role in generally mediating resistance to platinum-based agents. Further studies are warranted to elucidate MAST1 function in response to other platinum-based compounds and anti-cancer drugs.

3.6 Acknowledgements

We thank the shared resources facilities of the Winship Cancer Institute. This work was supported in part by NIH grants R01 CA175316 (S.K.), F31 CA183365 (G.N.A), and ACS grant RSG-11-081-01 (S.K.).

Chapter 4: General Discussion and Future Directions

Despite concerted efforts to better understand and treat cancer over the past several decades, cancer continues to be a leading cause of death worldwide. We have yet to gain a holistic understanding of the two key processes that are responsible for poor clinical outcomes: tumor metastasis and therapeutic resistance. The aberrant regulation of kinases is a pervasive theme underlying nearly every hallmark of cancer; indeed, dysregulated kinase activity is also implicated in metastasis and resistance. A more comprehensive understanding of kinase signaling is necessary before improvements in cancer therapy and clinical outcomes can be achieved.

4.1 RSK2 and Cancer Metastasis

RSK2 is a pro-metastatic kinase that phosphorylates nuclear and cytoplasmic proteins, predominantly at RRXS/T or RXRXXS/T motifs[46]. Our lab previously reported that RSK2 phosphorylates Hsp27, a protein that regulates actin dynamics and apoptosis, to promote stabilization of actin filaments[54]. Furthermore, we identified that RSK2 phosphorylates CREB at S133 to upregulate expression of Fascin-1, an actin filament bundling protein, to promote filopodia formation at the leading edge of protruding lamellipodia[55]. Aforementioned in Chapter 2, we identified that RSK2 phosphorylates the novel substrate stathmin to promote microtubule stabilization. Collectively, these RSK2 signaling effectors promote cancer cell invasion, which occurs through a process involving degradation of the local extracellular matrix, lamellipodia protrusion, focal adhesion formation, contraction, and retraction[134]. This suggests RSK2 plays an important role in cytoskeletal regulation to promote a pro-metastatic phenotype.

Considering the complex regulation underlying cancer cell invasion, it is worth exploring whether RSK2 can regulate other cytoskeletal proteins.

Stathmin acts globally to sequester free tubulin and promote microtubule destabilization, which increases microtubule (MT) dynamics in the cell. Dynamic MTs, which undergo distinct cycles of growth and catastrophe (i.e. dynamic instability), act as a scaffold to mediate the cell mechanics, intracellular trafficking, and signaling processes that are responsible for cell motility and invasion. The maintenance of dynamic MTs is highly regulated by stathmin and other MT-associated proteins[134, 135]. Conflicting reports link stathmin and MT dynamics to differing cellular responses. Several studies demonstrate that stathmin induces MT destabilization to promote migration[136] and invasion[75, 137, 138]; conversely, other studies show that stathmin-induced MT destabilization inhibits migration[139]. We find that RSK2-mediated inhibition of stathmin activity induces MT stabilization and promotes cancer cell invasion and tumor metastasis. It is important to note that many studies reporting pro-migratory and pro-invasive roles for stathmin majorly assess the contribution of expression of stathmin in cells, but not its microtubule polymerizing activity, in cell motility. Because stabilized MTs at the leading edge are necessary in promoting cell polarization and motility[140], stathmin is likely to be differentially regulated throughout the cell to stimulate increased motility and invasion. Indeed, studies show that MT stability influences cell motility in a cell-or context-dependent manner[141]. Thus, the contribution of context-specific deviations in stathmin function and MT regulation between these studies requires closer comparative evaluation.

N-terminal serine phosphorylation is indispensable for regulating stathmin-mediated cellular effects. However, very few studies have investigated the contribution of stathmin activity to tumor metastasis. Using a xenograft model, we demonstrate that RSK2 phosphorylation of stathmin at serine 16 promotes tumor metastasis. In addition, we show that S16 phosphorylation is progressively potentiated in malignant stages of human lung tumor tissues samples; moreover, stathmin S16 phosphorylation and RSK2 expression highly correlate, suggesting increased RSK2 signaling induces stathmin S16 phosphorylation in these samples. Thus, our study demonstrates that the regulation of stathmin activity at S16 is important for tumor metastasis. We acknowledge that four other kinases – CamKII/IV[77, 142], Aurora B[143], PKA-C[78, 144], and PAK1[145] – can also regulate stathmin at S16. These kinases may function in parallel with RSK2 in cancer cell migration and invasion or in different contexts to stimulate other cellular responses. Also, it is likely that phosphorylation of other N-terminal stathmin serines contributes to tumor metastasis. For instance, the soluble MET receptor ligand HGF induces stathmin expression and phosphorylation upon receptor binding and subsequent activation of ERK and Akt, both of which are kinases reported to phosphorylate stathmin at S38[146]. Thus, comprehensive studies are needed to investigate the prevalence and function of stathmin phosphorylation in tumor metastasis.

We observe that stathmin phosphorylation at S16 is significantly attenuated at the cortex of RSK2 knockdown cells; furthermore, this phenomenon correlates with a decreased amount of observable microtubules. Given that stathmin S16 is the only N-terminal residue that exclusively regulates microtubule catastrophe and RSK2 is known to

phosphorylate substrates at the cell membrane[147], it is likely that RSK2 phosphorylates and inhibits stathmin to prevent microtubule catastrophe at the leading edge of cancer cells. This would potentially promote microtubule elongation at the cell cortex and directional migration. Additionally, the fact that RSK2 is a pro-metastatic kinase suggests that decreased microtubule dynamicity at the leading edge is a common characteristic of motile and invasive cells. Indeed, many recent studies corroborate this hypothesis. Additional studies are needed to understand the link between RSK2 and stathmin activity in cancer cell migration and invasion.

Interestingly, $p27^{kip1}$ – a RSK2 substrate involved in cell cycle regulation – can bind, sequester, and inhibit stathmin[138]. RSK2-dependent phosphorylation of $p27^{kip1}$ is reported to induce nuclear export and cytoplasmic localization, enforced by 14-3-3 binding. Thus, it is possible that RSK2 also influences the tubulin sequestering activity of stathmin indirectly by encouraging $p27^{kip1}$-stathmin binding in the cytosol. The role of $p27^{kip1}$ in pro-invasive signaling is unclear, although many reports indicate an antimigratory activity. Complicating matters further, STAT3 is also reported to bind, sequester, and inhibit stathmin; however, STAT3, functioning in the same manner as $p27^{kip1}$, promotes invasive signaling[139, 148]. Thus, the possibility that RSK2-mediated phosphorylation of $p27^{kip1}$ indirectly modulates stathmin activity to further promote MT stabilization and pro-migratory phenotypes warrants further investigation.

4.2 MAST1 and Therapeutic Resistance

Oncogenic tyrosine kinase signaling plays an important role in the maintenance of

cisplatin resistance. Several recent studies show that therapeutic inhibition of JNK (using SP600125)[149], EGFR/HER2/HER4 (using afatinib)[150], PI3K/Akt (using wortmannin and MK-2206)[151] sensitizes lung cancer, gastric cancer, and hepatocellular carcinoma cells to cisplatin treatment. In addition to these studies and others, our finding that MAST1 inhibition sensitizes cancer cells to cisplatin therapy supports a role for kinases as prosurvival signaling effectors outside of pre-defined DNA damage repair/cell cycle/apoptotic pathways in mediating chemoresistance.

MAST1 was first cloned in 1999 and subsequently identified as a cytoskeleton-related protein highly expressed in brain tissue; since then, little progress has been made in identifying upstream activators, downstream substrates, and protein binding partners that influence MAST1 signaling. However, a few recent studies implicate MAST1 in human cancers. PTEN, a tumor suppressor gene, is demonstrated to be stabilized by MAST1 binding and phosphorylation[117], suggesting an anticancer function for MAST1. Conversely, overexpression of MAST1 fusion genes identified in breast cancer cell lines and tissue samples promotes cancer cell proliferation *in vitro* and *in viv*o[118]. Another report suggests that MAST1 mutations drive oncogenesis in a case of familial lung cancer[152]. We found MAST1 is important for sensitizing cancer cells to cisplatin treatment. Our study builds on previous reports implicating MAST1 in cancer, and suggests that MAST1 is important for the maintenance of a malignant phenotype. Since MAST1 signaling is relatively uncharacterized, it is likely that MAST1 interacts with other proteins to promote cisplatin resistance. PPI data from the IntAct database suggests that MAST1 interacts with proteins involved in lysosome vesicle biogenesis, trans-Golgi

network vesicle budding, and clathrin derived vesicle budding[153]. Intracellular vesicle transport is fundamental to cell growth, homeostasis, and survival[154, 155]. Therefore, MAST1 may regulate additional substrates that contribute to cisplatin resistance and other cancer phenotypes.

Polo-like kinase 1 (PLK1) promotes G2/M checkpoint recovery and adaptation after genotoxic stress in cancer[156]. The currently accepted paradigm of PLK1 signaling during DNA damage-induced G2/M phase checkpoint recovery starts with activation of PLK1 by Aurora A/Bora at threonine 210 (T210)[157]. PLK1 subsequently phosphorylates DNA repair-associated proteins (RAD 51[158], TP53BP1[159, 160]) and negative regulators of cell cycle progression (Wee1, Claspin, CHK2) to stimulate DNA repair and mitotic progression. In Chapter 3, we show MAST1 phosphorylation of PLK1 also induces mitotic progression past the G2/M cell cycle checkpoint during cisplatin treatment. However, MAST1 signaling does not influence DNA damage responses in the cancer cell lines we tested. This discrepancy between our results and the current PLK1 signaling paradigm suggests a spatio-temporal or context-dependent difference in PLK1 regulation between MAST1 and Aurora A/Bora. Of note, previous studies utilized doxorubicin[157], a chemotherapeutic compound that intercalates DNA bases, or ionizing radiation[159, 160] to induce DNA damage and G2/M arrest. Cisplatin primarily induces DNA intrastrand crosslinks[113], whereas doxorubicin stimulates a myriad of cytotoxic effects, including topoisomerase II poisoning, oxidative stress, ceramide overproduction, DNA torsion, and nucleosome destabilization[161]. Ionizing radiation creates single-strand, clustered, and double-strand DNA breaks[162]. These anticancer

agents engage distinct intracellular signaling pathways to promote apoptosis; therefore, our observations about MAST1-PLK1 signaling during cisplatin treatment may result from specific mechanisms underlying cisplatin activity. MAST1 regulation of PLK1 function in response to different modes of DNA damage warrants further study.

Therapeutic resistance is regulated in different ways across cancer types. This is best demonstrated by primary and secondary response rates to chemotherapy. Up to 20% of lung cancers initially respond to cisplatin based therapy; in contrast, close to 100% of testicular cancers respond[97]. Despite this cancer-specific variability, we found that MAST1 stimulates the same cellular responses in incredibly diverse cisplatin resistant cells, in which no two cell lines share the same tissue of origin or genetic background. This observation suggests the existence of one or more universal resistance pathway(s) regulated by MAST1 that can potentially be exploited for cisplatin chemosensitization. Whether these signaling commonalities and phenotypic outcomes are observed outside of tested *in vitro* experimental systems remains to be explored.

4.3 Conclusions

Cancer continues to be a leading cause of death worldwide. Clinical drug resistance and tumor metastasis are accountable for the vast majority of these deaths. Although therapeutic resistance and metastasis are typically considered to be separate entities, they are united on a molecular level by kinases. Given the commonality of substrates between kinase signaling pathways, it would not be surprising to find that certain aspects of pro-metastatic signaling may also regulate resistance to chemotherapeutics and vice versa. In

the case of RSK2, a recent report demonstrates that RSK2 knockdown promotes cisplatin chemosensitization [163]. Likewise, MAST1 may functionally promote invasive and metastatic phenotypes through effects on known or unknown substrates and signaling pathways. Thus, comprehensive characterization of protein kinase signaling in the many contexts of cancer progression, tumor metastasis, and therapeutic resistance will be critical for the development of future curative therapies.

Chapter 5: References

1. Fabbro, D., S.W. Cowan-Jacob, and H. Moebitz, *Ten things you should know about protein kinases: IUPHAR Review 14.* British Journal of Pharmacology, 2015. **172**(11): p. 2675-2700.
2. Shaw, A.S., et al., *Kinases and pseudokinases: lessons from RAF.* Mol Cell Biol, 2014. **34**(9): p. 1538-46.
3. Endicott, J.A., M.E. Noble, and L.N. Johnson, *The structural basis for control of eukaryotic protein kinases.* Annu Rev Biochem, 2012. **81**: p. 587-613.
4. Cohen, P., *The origins of protein phosphorylation.* Nat Cell Biol, 2002. **4**(5): p. E127-30.
5. Manning, G., et al., *The protein kinase complement of the human genome.* Science, 2002. **298**(5600): p. 1912-34.
6. Hanks, S.K., *Genomic analysis of the eukaryotic protein kinase superfamily: a perspective.* Genome Biol, 2003. **4**(5): p. 111.
7. Boudeau, J., et al., *Emerging roles of pseudokinases.* Trends Cell Biol, 2006. **16**(9): p. 443-52.
8. Taylor, S.S. and A.P. Kornev, *Protein kinases: evolution of dynamic regulatory proteins.* Trends Biochem Sci, 2011. **36**(2): p. 65-77.
9. Taylor, S.S., et al., *Evolution of the eukaryotic protein kinases as dynamic molecular switches.* Philos Trans R Soc Lond B Biol Sci, 2012. **367**(1602): p. 2517-28.
10. Hanahan, D. and R.A. Weinberg, *Hallmarks of cancer: the next generation.* Cell, 2011. **144**(5): p. 646-74.
11. Hanahan, D. and R.A. Weinberg, *The hallmarks of cancer.* Cell, 2000. **100**(1): p. 57-70.
12. Levinson, A.D., et al., *Evidence that the transforming gene of avian sarcoma virus encodes a protein kinase associated with a phosphoprotein.* Cell, 1978. **15**(2): p. 561-72.
13. Sefton, B.M., et al., *Evidence that the phosphorylation of tyrosine is essential for cellular transformation by Rous sarcoma virus.* Cell, 1980. **20**(3): p. 807-16.
14. Hunter, T. and B.M. Sefton, *Transforming gene product of Rous sarcoma virus phosphorylates tyrosine.* Proc Natl Acad Sci U S A, 1980. **77**(3): p. 1311-5.
15. Futreal, P.A., et al., *A census of human cancer genes.* Nat Rev Cancer, 2004. **4**(3): p. 177-83.
16. Fleuren, E.D., et al., *The kinome 'at large' in cancer.* Nat Rev Cancer, 2016. **16**(2): p. 83-98.
17. Gross, S., et al., *Targeting cancer with kinase inhibitors.* J Clin Invest, 2015. **125**(5): p. 1780-9.

18. Greenman, C., et al., *Patterns of somatic mutation in human cancer genomes.* Nature, 2007. **446**(7132): p. 153-8.

19. Holderfield, M., et al., *Targeting RAF kinases for cancer therapy: BRAF-mutated melanoma and beyond.* Nat Rev Cancer, 2014. **14**(7): p. 455-67.

20. Szerlip, N.J., et al., *Intratumoral heterogeneity of receptor tyrosine kinases EGFR and PDGFRA amplification in glioblastoma defines subpopulations with distinct growth factor response.* Proc Natl Acad Sci U S A, 2012. **109**(8): p. 3041-6.

21. Pawson, T. and P. Nash, *Protein-protein interactions define specificity in signal transduction.* Genes Dev, 2000. **14**(9): p. 1027-47.

22. Sun, C. and R. Bernards, *Feedback and redundancy in receptor tyrosine kinase signaling: relevance to cancer therapies.* Trends Biochem Sci, 2014. **39**(10): p. 465-74.

23. Cseh, B., E. Doma, and M. Baccarini, *"RAF" neighborhood: protein-protein interaction in the Raf/Mek/Erk pathway.* FEBS Lett, 2014. **588**(15): p. 2398-406.

24. Desideri, E., A.L. Cavallo, and M. Baccarini, *Alike but Different: RAF Paralogs and Their Signaling Outputs.* Cell, 2015. **161**(5): p. 967-70.

25. Tsai, C.J. and R. Nussinov, *The molecular basis of targeting protein kinases in cancer therapeutics.* Semin Cancer Biol, 2013. **23**(4): p. 235-42.

26. Wu, P., T.E. Nielsen, and M.H. Clausen, *FDA-approved small-molecule kinase inhibitors.* Trends Pharmacol Sci, 2015. **36**(7): p. 422-39.

27. *Cancer Facts & Figures 2016.* American Cancer Society, 2016.

28. Gupta, G.P. and J. Massague, *Cancer metastasis: building a framework.* Cell, 2006. **127**(4): p. 679-95.

29. Rofstad, E.K., et al., *The tumor bed effect: increased metastatic dissemination from hypoxia-induced up-regulation of metastasis-promoting gene products.* Cancer Res, 2005. **65**(6): p. 2387-96.

30. Vanharanta, S. and J. Massague, *Origins of metastatic traits.* Cancer Cell, 2013. **24**(4): p. 410-21.

31. Steeg, P.S., *Tumor metastasis: mechanistic insights and clinical challenges.* Nat Med, 2006. **12**(8): p. 895-904.

32. Neville-Webbe, H.L. and R.E. Coleman, *Bisphosphonates and RANK ligand inhibitors for the treatment and prevention of metastatic bone disease.* Eur J Cancer, 2010. **46**(7): p. 1211-22.

33. Pantel, K. and R.H. Brakenhoff, *Dissecting the metastatic cascade.* Nat Rev Cancer, 2004. **4**: p. 448-56.

34. Nguyen, D.X., P.D. Bos, and J. Massague, *Metastasis: from dissemination to organ-specific colonization.* Nat Rev Cancer, 2009. **9**(4): p. 274-84.

35. Sleeman, J. and P.S. Steeg, *Cancer metastasis as a therapeutic target.* Eur J Cancer, 2010. **46**(7): p. 1177-80.

36. Longley, D.B. and P.G. Johnston, *Molecular mechanisms of drug resistance.* J Pathol, 2005. **205**(2): p. 275-92.

37. Holohan, C., et al., *Cancer drug resistance: an evolving paradigm.* Nat Rev Cancer, 2013. **13**(10): p. 714-726.

38. Weng, L., et al., *Pharmacogenetics and pharmacogenomics: a bridge to individualized cancer therapy.* Pharmacogenomics, 2013. **14**(3): p. 315-24.

39. McLeod, H.L. and C. Siva, *The thiopurine S-methyltransferase gene locus -- implications for clinical pharmacogenomics.* Pharmacogenomics, 2002. **3**(1): p. 89-98.

40. Siddik, Z.H., *Cisplatin: mode of cytotoxic action and molecular basis of resistance.* Oncogene, 2003. **22**(47): p. 7265-79.

41. Azam, M., et al., *Activation of tyrosine kinases by mutation of the gatekeeper threonine.* Nat Struct Mol Biol, 2008. **15**(10): p. 1109-18.

42. Benson, J.D., et al., *Validating cancer drug targets.* Nature, 2006. **441**(7092): p. 451-6.

43. Kang, S., et al., *FGFR3 activates RSK2 to mediate hematopoietic transformation through tyrosine phosphorylation of RSK2 and activation of the MEK/ERK pathway.* Cancer Cell, 2007. **12**(3): p. 201-14.

44. Kang, S., et al., *Fibroblast growth factor receptor 3 associates with and tyrosine phosphorylates p90 RSK2, leading to RSK2 activation that mediates hematopoietic transformation.* Mol Cell Biol, 2009. **29**(8): p. 2105-17.

45. Elf, S., et al., *p90RSK2 is essential for FLT3-ITD- but dispensable for BCR-ABL-induced myeloid leukemia.* Blood, 2011. **117**(25): p. 6885-94.

46. Kang, S. and J. Chen, *Targeting RSK2 in human malignancies.* Expert Opin Ther Targets, 2011. **15**(1): p. 11-20.

47. Alesi, G.N., et al., *RSK2 signals through stathmin to promote microtubule dynamics and tumor metastasis.* Oncogene, 2016.

48. Fidler, I.J., *The pathogenesis of cancer metastasis: the 'seed and soil' hypothesis revisited.* Nat Rev Cancer, 2003. **3**(6): p. 453-8.

49. Nguyen, D.X. and J. Massague, *Genetic determinants of cancer metastasis.* Nat Rev Genet, 2007. **8**(5): p. 341-52.

50. Sahai, E., *Mechanisms of cancer cell invasion.* Curr Opin Genet Dev, 2005. **15**(1): p. 87-96.

51. Li, Y., et al., *Estrogen stimulation of cell migration involves multiple signaling pathway interactions.* Endocrinology, 2010. **151**(11): p. 5146-56.

52. Persad, S. and S. Dedhar, *The role of integrin-linked kinase (ILK) in cancer progression.* Cancer Metastasis Rev, 2003. **22**(4): p. 375-84.

53. Jin, L., et al., *p90 RSK2 Mediates Antianoikis Signals by both Transcription-Dependent and -Independent Mechanisms.* Mol Cell Biol, 2013. **33**(13): p. 2574-

85.

54. Kang, S., et al., *p90 ribosomal S6 kinase 2 promotes invasion and metastasis of human head and neck squamous cell carcinoma cells.* J Clin Invest, 2010. **120**(4): p. 1165-77.

55. Li, D., et al., *The prometastatic ribosomal S6 kinase 2-cAMP response element-binding protein (RSK2-CREB) signaling pathway up-regulates the actin-binding protein fascin-1 to promote tumor metastasis.* J Biol Chem, 2013. **288**(45): p. 32528-38.

56. Buck, M., et al., *C/EBPbeta phosphorylation by RSK creates a functional XEXD caspase inhibitory box critical for cell survival.* Mol Cell, 2001. **8**(4): p. 807-16.

57. Palmer, A., A.C. Gavin, and A.R. Nebreda, *A link between MAP kinase and p34(cdc2)/cyclin B during oocyte maturation: p90(rsk) phosphorylates and inactivates the p34(cdc2) inhibitory kinase Myt1.* EMBO J, 1998. **17**(17): p. 5037-47.

58. Shimamura, A., et al., *Rsk1 mediates a MEK-MAP kinase cell survival signal.* Curr Biol, 2000. **10**(3): p. 127-35.

59. Dehan, E., et al., *betaTrCP- and Rsk1/2-mediated degradation of BimEL inhibits apoptosis.* Mol Cell, 2009. **33**(1): p. 109-16.

60. Blenis, J., *Signal transduction via the MAP kinases: proceed at your own RSK.* Proc Natl Acad Sci U S A, 1993. **90**(13): p. 5889-92.

61. Frodin, M. and S. Gammeltoft, *Role and regulation of 90 kDa ribosomal S6 kinase (RSK) in signal transduction.* Mol Cell Endocrinol, 1999. **151**(1-2): p. 65-77.

62. Anjum, R. and J. Blenis, *The RSK family of kinases: emerging roles in cellular signalling.* Nat Rev Mol Cell Biol, 2008. **9**(10): p. 747-58.

63. Schoumacher, M., et al., *Actin, microtubules, and vimentin intermediate filaments cooperate for elongation of invadopodia.* J Cell Biol, 2010. **189**(3): p. 541-56.

64. Desai, A. and T.J. Mitchison, *Microtubule polymerization dynamics.* Annu Rev Cell Dev Biol, 1997. **13**: p. 83-117.

65. Belmont, L.D. and T.J. Mitchison, *Identification of a protein that interacts with tubulin dimers and increases the catastrophe rate of microtubules.* Cell, 1996. **84**(4): p. 623-31.

66. Belletti, B., et al., *Stathmin activity influences sarcoma cell shape, motility, and metastatic potential.* Mol Biol Cell, 2008. **19**(5): p. 2003-13.

67. Tan, H.T., et al., *Proteomic analysis of colorectal cancer metastasis: stathmin-1 revealed as a player in cancer cell migration and prognostic marker.* J Proteome Res, 2012. **11**(2): p. 1433-45.

68. Hsieh, S.Y., et al., *Stathmin1 overexpression associated with polyploidy, tumor-cell invasion, early recurrence, and poor prognosis in human hepatoma.* Mol Carcinog, 2010. **49**(5): p. 476-87.

69. Cheng, A.L., et al., *Identification of novel nasopharyngeal carcinoma biomarkers by laser capture microdissection and proteomic analysis.* Clin Cancer Res, 2008. **14**(2): p. 435-45.

70. Jeon, T.Y., et al., *Overexpression of stathmin1 in the diffuse type of gastric cancer and its roles in proliferation and migration of gastric cancer cells.* Br J Cancer, 2010. **102**(4): p. 710-8.

71. Polzin, R.G., et al., *E2F sites in the Op18 promoter are required for high level of expression in the human prostate carcinoma cell line PC-3-M.* Gene, 2004. **341**: p. 209-18.

72. Kinoshita, I., et al., *Identification of cJun-responsive genes in Rat-1a cells using multiple techniques: increased expression of stathmin is necessary for cJun-mediated anchorage-independent growth.* Oncogene, 2003. **22**(18): p. 2710-22.

73. Carr, J.R., et al., *FoxM1 mediates resistance to herceptin and paclitaxel.* Cancer Res, 2010. **70**(12): p. 5054-63.

74. San-Marina, S., et al., *Suspected leukemia oncoproteins CREB1 and LYL1 regulate Op18/STMN1 expression.* Biochim Biophys Acta, 2012. **1819**(11-12): p. 1164-72.

75. Li, N., et al., *Siva1 suppresses epithelial-mesenchymal transition and metastasis of tumor cells by inhibiting stathmin and stabilizing microtubules.* Proc Natl Acad Sci U S A, 2011. **108**(31): p. 12851-6.

76. Daub, H., et al., *Rac/Cdc42 and p65PAK regulate the microtubule-destabilizing protein stathmin through phosphorylation at serine 16.* J Biol Chem, 2001. **276**(3): p. 1677-80.

77. Marklund, U., et al., *Serine 16 of oncoprotein 18 is a major cytosolic target for the Ca2+/calmodulin-dependent kinase-Gr.* Eur J Biochem, 1994. **225**(1): p. 53-60.

78. Beretta, L., T. Dobransky, and A. Sobel, *Multiple phosphorylation of stathmin. Identification of four sites phosphorylated in intact cells and in vitro by cyclic AMP-dependent protein kinase and p34cdc2.* J Biol Chem, 1993. **268**(27): p. 20076-84.

79. Cassimeris, L., *The oncoprotein 18/stathmin family of microtubule destabilizers.* Curr Opin Cell Biol, 2002. **14**(1): p. 18-24.

80. Belletti, B. and G. Baldassarre, *Stathmin: a protein with many tasks. New biomarker and potential target in cancer.* Expert Opin Ther Targets, 2011. **15**(11): p. 1249-66.

81. Misek, D.E., et al., *Transforming properties of a Q18-->E mutation of the microtubule regulator Op18.* Cancer Cell, 2002. **2**(3): p. 217-28.

82. Holmfeldt, P., et al., *Aneugenic activity of Op18/stathmin is potentiated by the somatic Q18-->e mutation in leukemic cells.* Mol Biol Cell, 2006. **17**(7): p. 2921-30.

83. Clark, D.E., et al., *Rsk2 allosterically activates estrogen receptor alpha by docking to the hormone-binding domain.* EMBO J, 2001. **20**(13): p. 3484-94.

84. Kang, Y., et al., *Breast cancer bone metastasis mediated by the Smad tumor suppressor pathway.* Proc Natl Acad Sci U S A, 2005. **102**(39): p. 13909-14.

85. Hitosugi, T., et al., *Tyrosine phosphorylation of mitochondrial pyruvate dehydrogenase kinase 1 is important for cancer metabolism.* Mol Cell, 2011. **44**(6): p. 864-77.

86. Morrison, K.C. and P.J. Hergenrother, *Whole cell microtubule analysis by flow cytometry.* Anal Biochem, 2012. **420**(1): p. 26-32.

87. Ng, D.C., et al., *Stat3 regulates microtubules by antagonizing the depolymerization activity of stathmin.* J Cell Biol, 2006. **172**(2): p. 245-57.

88. Jin, L., et al., *Glutamate Dehydrogenase 1 Signals through Antioxidant Glutathione Peroxidase 1 to Regulate Redox Homeostasis and Tumor Growth.* Cancer Cell, 2015. **27**(2): p. 257-70.

89. Tournebize, R., et al., *Distinct roles of PP1 and PP2A-like phosphatases in control of microtubule dynamics during mitosis.* EMBO J, 1997. **16**(18): p. 5537-49.

90. Mistry, S.J., H.C. Li, and G.F. Atweh, *Role for protein phosphatases in the cell-cycle-regulated phosphorylation of stathmin.* Biochem J, 1998. **334 (Pt 1)**: p. 23-9.

91. Mizumura, K., et al., *Identification of Op18/stathmin as a potential target of ASK1-p38 MAP kinase cascade.* J Cell Physiol, 2006. **206**(2): p. 363-70.

92. Prestayko, A.W., et al., *Cisplatin (cis-diamminedichloroplatinum II).* Cancer Treat Rev, 1979. **6**(1): p. 17-39.

93. Lebwohl, D. and R. Canetta, *Clinical development of platinum complexes in cancer therapy: an historical perspective and an update.* Eur J Cancer, 1998. **34**(10): p. 1522-34.

94. Galanski, M., *Recent developments in the field of anticancer platinum complexes.* Recent Pat Anticancer Drug Discov, 2006. **1**(2): p. 285-95.

95. Murata, T., et al., *Molecular mechanism of chemoresistance to cisplatin in ovarian cancer cell lines.* Int J Mol Med, 2004. **13**(6): p. 865-8.

96. Galluzzi, L., et al., *Molecular mechanisms of cisplatin resistance.* Oncogene, 2012. **31**(15): p. 1869-83.

97. Giaccone, G., *Clinical perspectives on platinum resistance.* Drugs, 2000. **59 Suppl 4**: p. 9-17; discussion 37-8.

98. Einhorn, L.H., *Curing metastatic testicular cancer.* Proc Natl Acad Sci U S A, 2002. **99**(7): p. 4592-5.

99. Koberle, B., et al., *Cisplatin resistance: preclinical findings and clinical implications.* Biochim Biophys Acta, 2010. **1806**(2): p. 172-82.

100. Nakayama, K., et al., *Prognostic value of the Cu-transporting ATPase in ovarian carcinoma patients receiving cisplatin-based chemotherapy.* Clin Cancer Res, 2004. **10**(8): p. 2804-11.

101. Aida, T., et al., *Expression of copper-transporting P-type adenosine triphosphatase (ATP7B) as a prognostic factor in human endometrial carcinoma.* Gynecol Oncol, 2005. **97**(1): p. 41-5.

102. Moreno-Smith, M., et al., *ATP11B mediates platinum resistance in ovarian cancer.* J Clin Invest, 2013. **123**(5): p. 2119-30.

103. Liedert, B., et al., *Overexpression of cMOAT (MRP2/ABCC2) is associated with decreased formation of platinum-DNA adducts and decreased G2-arrest in melanoma cells resistant to cisplatin.* J Invest Dermatol, 2003. **121**(1): p. 172-6.

104. Korita, P.V., et al., *Multidrug resistance-associated protein 2 determines the efficacy of cisplatin in patients with hepatocellular carcinoma.* Oncol Rep, 2010. **23**(4): p. 965-72.

105. Metzger, R., et al., *ERCC1 mRNA levels complement thymidylate synthase mRNA levels in predicting response and survival for gastric cancer patients receiving combination cisplatin and fluorouracil chemotherapy.* J Clin Oncol, 1998. **16**(1): p. 309-16.

106. Jun, H.J., et al., *ERCC1 expression as a predictive marker of squamous cell carcinoma of the head and neck treated with cisplatin-based concurrent chemoradiation.* Br J Cancer, 2008. **99**(1): p. 167-72.

107. Olaussen, K.A., *A new step ahead for the consideration of ERCC1 as a candidate biomarker to select NSCLC patients for the treatment of cetuximab in combination with cisplatin.* Cancer Biol Ther, 2009. **8**(20): p. 1922-3.

108. Erovic, B.M., et al., *Mcl-1, vascular endothelial growth factor-R2, and 14-3-3sigma expression might predict primary response against radiotherapy and chemotherapy in patients with locally advanced squamous cell carcinomas of the head and neck.* Clin Cancer Res, 2005. **11**(24 Pt 1): p. 8632-6.

109. Han, J.Y., et al., *Death receptor 5 and Bcl-2 protein expression as predictors of tumor response to gemcitabine and cisplatin in patients with advanced non-small-cell lung cancer.* Med Oncol, 2003. **20**(4): p. 355-62.

110. Ikeguchi, M. and N. Kaibara, *Changes in survivin messenger RNA level during cisplatin treatment in gastric cancer.* Int J Mol Med, 2001. **8**(6): p. 661-6.

111. Jain, H.V. and M. Meyer-Hermann, *The molecular basis of synergism between carboplatin and ABT-737 therapy targeting ovarian carcinomas.* Cancer Res, 2011. **71**(3): p. 705-15.

112. Ryan, B.M., N. O'Donovan, and M.J. Duffy, *Survivin: a new target for anti-cancer therapy.* Cancer Treat Rev, 2009. **35**(7): p. 553-62.

113. Kelland, L., *The resurgence of platinum-based cancer chemotherapy.* Nat Rev Cancer, 2007. **7**(8): p. 573-84.

114. Garland, P., et al., *Expression of the MAST family of serine/threonine kinases.* Brain Res, 2008. **1195**: p. 12-9.

115. Walden, P.D. and N.J. Cowan, *A novel 205-kilodalton testis-specific serine/threonine protein kinase associated with microtubules of the spermatid manchette.* Mol Cell Biol, 1993. **13**(12): p. 7625-35.

116. Lumeng, C., et al., *Interactions between beta 2-syntrophin and a family of microtubule-associated serine/threonine kinases.* Nat Neurosci, 1999. **2**(7): p. 611-7.

117. Valiente, M., et al., *Binding of PTEN to specific PDZ domains contributes to PTEN protein stability and phosphorylation by microtubule-associated serine/threonine kinases.* J Biol Chem, 2005. **280**(32): p. 28936-43.

118. Robinson, D.R., et al., *Functionally recurrent rearrangements of the MAST kinase and Notch gene families in breast cancer.* Nat Med, 2011. **17**(12): p. 1646-51.

119. Lin, C.J., et al., *Head and neck squamous cell carcinoma cell lines: established models and rationale for selection.* Head Neck, 2007. **29**(2): p. 163-88.

120. Zhao, M., et al., *Assembly and initial characterization of a panel of 85 genomically validated cell lines from diverse head and neck tumor sites.* Clin Cancer Res, 2011. **17**(23): p. 7248-64.

121. Richert, N., et al., *Multiply drug-resistant human KB carcinoma cells have decreased amounts of a 75-kDa and a 72-kDa glycoprotein.* Proc Natl Acad Sci U S A, 1985. **82**(8): p. 2330-3.

122. Akiyama, S., et al., *Isolation and genetic characterization of human KB cell lines resistant to multiple drugs.* Somat Cell Mol Genet, 1985. **11**(2): p. 117-26.

123. Smits, V.A., et al., *p21 inhibits Thr161 phosphorylation of Cdc2 to enforce the G2 DNA damage checkpoint.* J Biol Chem, 2000. **275**(39): p. 30638-43.

124. Kannan, N., et al., *The hallmark of AGC kinase functional divergence is its C-terminal tail, a cis-acting regulatory module.* Proceedings of the National Academy of Sciences, 2007. **104**(4): p. 1272-1277.

125. Johnson, L.N., M.E. Noble, and D.J. Owen, *Active and inactive protein kinases: structural basis for regulation.* Cell, 1996. **85**(2): p. 149-58.

126. Bayliss, R., et al., *On the molecular mechanisms of mitotic kinase activation.* Open Biol, 2012. **2**(11): p. 120136.

127. Hyun, S.Y., H.I. Hwang, and Y.J. Jang, *Polo-like kinase-1 in DNA damage response.* BMB Rep, 2014. **47**(5): p. 249-55.

128. Lee, K.S., et al., *Mutation of the polo-box disrupts localization and mitotic functions of the mammalian polo kinase Plk.* Proceedings of the National Academy of Sciences, 1998. **95**(16): p. 9301-9306.

129. Lens, S.M., E.E. Voest, and R.H. Medema, *Shared and separate functions of polo-like kinases and aurora kinases in cancer.* Nat Rev Cancer, 2010. **10**(12): p. 825-41.

130. Tsvetkov, L. and D.F. Stern, *Phosphorylation of Plk1 at S137 and T210 is inhibited in response to DNA damage.* Cell Cycle, 2005. **4**(1): p. 166-71.

131. Seong, Y.S., et al., *A spindle checkpoint arrest and a cytokinesis failure by the dominant-negative polo-box domain of Plk1 in U-2 OS cells.* J Biol Chem, 2002. **277**(35): p. 32282-93.

132. van Vugt, M.A.T.M., A. Brás, and R.H. Medema, *Polo-like Kinase-1 Controls Recovery from a G2 DNA Damage-Induced Arrest in Mammalian Cells.* Molecular Cell, 2004. **15**(5): p. 799-811.

133. Hauser, R., et al., *RsfA (YbeB) proteins are conserved ribosomal silencing factors.* PLoS Genet, 2012. **8**(7): p. e1002815.

134. Etienne-Manneville, S., *Microtubules in cell migration.* Annu Rev Cell Dev Biol, 2013. **29**: p. 471-99.

135. Kaverina, I. and A. Straube, *Regulation of cell migration by dynamic microtubules.* Semin Cell Dev Biol, 2011. **22**(9): p. 968-74.

136. Knight, L.M., et al., *Merkel cell polyomavirus small T antigen mediates microtubule destabilization to promote cell motility and migration.* J Virol, 2015. **89**(1): p. 35-47.

137. Akhtar, J., et al., *Lentiviral-mediated RNA interference targeting stathmin1 gene in human gastric cancer cells inhibits proliferation in vitro and tumor growth in vivo.* J Transl Med, 2013. **11**: p. 212.

138. Baldassarre, G., et al., *p27(Kip1)-stathmin interaction influences sarcoma cell migration and invasion.* Cancer Cell, 2005. **7**(1): p. 51-63.

139. Ng, D.C., et al., *Stat3 regulates microtubules by antagonizing the depolymerization activity of stathmin.* J Cell Biol, 2006. **172**: p. 245-57.

140. Ganguly, A., et al., *The role of microtubules and their dynamics in cell migration.* J Biol Chem, 2012. **287**(52): p. 43359-69.

141. Etienne-Manneville, S., *Actin and microtubules in cell motility: which one is in control?* Traffic, 2004. **5**(7): p. 470-7.

142. le Gouvello, S., V. Manceau, and A. Sobel, *Serine 16 of stathmin as a cytosolic target for Ca2+/calmodulin-dependent kinase II after CD2 triggering of human T lymphocytes.* J Immunol, 1998. **161**(3): p. 1113-22.

143. Gadea, B.B. and J.V. Ruderman, *Aurora B is required for mitotic chromatin-induced phosphorylation of Op18/Stathmin.* Proc Natl Acad Sci U S A, 2006. **103**(12): p. 4493-8.

144. Gradin, H.M., et al., *Regulation of microtubule dynamics by extracellular signals: cAMP-dependent protein kinase switches off the activity of oncoprotein 18 in intact cells.* J Cell Biol, 1998. **140**(1): p. 131-41.

145. Wittmann, T., G.M. Bokoch, and C.M. Waterman-Storer, *Regulation of microtubule destabilizing activity of Op18/stathmin downstream of Rac1.* J Biol Chem, 2004. **279**(7): p. 6196-203.

146. Schmitt, S., et al., *Stathmin regulates keratinocyte proliferation and migration during cutaneous regeneration.* PLoS One, 2013. **8**(9): p. e75075.

147. Gawecka, J.E., et al., *RSK2 Protein Suppresses Integrin Activation and Fibronectin Matrix Assembly and Promotes Cell Migration.* J Biol Chem, 2012. **287**: p. 43424-37.

148. Wei, Z., et al., *STAT3 interacts with Skp2/p27/p21 pathway to regulate the motility and invasion of gastric cancer cells.* Cell Signal, 2013.

149. Liu, X.Y., et al., *Inhibition of the JNK signaling pathway increases sensitivity of hepatocellular carcinoma cells to cisplatin by down-regulating expression of P-glycoprotein.* Eur Rev Med Pharmacol Sci, 2016. **20**(6): p. 1098-108.

150. Brands, R.C., et al., *Co-treatment of wildtype EGFR head and neck cancer cell lines with afatinib and cisplatin.* Mol Med Rep, 2016. **13**(3): p. 2338-44.

151. Tao, K., et al., *Akt inhibitor MK-2206 enhances the effect of cisplatin in gastric cancer cells.* Biomed Rep, 2016. **4**(3): p. 365-368.

152. Tomoshige, K., et al., *Germline mutations causing familial lung cancer.* J Hum Genet, 2015. **60**(10): p. 597-603.

153. Kerrien, S., et al., *The IntAct molecular interaction database in 2012.* Nucleic Acids Res, 2012. **40**(Database issue): p. D841-6.

154. Rothman, J.E., *The protein machinery of vesicle budding and fusion.* Protein Sci, 1996. **5**(2): p. 185-94.

155. Paknikar, K.M., *Landmark discoveries in intracellular transport and secretion.* J Cell Mol Med, 2007. **11**(3): p. 393-7.

156. Zitouni, S., et al., *Polo-like kinases: structural variations lead to multiple functions.* Nat Rev Mol Cell Biol, 2014. **15**(7): p. 433-52.

157. Macurek, L., et al., *Polo-like kinase-1 is activated by aurora A to promote checkpoint recovery.* Nature, 2008. **455**(7209): p. 119-123.

158. Yata, K., et al., *Plk1 and CK2 Act in Concert to Regulate Rad51 during DNA Double Strand Break Repair.* Molecular Cell, 2012. **45**(3): p. 371-383.

159. Benada, J., et al., *Polo-like kinase 1 inhibits DNA damage response during mitosis.* Cell Cycle, 2015. **14**(2): p. 219-31.

160. van Vugt, M.A.T.M., et al., *A Mitotic Phosphorylation Feedback Network Connects Cdk1, Plk1, 53BP1, and Chk2 to Inactivate the G₂/M DNA Damage Checkpoint.* PLoS Biol, 2010. **8**(1): p. e1000287.

161. Yang, F., et al., *Doxorubicin, DNA torsion, and chromatin dynamics.* Biochimica et Biophysica Acta (BBA) - Reviews on Cancer, 2014. **1845**(1): p. 84-89.

162. Lomax, M.E., L.K. Folkes, and P. O'Neill, *Biological Consequences of Radiation-induced DNA Damage: Relevance to Radiotherapy.* Clinical Oncology, 2013. **25**(10): p. 578-585.

163. van Jaarsveld, M.T., et al., *The kinase RSK2 modulates the sensitivity of ovarian*

cancer cells to cisplatin. Eur J Cancer, 2013. **49**(2): p. 345-51.